

MARSHALL ISLANDS FILE TRACKING DOCUMENT

Record Number: 352

File Name (TITLE): Chem., Phys., and Radchem.
Characteristics of the Contaminant

Document Number (ID): WT-917

DATE: 9/1955

Previous Location (FROM): CIC

AUTHOR: E. R. Tompkins

Additional Information: _____

OrMIbox: 19

CyMIbox: 12

15434

WT-917 (EX)
EXTRACTED VERSION

OPERATION CASTLE

Project 2.6a

Chemical, Physical, and Radiochemical Characteristics of the Contaminant

Pacific Proving Grounds
March — May 1954

Headquarters Field Command
Armed Forces Special Weapons Project
Sandia Base, Albuquerque, New Mexico

September 1955

NOTICE

This is an extract of WT-917, Operation CASTLE, Project 2.6a, which remains classified SECRET/RESTRICTED DATA as of this date.

Extract version prepared for:

Director
DEFENSE NUCLEAR AGENCY
Washington, D.C. 20305

15 May 1981

Approved for public release;
distribution unlimited.

REPORT DOCUMENTATION PAGE		READ INSTRUCTIONS BEFORE COMPLETING FORM
1. REPORT NUMBER WT-917 (EX)	2. GOVT ACCESSION NO.	3. RECIPIENT'S CATALOG NUMBER
4. TITLE (and Subtitle) Operation CASTLE - Project 2.6a Chemical, Physical, and Radiochemical Characteristics of the Contaminant	5. TYPE OF REPORT & PERIOD COVERED	
	6. PERFORMING ORG. REPORT NUMBER WT-917 (EX)	
7. AUTHOR(s) E. R. Tompkins L. B. Werner	8. CONTRACT OR GRANT NUMBER(s)	
9. PERFORMING ORGANIZATION NAME AND ADDRESS U.S. Naval Radiological Defense Laboratory San Francisco, California	10. PROGRAM ELEMENT, PROJECT, TASK AREA & WORK UNIT NUMBERS	
11. CONTROLLING OFFICE NAME AND ADDRESS Headquarters Field Command Armed Forces Special Weapons Project Sandia Base, Albuquerque, New Mexico	12. REPORT DATE September 1955	
	13. NUMBER OF PAGES	
14. MONITORING AGENCY NAME & ADDRESS (if different from Controlling Office)	15. SECURITY CLASS. (of this report) Unclassified	
	15a. DECLASSIFICATION/DOWNGRADING SCHEDULE	
16. DISTRIBUTION STATEMENT (of this Report) Approved for public release; unlimited distribution.		
17. DISTRIBUTION STATEMENT (of the abstract entered in Block 20, if different from Report)		
18. SUPPLEMENTARY NOTES This report has had the classified information removed and has been republished in unclassified form for public release. This work was performed by Kaman Tempo under contract DNA001-79-C-0455 with the close cooperation of the Classification Management Division of the Defense Nuclear Agency.		
19. KEY WORDS (Continue on reverse side if necessary and identify by block number) Operation CASTLE Bomb Debris Chemical Measurements Physical Measurements Radiochemical Measurements		
20. ABSTRACT (Continue on reverse side if necessary and identify by block number)		

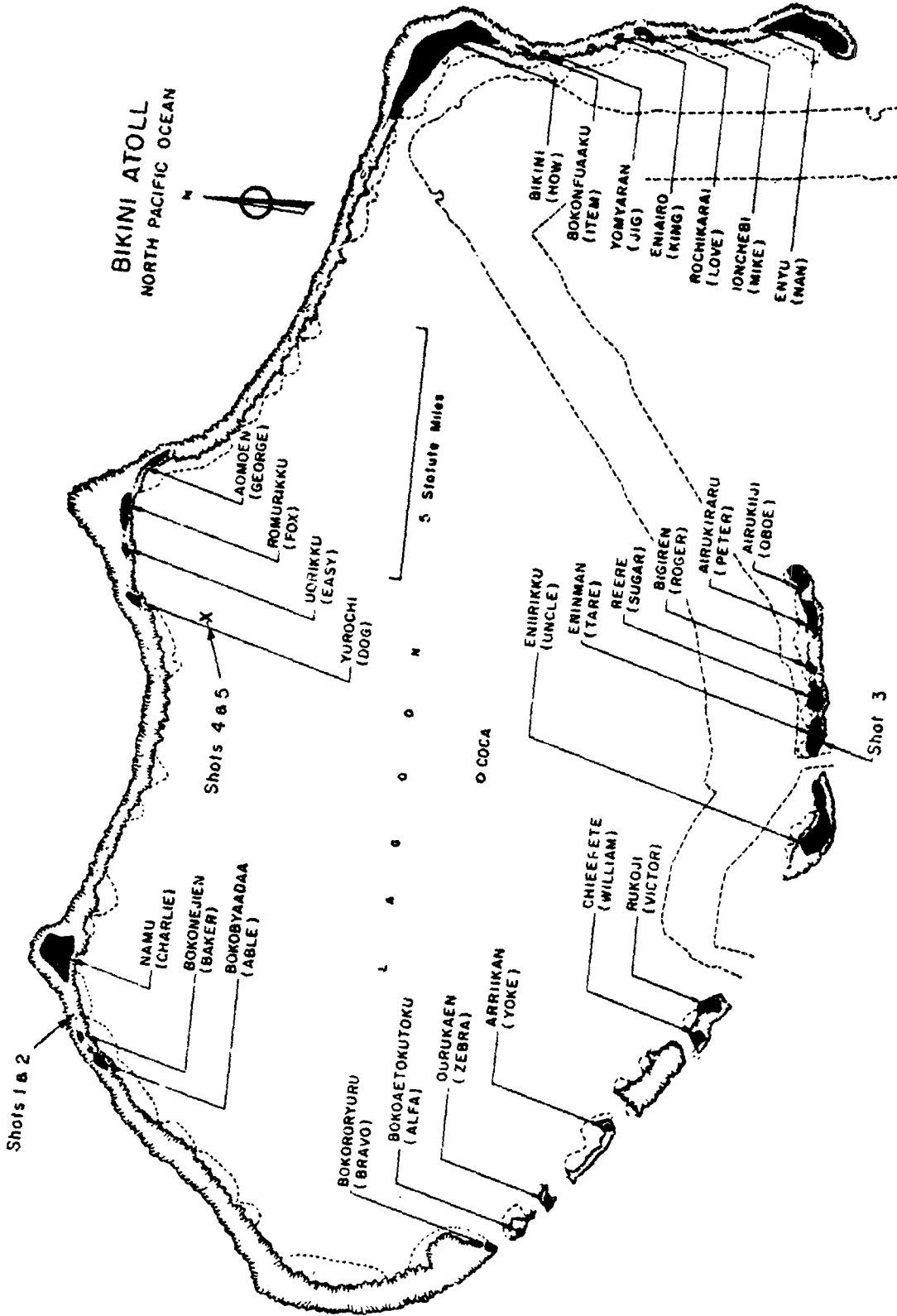
FOREWORD

This report has had classified material removed in order to make the information available on an unclassified, open publication basis, to any interested parties. This effort to declassify this report has been accomplished specifically to support the Department of Defense Nuclear Test Personnel Review (NTPR) Program. The objective is to facilitate studies of the low levels of radiation received by some individuals during the atmospheric nuclear test program by making as much information as possible available to all interested parties.

The material which has been deleted is all currently classified as Restricted Data or Formerly Restricted Data under the provision of the Atomic Energy Act of 1954, (as amended) or is National Security Information.

This report has been reproduced directly from available copies of the original material. The locations from which material has been deleted is generally obvious by the spacings and "holes" in the text. Thus the context of the material deleted is identified to assist the reader in the determination of whether the deleted information is germane to his study.

It is the belief of the individuals who have participated in preparing this report by deleting the classified material and of the Defense Nuclear Agency that the report accurately portrays the contents of the original and that the deleted material is of little or no significance to studies into the amounts or types of radiation received by any individuals during the atmospheric nuclear test program.



GENERAL SHOT INFORMATION

	Shot 1	Shot 2	Shot 3	Shot 4	Shot 5	Shot 6
DATE	1 March	27 March	7 April	26 April	5 May	14 May
CODE NAME (Unclassified)	Bravo	Romeo	Koon	Union	Yankee	Nectar
TIME*	06:40	06:25	06:15	06:05	06:05	06:15
LOCATION	Bikini, West of Charlie (Namu) on Reef	Bikini, Shot 1 Crater	Bikini, Tare (Eninman)	Bikini, on Barge at Intersection of Arcs with Radius of 6900' from Dog (Yurochi) and 3 Statute Miles from Fox (Aomoe).		Eniwetok, IVY Mike Crater, Flora (Elugelab)
TYPE	Land	Barge	Land	Barge	Barge	Barge
HOLMES & NARVER COORDINATES	N 170,617.17 E 76,163.98	N 170,635.05 E 75,950.46	N 100,154.50 E 109,799.00	N 161,698.83 E 116,800.27	N 161,424.43 E 116,688.15	N 147,750.00 E 67,790.00

* APPROXIMATE

ABSTRACT

The bomb debris from surface, land and water shots at Operation CASTLE was studied to determine the physical, chemical, and radiochemical characteristics.

The fallout from the surface land shots consisted chiefly of irregular white particles 25 μ to 2 mm in diameter. They were derived from coral and had the radioactivity concentrated near their surfaces. About 5 per cent of the activity in the solid fallout was water soluble; 95 per cent dissolved in dilute acetic acid. The fallout from the surface water shots was invisible both in the air and after it had deposited. It was collected on special filters and on a film by electrostatic precipitation. The filters and film and their autoradiographs were studied microscopically. These studies showed that the fallout consisted of microscopic solid crystals and small droplets. The autoradiographs indicated the presence on the filters of many particles which were invisible under the microscope. The major part of the radioactivity was associated with crystalline aggregates and droplets up to about 2 mm in diameter. Water dissolved from 60 to 90 per cent of the radionuclides from this type of fallout.

Fallout and cloud samples from land and water shots were analyzed chemically for major constituents and trace elements including many of the radionuclides. Coral and sea water contributed the major constituents, bomb products being present in trace concentrations. Radiochemical analysis showed the valley of the fission product yield curve was about 20 times higher and the heavy wing at mass 156 about 6 times higher than the yield curve from thermal neutrons on U^{235} . The important induced radionuclides were U^{239} - Np^{239} , U^{237} , and U^{240} . The presence of these had a marked effect on the decay curves and energy spectra especially at intermediate times after detonation. The neptunium was distributed between oxidation states; iodine occurred principally as iodide.

The information obtained from these studies has aided in (a) an understanding of the mechanism of formation of the fallout, (b) assessing the radiological situation in fallout areas, (c) synthesizing simulants for laboratory studies, and (d) interpreting data obtained in proof tests of countermeasures for ships.

FOREWORD

This report is one of the reports presenting the results of the 34 projects participating in the Military Effects Tests Program of Operation CASTLE, which included six test detonations. For readers interested in other pertinent test information, reference is made to WT-934, Summary Report of the Commander, Task Unit 13, Programs 1-9, Military Effects Program. This summary report includes the following information of possible general interest.

- a. An over-all description of each detonation, including yield, height of burst, ground zero location, time of detonation, ambient atmospheric conditions at detonation, etc., for the six shots.
- b. Discussion of all project results.
- c. A summary of each project, including objectives and results.
- d. A complete listing of all reports covering the Military Effects Tests Program.

PREFACE

The treatment and analyses of samples and the interpretation of the results in determining the characteristics of the bomb debris from Operation CASTLE required extensive participation by many individuals. The experimental measurements consisting of (a) Chemical, (b) Physical, and (c) Radiochemical Studies are presented in Chapters 3,4, and 5, respectively. The participation in each phase of the work is described below.

The Chemical Studies consisted of observations and measurements made at the site and analyses for major and minor constituents at the U.S. Naval Radiological Defense Laboratory (USNRDL). The field studies and the preparation of Chapter 3 were directed by C.F. Miller. D.Sam, A.E. Greendale, and M.J. Nuckolls carried on the preparation of the samples including the general observations, pre-treatment and aliquoting. The Physical State Studies were performed by R.Cole who also prepared the portion of Chapter 3 presenting the results of these studies. The oxidation states of Np and I were determined by W.J. Heiman and J.F. Pestaner,

respectively. M. Honma aided by J.D. O'Connor determined the major constituents in the fallout samples and the background samples of coral and sea water; R.W. Rinehart aided by J.A. Seiler analyzed them for the trace elements. An ion exchange procedure for separating some of the radionuclides was developed at the site by C.F. Miller and J.F. Pestaner.

Studies of the physical properties of fallout material involved development of collecting devices, collection of samples in the field, and analyses of samples at USNRDL. This work was done under the direction of T.C. Goodale. Chapter 4 was prepared by P.D. LaRiviere and C.E. Adams. In it are discussed the measurements of the physical properties of the fallout made on samples from an electrostatic precipitator, liquid droplet collector, and filter samplers. The sample collections were made by E.C. Evans III, J.P. Wittman, J.V. Zaccor, and N.R. Wallace. The physical analyses were performed at USNRDL by P.D. LaRiviere, T.C. Goodale, N.H. Farlow, C.E. Adams, S.K. Ichiki, J.P. Wittman, N.R. Wallace, J.V. Zaccor, and J.T. Quan. The special film used in the electrostatic precipitator was developed by N.H. Farlow and F.A. French.

Chapter 5 which described the Radiochemical Studies was prepared by L.R. Bunney and C.F. Miller aided by B. Singer, L.H. Gevantman and W.J. Heiman. Studies of neutron induced radionuclides were directed by L.H. Gevantman. The decay and adsorption measurements were started at the site by C.F. Miller, D. Sam and W.J. Heiman, and followed at later times at USNRDL by L.D. McIsaac, L.R. Bunney and E.W. Roberts. The interpretation of these data as presented in this report was made by W.J. Heiman. The gamma analyser was converted from an alpha analyser at the site by D.F. Covell and M.S. Eichen. The field readings of the samples were made by all members of Project 2.6a present at the site. W.J. Heiman and C.F. Miller interpreted the data for the report. The analysis of Na²⁴ was performed by B. Singer. Radiochemical analyses for fission product and heavy element radionuclides were performed at USNRDL under the direction of L.R. Bunney, E.C. Freiling, and L. Wish. Fission product measurements were made by E.M. Scadden, S.A. Ring, L.D. McIsaac, J.A. Seiler, and S.C. Foti. Heavy element measurements were made by M.H. Rowell and J.N. Pascual.

L.H. Gevantman prepared the pretest report.

Lt. Col. E.A. Martell, USA, provided valuable suggestions throughout the planning and execution of the project. Capt. B. Bennett, USN, contributed both by his advice and aid in making the scintillation spectrometer measurements at the site.

E.R. Tompkins was the project officer and L.B. Werner was his deputy.

CONTENTS

ABSTRACT	5
FOREWORD	7
PREFACE	7
ILLUSTRATIONS	12
TABLES	13
CHAPTER 1 INTRODUCTION	15
1.1 Objectives and Background	15
1.1.1 Mechanism of Contamination Formation	15
1.1.2 Assessment of Radiological Situations	16
1.1.3 Specifications of Simulants for Radiological Contaminants	16
1.1.4 Proof Testing Atomic Warfare Countermeasures for Ships	18
CHAPTER 2 EXPERIMENT DESIGN	19
2.1 Determinations Undertaken	19
2.2 Collection of Samples	20
2.3 Equipment	20
2.3.1 Sample Collectors	20
2.3.2 Beta Counters	20
2.3.3 Gamma Counters	21
2.3.4 Gamma Analyzer	22
2.3.5 Emission Spectrograph	22
2.3.6 Spectrophotometers	22
2.3.7 X-ray Diffraction Apparatus	24
2.3.8 Petrographic Microscopes	24
2.3.9 Ion Exchange Equipment	24
2.3.10 Film Coating Apparatus	24
2.3.11 Sun Lamp Unit	25
2.3.12 Radioactivity Monitor	25
2.3.13 Vapor Phase Reducing Unit	25

2.3.14	Microscope Traversing Mechanism	25
2.3.15	Aerosol Sampling Devices	26
CHAPTER 3 CHEMICAL MEASUREMENTS		27
3.1	Description of Fallout Samples	28
3.1.1	Samples from Shot 1	28
3.1.2	Samples from Shot 2	29
3.1.3	Samples from Shot 3	30
3.1.4	Samples from Shot 4	30
3.1.5	Evaluation of Samples	32
3.2	Physical State Separations	33
3.2.1	Physical Treatment of Samples	33
3.2.2	Results	34
3.2.2.1	Gamma Activity Distribution Among Physical State Fractions	34
3.2.2.2	Gamma Decay of Physical State Fractions	36
3.2.2.3	Gamma Energy Distribution of Physical State Fractions	41
3.2.2.4	Quantitative Analysis of Physical State Fractions	48
3.3	Chemical State of Neptunium and Iodine	56
3.3.1	Oxidation State of Neptunium	56
3.3.1.1	Chemical Treatment of Samples	56
3.3.1.2	Neptunium Results	56
3.3.2	Chemical State of Iodine	57
3.3.2.1	Chemical Treatment of Samples	57
3.3.2.2	Results	58
3.4	Composition of the Fallout Material	58
3.4.1	Physical Treatment of Samples	59
3.4.2	Chemical Treatment of Samples	59
3.4.3	Results	61
CHAPTER 4 PHYSICAL MEASUREMENTS		82
4.1	Properties of Aerosols	82
4.1.1	Operational Record	82
4.1.2	Observations and Results	83
4.1.2.1	General Observations, Shot 1	83
4.1.2.2	General Observations, Shot 2	83
4.1.2.3	General Observations, Shot 4	88
4.1.2.4	General Observations, Shot 5	88
4.1.2.5	Physical State of Activity on Air Filters	92
4.1.2.6	Specific Gravity of Settled Radioactive Aerosol	93
4.2	Properties of Fallout (Shot 1)	93
4.2.1	Distribution of Activity with Particle Size	95
4.3	Individual Particle Composition and Characteristics	95
4.3.1	General Description	95
4.3.2	Distribution of Activity	97

4.3.3	Solubility Studies	97
4.3.4	Mechanism of Formation	98
CHAPTER 5 RADIOCHEMICAL MEASUREMENTS		100
5.1	Radiation Characteristics of Gross Fallout Samples . . .	100
5.1.1	Preparation of Counting Samples	100
5.1.2	Gross Decay	101
5.1.2.1	Shot 1	101
5.1.2.2	Shot 2	101
5.1.2.3	Shot 3	101
5.1.2.4	Shot 4	101
5.1.3	Gamma Spectrometer Measurements	112
5.1.3.1	Shot 1	114
5.1.3.2	Shot 2	114
5.1.3.3	Shot 3	115
5.1.3.4	Shot 4	115
5.1.3.5	Comparisons of Spectra of Samples from Shots 1 through 4	116
5.1.4	Absorption Measurements	117
5.1.4.1	Lead Absorption	117
5.1.4.2	Aluminum Absorption	119
5.2	Fission Product Determinations	120
5.2.1	Radiochemical Procedures	121
5.2.2	Results	121
5.2.3	Fractionation	123
5.2.4	Fission Yield Curves	123
5.3	Induced Activities	123
5.3.1	Radiochemical Procedures	123
5.3.2	Activities Induced in Environmental Substances .	124
5.3.2.1	Chemical Treatment of Samples	124
5.3.2.2	Results	125
5.3.3	Activities Induced in Device Components	129
5.3.3.1	Results	129
5.4	Fraction of Bomb in Fallout Samples	129
5.4.1	Results	129
CHAPTER 6 SUMMARY		132
6.1	General	132
6.2	Mechanism of Formation and Subsequent Reactions of Nuclear Detonation Debris	132
6.3	Assessment of Radiological Situation in Fallout Areas .	133
6.4	Synthesis of Simulants for Decontamination Tests	134
6.5	Proof Testing AN Countermeasures for Ships	134
APPENDIX A CHEMICAL AND RADIOCHEMICAL PROCEDURES		135
A.1	Determination of Oxidation States of Neptunium	135
A.2	Separation of Sodium Activity	136
A.2.1	Notes	137

A.3	Separation of Potassium Activity	137
A.4	Separation of Chlorine Activity	138
A.4.1	Notes	138
APPENDIX B PARTIAL FRACTIONATION OF FALLOUT COMPONENTS BY		
	CATION EXCHANGE	139
B.1	Exchange Column Procedure	139
B.2	Results	139
BIBLIOGRAPHY		149

ILLUSTRATIONS

2.1	Relative Photon Efficiency for Scintillation Counters Using 1-1/2 by 1-1/2 in. NaI Crystal and 1600 mg/sq cm Aluminum Absorber	23
3.1	Gamma Decay of Physical State Fractions of Sample 1-251.03	37
3.2	Gamma Decay of Physical State Fractions of Sample 2-A4	38
3.3	Gamma Decay of Physical State Fractions of Sample 3-Coca TC	39
3.4	Gamma Decay of Physical State Fractions of Sample 4-Y39	40
3.5	Lead Absorption Curves at 8.3 Days for Sample 251.03, Shot 1	43
3.6	Lead Absorption Curves at 3.6 Days for Sample 2-A4, Shot 2	44
3.7	Lead Absorption Curves at 5.3 Days for Sample 2-A4, Shot 2	45
3.8	Gamma Spectra of NpV-VI, Sample 3-251.02 at + 7 Days	49
3.9	Gamma Spectra of Solid, Sample 3-251.02 at + 7 Days	50
3.10	Gamma Spectra of Ultrafiltrate, Sample 3-251.02 at + 7 Days	51
3.11	Gamma Spectra of Colloid Fraction, Sample 3-251.02 at + 7 Days	52
3.12	Density Distribution of Equivalent Coral for Shots 1,2, and 3	72
3.13	Density Distribution of Equivalent Sea Water for Shots 2,3, and 4	73
3.14	Density Distribution of Device Fraction for Shots 1,2, 3, and 4	74
3.15	Distribution of the Ratio of the Radiation Field to the Surface Density of the Coral Component	78
3.16	Distribution of the Ratio of the Radiation Field to the Surface Density of the Sea Water Component	79
3.17	Distribution of the Ratio of the Radiation Field to the Surface Density of the Device Fraction Component	80
4.1	Photomicrographs of Aerosol Samples from Shot 1	84

4.2	Size Distribution of Active Aerosol Particles from Shot 1	85
4.3	Autoradiographs of Millipore Filters, Shot 2	86
4.4	Photomicrograph of Radioactive Aggregate, Shot 2	87
4.5	Autoradiographs of Millipore Filters, Shot 4	89
4.6	Photomicrographs of Radioactive Areas of Millipore Filters, Shot 4	90
4.7	Autoradiographs of Fragments of Millipore Filters, Shot 5.	91
5.1	Gross Beta Decay of Fallout Samples from Shots 1,2,3, and 4	104
5.2	Gross Gamma Decay of Fallout Samples from Shots 1,2,3, and 4	107
5.3	Ionization Decay as a Function of Relative Ionization Rate	110
5.4	Calculated Beta Curves	113
5.5	Decay Curve of Na ²⁴ Sample from Shot 2	126
5.6	Decay Curve of Na ²⁴ Sample from Shot 3	127
5.7	Aluminum Absorption Curve for Na ²⁴ Sample from Shot 3	128
B.1	Facsimile of Chromatogram Taken from the Esterline-Angus Recorder	140
B.2	Decay of Fraction 4-34	142
B.3	Decay of Fraction 4-31	143
B.4	Decay of Fraction 4-32	144
B.5	Decay of Fraction 4-33	145
B.6	Decay of Fraction 4-24	147

TABLES

3.1	Samples from Shot 1	29
3.2	Samples from Shot 2	30
3.3	Samples from Shot 3	31
3.4	Samples from Shot 4	32
3.5	Physical State Fractionation of Gamma Activity	35
3.6	Summary, Physical State Fractionation of Gamma Activity	35
3.7	Summary of Log-Log Decay Slopes	42
3.8	Gamma Energy Distribution of Physical State Fractions Determined by Lead Absorption	46
3.9	Concentration of Elements of Interest in Solutions of Physical State Fractions	53
3.10	Mass Distribution of Elements of Interest in Liquid and Solid Fractions	54
3.11	Summary of Analysis of Neptunium Oxidation States	57
3.12	Summary of Results for State of Iodine	59
3.13	Summary of Analytical Methods	60
3.14	Spectrophotometric Analysis of Minor Constituents	60

3.15	Analysis of Background Components	62
3.16	Physical Measurements of the Fallout Samples	63
3.17	Concentration Analysis of Liquid Fractions from Fallout . . .	64
3.18	Concentration Analysis of Solid Fractions from Fallout Samples	65
3.19	Component Analysis of Fallout Samples	66
3.20	Surface Density of Fallout Components	71
3.21	Comparison of Radiation Field with Surface Density of Fallout Components	76
4.1	Physical State of Activity	92
4.2	Specific Gravity of Active Material Settling on Decks of Ships Compartments	94
4.3	Distribution of Fallout Activity with Particle Size, Shot 1 .	96
5.1	Gross Beta Decay	102
5.2	Gross Gamma Decay	105
5.3	Gamma Ionization Decay of Sample 4-Y39	109
5.4	Data for Coincidence Loss from High Counting Samples from YAG 39	111
5.5	Calculation of Background from Shelf Ratios and Contaminated Plate Readings	111
5.6	Gamma Energy Measurements from Rongelap Sample, Shot 1 . . .	114
5.7	Gamma Energy Measurements from Sample 2-A5, Shot 2	115
5.8	Gamma Energy Measurements from Sample 3-Coca TC, Shot 3 . . .	115
5.9	Gamma Energy Measurements from Sample 4-Y39, Shot 4	116
5.10	Energies and Gross Distribution of Gamma Rays from Gross Fallout Samples	118
5.11	Average Hard Gamma Energy for Each Shot	119
5.12	Average Energy and Average Percentage of "Apparent" Gamma Components for Each Shot at Times Less than 14 Days	119
5.13	Preliminary Summary of Beta Energies	120
5.14	Fission Product R Values Referred to Nuclide Mo ⁹⁹	122
5.15	Amounts of Neutron Induced Radionuclides Produced per Fission Event	129
5.16	Relative Activity Levels of Np ²³⁹ , U ²³⁷ , U ²⁴⁰ , and Mo ⁹⁹ Extrapolated to Zero Time	130
5.17	Number of Atoms of U ²³⁷ and U ²³⁹ Relative to Number of Fissions	130
B.1	Summary of Major Photon Spectra Peaks of Ion Exchange Fractions	146
B.2	Major Gamma Emitters in Ion Exchange Fractions	148

CHAPTER 1

INTRODUCTIONS

Radiation fields produced by fallout from a nuclear detonation create debilitating effects far beyond the range of its blast damage. Information on transport and distribution of fallout and knowledge of its physical, chemical, and radiochemical properties are prerequisite to development of countermeasures against its radiation fields. At Operation CASTLE the transport and distribution of fallout was principally the concern of Projects 2.5a and 6.4; Project 2.5b studied the fallout on islands near the shot point; investigation of fallout properties was the concern of Projects 2.6a and 2.6b.

1.1 OBJECTIVES AND BACKGROUND

The purpose of Project 2.6a was to investigate the chemical, physical, and radiochemical properties of the fallout for:

- a. Deducing the mechanism whereby contaminant is formed.
- b. Assessing radiological situations.
- c. Specifying realistic simulants of radiological contaminants for use in contamination and decontamination tests.
- d. Interpreting the data obtained in proof testing atomic warfare countermeasures for ships.

1.1.1 Mechanism of Contamination Formation

The contamination formed from surface or sub-surface detonation of a nuclear weapon has important military consequences. It was found at Operations CROSSROADS,⁸ JANGLE,¹⁷ and IVY¹² that high levels of surface contamination were produced as a result of surface or sub-surface detonations. Each of these operations represented a unique condition of detonation, but provided insufficient data to establish bases for predicting radiological effects for a wide range of probable conditions of detonation. An understanding of the mechanism whereby contamination is produced is necessary in making such predictions. Data obtained in CASTLE are applicable in answering such questions on the mechanics of the event as: To what extent is wet contaminant formed by condensation phenomena? With what type of particles do the primary particles of

radioactive debris associate? What is the rate and extent of settling out and mixing of fallout deposited on the water surface?

Owing to the incompleteness of the data taken at Shot Baker, CROSSROADS, essentially nothing was known prior to CASTLE concerning the mechanism of formation of wet contamination from this type of burst. The relative contributions of base surge and fallout were uncertain; the roles of condensation, evaporation and mixing with sea water in the production of either base surge or fallout were unknown. Particle size and individual particle studies undertaken at JANGLE and IVY have yielded considerable information on the mechanism of formation, dispersion and reactions of dry contaminants from these operations. ^{25, 20, 1, 2/}

1.1.2 Assessment of Radiological Situations

Extensive laboratory contamination-decontamination programs have been undertaken to solve presumed field radiological problems but in many cases lack of full-scale test data has made it impossible to define them clearly. For example, before CASTLE it had not been determined whether an internal contamination hazard would be produced on ships by radioactive aerosols from an underwater detonation, because the nature of such aerosols was unknown; the relative contribution of gamma radiation from fallout in the water with that on contaminated ships could not be calculated because the rate of settling or mixing of the contaminant in the water was unknown. Insoluble particles will settle depending on size and density while dissolved (ionic) contaminants will mix; colloidal material, if present, will mix and settle slowly. The assessment of such radiological situations and the development of countermeasures require a knowledge of many physical and chemical properties of the contaminant.

Limited data exist with regard to the contaminants which may be produced by surface and underground detonations because of the atypical nature of the soils at IVY and JANGLE. No direct information has been obtained on the nature of contaminants from underwater detonations. For this reason, there is special interest in surface water shots which should produce a contaminant most similar in nature to that from an underwater detonation.

1.1.3 Specifications of Simulants for Radiological Contaminants

If meaningful laboratory contamination-decontamination results are to be obtained, it is essential that the artificial contaminants used must simulate real ones in chemical and radiochemical composition and in important chemical and physical characteristics. In the past, the radiochemical composition of artificial contaminants ^{14/} has been based upon yields of various radioelements from slow fission of U²³⁵. It is important to know the extent of difference in fission yields for nuclear processes other than slow fission and whether induced activities contribute appreciably to the contamination. Finally, it is necessary to evaluate the relative contribution of each radioelement to contamination fields on the basis of its yield and the number and energy of the gamma rays emitted by the various radionuclides of that element.

Fission yield curves have been determined for various fission weapons detonated to date. Although some such information exists for the fusion-fission device detonated at IVY, it was necessary to determine the important radionuclides produced by the detonation of new types of devices at CASTLE.

The presence of activities induced in elements found in sea water was reported for Shot Baker at CROSSROADS. An analysis for induced activities was also made at JANGLE.^{19,4/} It was shown that the single important induced activity present in JANGLE fallout any time during the first 90 days after detonation was Np²³⁹, formed from U²³⁸ present in the device. No important induced activities have been reported for IVY. However, some unconfirmed data indicated an activity present in high yield at early times.^{12/} Detonation of certain of the CASTLE devices over water posed the question of the extent to which important induced activities would be formed under these conditions.

Calculations for estimating the contribution of different chemical elements to the rate of gamma radiation have been made. Yields from slow neutron fission were used. Data regarding the number and energy of the gamma rays emitted by various radionuclides were incomplete. To improve the validity of these important calculations better radionuclide yield data were required. Also it was important to measure the gamma energies of a few radionuclides, for which the energies had not been adequately defined.

It has been shown that contamination-decontamination behavior is a function of the physical and chemical properties of the contaminant system. This is illustrated by the ease with which gross particulate contaminants are removed,^{32/} by the relation of particle size to decontamination efficiency,^{18/} and by the influence which composition and oxidation state of liquid contaminants exert on decontamination effectiveness.^{22,23,24,10/} Definition of the real contaminant system was therefore an important prerequisite for specification of contaminant simulants.

Definition of any chemical system requires a knowledge of the identity and amounts of its various components. The contaminating fallout from each shot consists largely of nonradioactive materials. The production of realistic laboratory contaminants for more basic information about radiological decontamination has, in the past, suffered severely from the absence of elementary information about the actual contamination-decontamination system in question. Since real contamination had not been available, many investigations were conducted using highly questionable contamination procedures with no available means of relating the data to real events. Knowledge of the concentrations of macro constituents along with radiochemical analytical data provide all the information needed to prepare laboratory contaminants which would consistently have the same general decontamination characteristics. With such added information as field isodose data in conjunction with isoconcentration plots from these data, laboratory experiments on the effect of level on decontamination can be investigated reliably.

The thermodynamic states of inactive or bulk materials usually are of greater importance than those of the radioactive constituents. It is inconceivable, for any radiological contamination of interest,

that the radioactive constituents can comprise as much as 0.01 per cent of the total fallout. Hence, most of the properties of the contaminant except the radiation characteristics will be essentially determined by the inactive elements. Therefore, emphasis was placed on determining the states of the inactive constituents and the states of a few important gamma emitting elements.

1.1.4 Proof Testing Atomic Warfare Countermeasures for Ships

There has been extensive laboratory and field scale development work on atomic warfare (AW) countermeasures for ships.^{5/} Project 6.4 tested the washdown system at CASTLE and conducted decontamination operations on the ships used in the operation. Since the contamination found from certain of the shots of CASTLE differed from either real or simulated contaminants previously studied, detailed knowledge of the properties of the contaminant was needed for interpreting these results.

Information on the rate of radioactive decay, gross gamma energy spectrum, and the ratio of beta to gamma radiation was furnished by Project 2.6a.

CHAPTER 2

EXPERIMENT DESIGN

Chemical, physical, and radiochemical measurements were made on the fallout samples collected at lagoon, island, and sea stations. Short lived radioactive species were analyzed in the forward area; the remainder of the analyses were made at U.S. Naval Radiological Defense Laboratory. Owing to many unforeseen difficulties early samples for the radiochemical analyses were not obtained, although early decay data were obtained from several shots. The number of samples collected was much smaller than planned. However, it was possible to get considerable information concerning all planned phases except those involving very short lived radioisotopes.

2.1 DETERMINATIONS UNDERTAKEN

To investigate the chemical, physical, and radiochemical properties of the fallout the following determinations were undertaken:

- a. Amounts of radioactivity in soluble (ionic), colloidal, and insoluble fractions.
- b. Concentration of macro constituents, primarily the elements which occur naturally in coral and sea water, but also the elements present in large amounts in the weapon assembly and associated equipment.
- c. Oxidation state of certain radionuclides whose final state under the conditions of the detonation could not be predicted, and whose contamination-decontamination behavior is believed to depend upon their oxidation state.
- d. Size distributions of fallout drops and particles, and the variation of these distributions throughout the sampling array.
- e. Specific radioactivities and salt content of various particle and drop size fractions in fallout.
- f. Chemical and crystalline composition of individual particles.
- g. Size distributions and presence of radioactivity in both liquid and dry aerosol particles; presence of salt in liquid aerosol particles.
- h. Radiochemical composition of fallout, especially determination of the fission yield curve and the degree of chemical fractionation among the fission products.

2.2 COLLECTION OF SAMPLES

The fallout samples were collected at stations established by the personnel of Projects 2.5a and 6.4. The location of these stations and details of the collectors used are given in the reports of Projects 2.5a and 6.4.

Chemical and radiochemical studies were made on samples from Shots 1,2,3, and 4. Limited radiochemical measurements were made on samples from Shots 5 and 6.

Physical data on the nature of the fallout were obtained from Shots 1,2,4, and 5.

2.3 EQUIPMENT

The analyses at the site were performed in mobile laboratories built in trailers. These laboratories were equipped with conventional chemical apparatus and several types of special apparatus as well as beta and gamma counters. A gamma spectrometer was located in an air conditioned building near the mobile laboratories.

The equipment at USNRDL consisted of conventional apparatus for chemical, radiochemical, and physical studies as well as several special types of apparatus. Included in the conventional equipment were beta and gamma counters, an emission spectrograph, spectrophotometers, X-ray diffraction apparatus, a petrographic microscope, a crystalab ultrasonicator, Model SL 520, Beckman pH meters, ion-exchange columns with accessory equipment, and the standard apparatus found in chemical laboratories. The special equipment included aerosol sampling devices and film coating, developing, and scanning apparatus.

2.3.1 Sample Collectors

Samplers of two types were used for collecting fallout for chemical and radiochemical studies. Also, some of the samples from Project 2.5a collectors were studied on this project.

One type of collector consisted of three 1-gal polyethylene bottles fitted with 7-in. diameter funnels of the same material mounted in a frame with a mechanical device arranged to uncover the three funnels at detonation time and cover them again after 3 hr. These samplers did not operate originally as well as had been anticipated but after some modification operated satisfactorily.

The other type of collector was a collecting funnel 6-1/2 ft x 11 ft built onto a life raft and arranged to drain into a 13-gal polyethylene bottle. Because this apparatus was inadequately designed and constructed to cope with conditions found in the field only a limited number of samples were obtained from it.

2.3.2 Beta Counters

The beta detectors were NRDL Model PG-1 proportional counters. These detectors were of the cylindrical, side-window, coaxial anode type,

made from an aluminum block supported by end pieces which were notched at several discrete positions to accommodate a standard planchet holder. The detectors afforded a fair range of geometry variation. All pieces were made of aluminum and machined to close tolerances so that geometrical orientation of the counting samples could be readily reproduced and identical operating characteristics could be assured from detector to detector. The detectors were the continuous gas-flow type, using a gas consisting of 90 per cent argon and 10 per cent carbon dioxide at a flow rate of 10 to 15 cu cm per min. Doubly aluminized Mylar (0.95 mg/sq cm) was used for the window which was nominally 1 in. in diameter and collimated by 1/16 in. aluminum and 1/16 in. lead. A pre-amplifier of wide dynamic range and gain of approximately 1000 was built on a chassis assembled directly with the detector in such a way that the entire assembly fitted into a commercial lead castle. The detector assembly had about a 200-v plateau with less than 1 per cent slope per 100 v, and operated at about 1900 v.

Decade scalars NRDL Model 2 with self-contained register, high voltage, and automatic clock were used. Time accuracy was about 1/2 sec. A scale factor of 1000 was employed.

The dead time of the beta counting system was 5 μ sec which gave a coincidence loss of 1 per cent at a counting rate of 100,000 events per minute.

2.3.3 Gamma Counters

The gamma detectors consisted of an RCA type 5819 photomultiplier with a light-pipe adapter and a commercially mounted* cylindrical crystal of sodium iodide, 1-1/2 in. in diameter by 1/2 in. thick. A removable aluminum absorber (1600 mg/sq cm) was used to shield out beta rays. The shelf geometry was the same as that described for the beta counters so that the same planchet holders could be used in both systems. The detector assembly was attached directly to an amplifier chassis, and the whole assembly was mounted within a commercial lead castle. The amplifier was of a wide dynamic range design with a nominal gain of 1000.

The scaler, (Navy Model AN-4DR19) supplied high voltage and power needed for the detector unit. Two types of timers were provided with this scaler; an electromechanical automatic-terminating timer with an accuracy of 1/2 sec, and an electronic timer. The electronic timer** accepted pulses from a crystal oscillator within the scaler on a 1 sec schedule, scaled these down by means of glow-transfer type decades with provisions for presetting any scale factor from 1 to 9999 and feeding the carry-over pulse into the gating jack on the scaler which stopped the scaler with an accuracy of about 100 μ sec. With this timing device short time intervals of counting could be used while maintaining a counting error within allowable counting statistics (i.e., minimum timing error).

* Supplied by Harshaw Chemical Co., Cambridge, Mass.

** Model GS-10C, manufactured by Atomic Instrument Co., Cleveland, Ohio.

The above counting system had a coincidence loss of about 2 per cent at 1,000,000 c/m and 7 per cent at 2,000,000 c/m as determined by the split sample method. The voltage plateau extended about 200 v with a slope around 2 per cent per 100 v. However, the extent and quality of the plateau was influenced by the energy of the incident photon. The discriminator and high voltage settings were determined from data taken on Cd¹⁰⁹ (80 kev gamma) and Co⁶⁰ (1.1 and 1.3 Mev gammas) sources so that both the high and low energy photons were on some part of both plateaus.

The calculated energy response of the system is shown in Fig.2.1. The discriminator and high voltage, when determined as described above, have little effect on the energy response of the system. The curve is a combined effect of aluminum absorber and crystal capture efficiency showing a virtual cut off at 50 kev due to the adsorber, a fall in efficiency about 200 kev due to the thin crystal, and a maximum efficiency at about 125 kev.

2.3.4 Gamma Analyzer

A 10-channel alpha energy analyzer (using an alpha ionization chamber) was sent to the site for planned alpha analysis. After Shot 1, when it became evident that the requirements of sample collection and delivery could not be fulfilled, this analyzer was converted to a gamma analyzer. To achieve this, certain time constants in the analyzer were reduced, a scintillation detector-preamplifier was constructed, and an auxiliary high-voltage supply was provided. The detector consisted of a Dumont 6292 phototube and a sodium iodide crystal 1 in. in diameter and 1 in. long. The detector was attached directly to the preamplifier (nominal gain of 100) and the whole mounted within a commercial lead shield which was covered with 2-in. thick lead bricks to minimize the background.

The analyzer itself had an internal gain of 100, followed by a window amplifier and 10 different discriminators, each with its own scaling and registering circuits. The discriminator circuitry was the Johnstone design.^{15/} The long-term stability and linearity of the system were excellent as long as the ambient temperature was kept below 80°F; the resolution was about 10 per cent under the usual operating conditions. An external filter was provided to reduce the ripple in the high voltage supplied by a Navy Model AN-4DR/9 scaling unit.

2.3.5 Emission Spectrograph

An ARL 2-meter grating spectrograph was used for exploratory examination of samples. A special chamber^{6/} was used to collect the radioactive debris from the arced samples.

2.3.6 Spectrophotometers

A Beckman Model 9200 flame photometer was used for the analysis of the major constituents in coral and sea water. This photometer was equipped with a special device^{13/} to collect the combustion products from

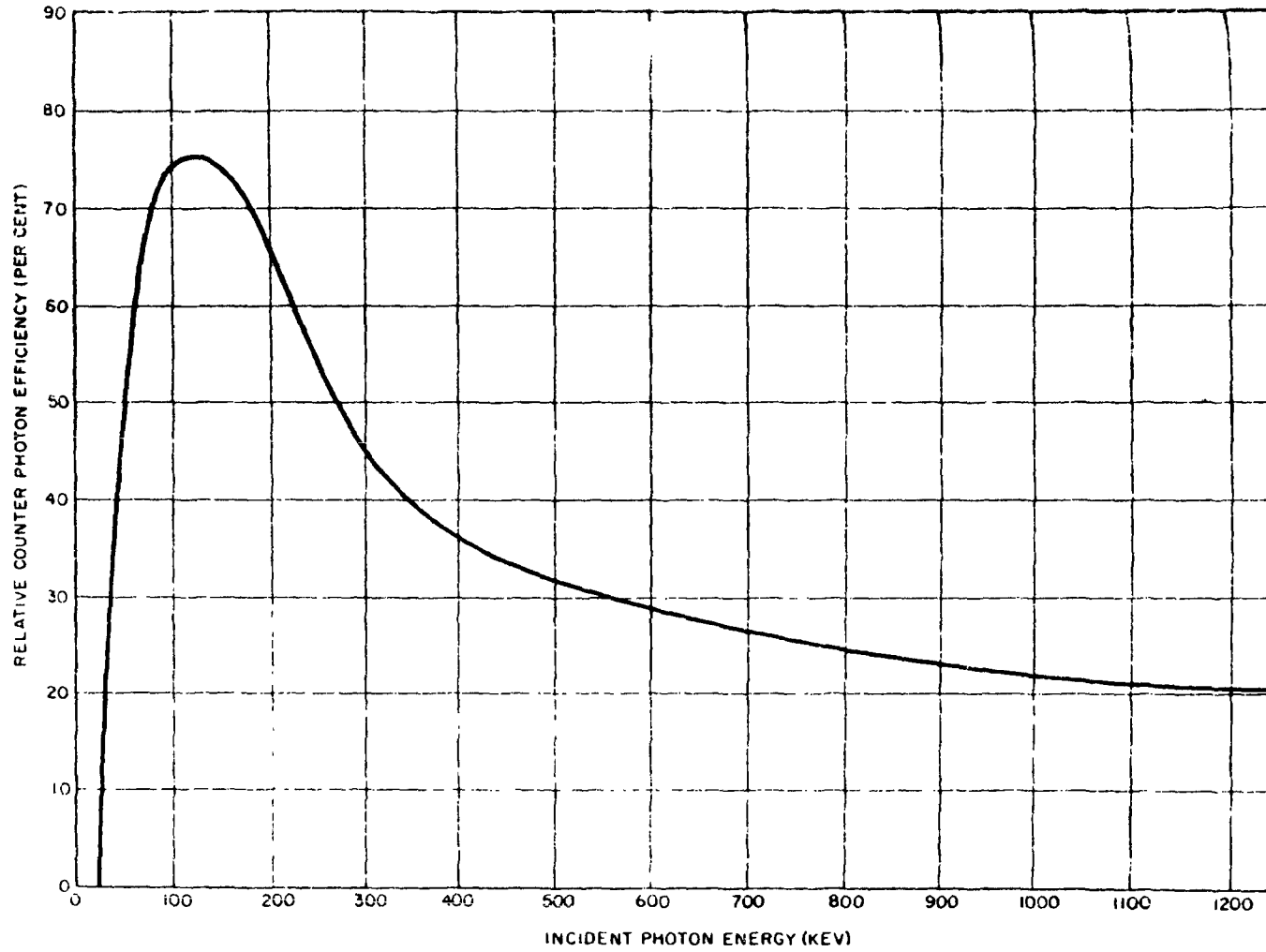


Fig. 2.1 Relative Photon Efficiency for Scintillation Counters, Using 1-1/2 by 1-1/2 in. NaI Crystal and 1600 mg/sq cm Aluminum Absorber

the exhaust gases so that the radioactive substances in the samples could be removed. A Beckman Model DU spectrophotometer was used to analyse for some of the minor constituents of coral and sea water.

2.3.7 X-ray Diffraction Apparatus

A General Electric XRD-3 X-ray diffraction unit was used in the X-ray analysis of Project 2.6a samples. The essential components of this unit are a high-intensity sealed-off X-ray tube energized by a voltage-stabilized power supply, a collimating system which permits the use of slit or pinhole collimators, an X-ray camera using the Straumanis method of film loading, and two types of sample mounts (rotating and oscillating wedge).

The samples were fine, crystalline materials. Some were individual pellets of 1 to 2 cu mm, others were friable powders. All were in a very satisfactory state for X-ray analysis.

For individual particle analysis, a pellet of approximately 1 mm long and 0.5 mm in diameter was cemented to the end of a fine glass fiber, supported on the rotating sample mount with the particle centered in the path of a collimated beam of filtered copper K_{α} radiation. The diffracted rays were registered on film. Normal exposure time was 7 hr.

The friable material was crushed to reduce the large aggregates to smaller uniform size powder, which was packed into the shape of a wedge and mounted on the oscillating mount. The edge of the wedge was adjusted to intercept one-half of a slit-collimated beam of filtered copper K_{α} radiation. The diffracted rays were registered on film during a 1-1/2 hr exposure.

A comparator^{26/} was used to compare the diffraction patterns from fallout with those from coral sand collected near the site of the detonation.

2.3.8 Petrographic Microscope

A Bausch and Lomb Petrographic Microscope, model WL 3238 with a Leitz 4-axis universal stage was used to examine sections of radioactive particles.

2.3.9 Ion Exchange Equipment

Ion exchange columns and assessorry equipment were used for the separation of rare earth fission products. The column was eluted with lactate at a controlled pH at a temperature of 87°C. The effluent was collected in small fractions by a fraction collector.

2.3.10 Film Coating Apparatus

This equipment was developed to produce specially coated water droplet sensitive 35-mm film. The apparatus consists of a variable speed drive motor which pulled the film through a series of etching, washing, and coating baths and thence through a thermal drying chamber to a reel onto which the film was wound in 500-ft lengths. The film was

produced from blank 35-mm leader by first etching it in saturated potassium hydroxide solution, then rinsing it in three water baths, in the last of which it was dip coated with water soluble plastic mix. A simple suction apparatus mounted beyond the plastic dip bath cleaned the viscous plastic from the sprocket holes. Three 500-ft reels of film can be processed at one time at the rate of about 3/4-ft/min.

2.3.11 Sun Lamp Unit

To properly sensitize sea water droplet impressions collected on the sensitive film, they must be exposed to high intensity solar radiation. This was accomplished with a hood-like arrangement containing six sun lamps which fitted onto the film coater over the empty wash tanks; the drive system pulled the film beneath the lighted lamps. The sun lamp hood was connected to the ventilating system through filters and the movement of air both cooled the film and entrapped any loosened radioactive particles.

2.3.12 Radioactivity Monitor

It was necessary to define the areas of activity on droplet exposed film so that radioautographs could be made. For this purpose, an end window Geiger tube was suspended above the film and connected to a count rate meter, thence to an Esterline Angus recorder. Activity recording was combined with the sun lamp exposure. By calibrating the coater drive speed with the recorder speed, the exact location of any active areas could be determined.

2.3.13 Vapor Phase Reducing Unit

To properly develop sea water and distilled water spots on the sensitive film, vapors of certain chemicals in controlled amounts and under controlled conditions must be brought into contact with the film surface. The developing apparatus consisted of three temperature controlled units; one for the saturation of air with phenylhydrazine vapors, one to saturate air with water vapor, and the central unit where the two vapors were mixed with ammonia gas. The central reducing chamber was an oil jacketed tank through which the film was drawn into contact with the reducing chemical vapors. All of the saturation units, temperature control systems, and heat exchanger coils were completely immersed in oil baths contained in stainless steel tanks surrounded with fiberglass insulation. The sunlamp treated film was led from the reducing chamber through a thermal drying chamber to a wind-up reel.

2.3.14 Microscope Traversing Mechanism

This unit was built to allow a rapid survey of hundreds of feet of processed film. A precision stage was devised which allowed the film to be tracked under the lens system without scratching the silvered surfaces. A counting device mounted on the stage allowed an accurate computation of the film footage passing across the stage.

2.3.15 Aerosol Sampling Devices

The aerosol sampling devices were an electrostatic precipitator (ESP), employing a moving film coated with a drop sensitive emulsion, accompanied by millipore filter and dimethyl-terephthalate (DMT) air samplers.

The millipore filter (MP) consists of a specially prepared thin (150μ) sheet of cellulose, of uniform cell structure, submicroscopically honeycombed such that the volume of the filter is 80 per cent voids, or 5×10^7 pores/sq cm. The aerosol type filter has a theoretical pore size slightly larger than 0.5μ , although it is claimed that 0.2μ particles are retained within 50μ of the surface. Tests at USNRDL on the NRL smoke penetrometer at operational face velocities (70 cm/sec) indicated 100 per cent efficiency for 0.3μ diethylphthalate particles.

The DMT filters consisted of DMT crystals packed to a thickness of 0.7 cm between two supporting screens. The DMT filters were sublimed off at USNRDL under reduced pressure and elevated temperature, leaving the captured aerosol material on microscope slides or in centrifuge tubes, as desired. Calibration tests as described above yielded a capture efficiency of 98 to 99 per cent.

The air sampler suction units, ²⁷/designed to collect a total sample for a 6-hr period following a shot, drew 10 cfm through an effective sampling area of 64 sq cm for both the MP and DMT filters.

CHAPTER 3

CHEMICAL MEASUREMENTS

The significant properties which determine the relative thermodynamic stability of a contaminated system are: (1) the composition of the fallout material, (2) the phase distribution of the various constituents, and (3) the chemical and physical state of certain elements. Most of these properties of the fallout were found to be determined by or dependent on the location of the point of detonation. Reef shots produced largely coral-derived material; barge shots produced largely sea water derived material. The distribution of the radioactive elements and the stable or carrier material between the liquid and solid phases and further between colloidal and ionic fractions gives information on chemical and physical states of components known to be important contamination-decontamination parameters. In addition, the oxidation states of certain radioactive elements determines their chemical behavior in the fallout mixture during the period of contamination. Thus the thermodynamic environment in which radioactive species of the fallout occur influences their contamination potential to the extent of controlling it. Chemical measurements of the significant properties were made on samples collected from Shots 1,2,3, and 4.

The characterization of the fallout samples consisted of: (1) measuring the total activity of each sample with a survey meter; (2) determining the total quantities of solids and liquids in them; (3) measuring the pH of the liquid phase of those samples which had sufficient liquid; (4) determining the total beta and gamma activities in each sample; (5) fractionating representative samples into solid, colloidal, and ionic constituents and measuring the radioactive characteristics of each fraction; and (6) analyses for the major and minor constituent elements in fallout samples and in several samples of sea water and coral.

The samples received for analysis were not always representative of the actual fallout owing to the collection of rain water, sea water spray, and extraneous coral and organic material in the open collectors. Nevertheless, from the analytical data an estimate of the composition of the actual fallout has been made by subtracting the extraneous sea water and coral constituents found in the diluted samples.

3.1 DESCRIPTION OF FALLOUT SAMPLES

Upon delivery of the samples to the site laboratory, the exterior of all the sample bottles was decontaminated with dilute acid and rinsed in water after which a reading of each sample was taken with a survey meter in contact with the bottom of the cleaned bottle. On Shots 2 and 4, much of the fallout activity was retained by the funnel. In these cases, the exterior of the funnel was cleaned and the interior monitored by inverting the funnel carefully over the meter. The funnel was then rinsed with dilute acid into the bottle until it had been sufficiently decontaminated. The inside of the bottle was similarly washed and the rinsings collected in a graduated cylinder and appropriately aliquoted for counting and other treatments. Samples of both Projects 2.5a and 2.6a which were not treated at the field laboratory were packed for shipment to USNRDL after the sample bottles had been decontaminated and the survey meter reading had been observed.

The samples retained at the field laboratory were removed from the polyethylene bottles. For larger samples, the bulk of the material was transferred to weighing bottles or graduated cylinders and the remainder rinsed into the cylinders with water or dilute acid. For smaller samples, the bottle was cut and the material collected by use of a large rubber policeman or brush depending on whether the material was wet or dry. After obtaining the total weight or volume, the sample was aliquoted. Most of the samples were slurries, or mixtures of solid and liquid. These were subjected to vigorous stirring and aliquoted with pipettes, the tips of which had been removed. In numerous cases it was extremely difficult to aliquot the untreated material because of large coral particles, organic debris, and other material. A number of experiments required samples just as they had been collected. As the samples generally were small and triplicate samples from a given station were not available as had been planned, they had to be aliquoted by the best means available. In cases where the samples could be acidified the aliquoting was greatly simplified.

3.1.1 Samples from Shot 1

These samples, described in Table 3.1, were received by the field laboratory on B+5.3 days. Stations 250 were lagoon rafts and stations 251 were island positions. The latter were concrete pits at ground level which permitted considerable coral to drift into the collectors. Due to a short supply of bottles for refitting the stations for subsequent shots, collecting teams were obliged to combine all three bottles from each collector or occasionally discard two of the three fallout samples. Consequently, a comparison of the collecting efficiency of three adjacent collectors at a given station could not be determined as had been planned. For lagoon stations, samples from two bottles were rinsed into the third with sea water; samples from the island stations were combined without rinsing. This procedure resulted in uncertainties in the total quantity of fallout collected per unit area. Furthermore, since the samples collected on the lagoon were diluted with sea water their original compositions were difficult to determine.

No rain fell between shot time and sample recovery so the chemical composition of island stations was affected only by the coral sand which was blown in by the wind.

TABLE 3.1 - Samples from Shot 1

Station	Weight(a) (grams)	Total Count(a) at B+14.1 days (c/m x 10 ⁻⁷)		Description	Comments(c)
		Gamma	Beta		
1-250.04	14.85	3.02	2.25	Slurry ^(b)	3;sampler lid open
1-250.05	61.98	5.97	4.93	Slurry	3;sampler lid open
1-250.06	23.11	1.82	1.67	Slurry	3;sampler lid open
1-250.17	14.90	0.0188	0.0035	Slurry	3;sampler worked
1-250.22	2.87	0.183	0.112	Slurry	3;sampler lid open
1-250.24	37.31	2.63	1.47	Slurry	3;sampler lid open
1-250.25	3.85	0.0607	0.0275	Slurry	3;sampler worked
1-251.02	120.69	111.0	61.0	Solid and liquid	1;sampler may have worked
1-251.03	15.46	14.0	11.4	Solid and liquid	3;sampler open
1-251.04	32.54	8.59	7.34	Solid(wet)	1;sampler open
1-251.05	107.01	0.246	0.045	Solid and liquid	1;sampler open
1-251.06	1.53	3.67	0.194	Solid(wet)	3;sampler open
1-251.07	0.802	0.0090	0.0053	Solid(dry)	1;may not have opened
1-251.08	0.373	-	-	Solid(dry)	3;no information
1-251.10	1.50	0.0279	0.0113	Solid(dry)	1;sampler worked

(a) Data on single bottle basis

(b) Slurry - appearance of sea water plus slaked lime suspension

(c) Number indicates bottles combined at the time of pickup

3.1.2 Samples from Shot 2

Samples collected on Elmer at R+15 hr from very light fallout were used only for decay measurements. The samples from Project 2.5a were received at the field laboratory on R+2 days; they are described in Table 3.2. The total counts, as given, include the activity on the funnels as well as that in the bottles. In general, the funnels were more contaminated than the bottles, especially for the dry samples. The flags on the buoy mast of the floating stations collected very large amounts of fallout. On station R4, for example, the bottle read 60 mr/h, the funnel 400 mr/h, and the flag 9000 mr/h at R+2.1 days. Rain fell over scattered areas between the placement and recovery of the samplers for Shot 2.

TABLE 3.2 - Samples from Shot 2

Station	Volume (ml)	Total Count at R+5.2 days (c/m x 10 ⁻⁷)		Description	Comments
		Gamma	Beta		
2-A4	39.5	13.5	17.8	liquid	Buoy - TC(a)
2-A5	12.9	10.3	16.1	liquid	Buoy - TC
2-Q4	0	0.222	0.292	dry	Buoy - TC
2-P4	0	0.0145	0.0095	dry	Buoy - TC
2-Q4	11.0	12.5	14.7	liquid	Buoy - TC
2-R4	0	55.4	88.3	dry	Buoy - TC
2-T4	21.0	10.2	15.1	liquid	Buoy - TC
2-Y39(b)	373.0	1.90	2.16	liquid	TC
2-Y40(b)	579.0	15.8	23.5	liquid	TC

(a) Project 2.5a total collector

(b) Project 6.4 YAG

3.1.3 Samples from Shot 3

These samples were received by the field laboratory on K+3 days; they are described in Table 3.3. The samples contained large volumes of liquid as a result of heavy rainfall on both the day of the shot and the following day. The samples consisted of a suspension of light-gray material (like slaked lime) as did those from Shot 1; however, they appeared to contain a larger amount of unchanged coral sand than did those from Shot 1, especially for the samples recovered from lagoon stations. The triple collector on Coca Head operated exposing the bottles for 3 hr, but the contents of the three bottles were combined before being received. The values in the table are therefore one-third of those determined for the total sample. Values for samples from duplicate total collectors at station 250.05 show good agreement except in total volume while those for station 250.07 differ by almost a factor of two, the more radioactive sample having the lesser volume. Bottles from 250.05 read 120 and 160 mr/hr at contact at K+3 days while those from 250.07 both read 80 mr/hr. The large (and different) volumes in the 250.07 samples would account for the relative differences in the mr/hr readings and the total counts. The heavy rainfall decontaminated the funnels to essentially background.

3.1.4 Samples from Shot 4

Samples collected by Project 2.6a personnel from Project 6.4 YAG 39 and YAG 40 are described in Table 3.4. Twelve bottles and funnels were placed on each ship. On the YAG 40, six bottles were placed on the port side of the bridge and six bottles on the starboard side at U-12 days and recovered on U+4 days. On the YAG 39, all 12 bottles were placed on the No. 1 kingpost. The YAG 39 was manned during this shot. The bottles were exposed at U-1 hr and recovered at U+8 hr. In addition,

samples of washdown water were collected on the YAG 39 with a 7-in. funnel which was fitted into a hole in the deck and connected by a long piece of tygon tubing to a collecting bottle just above the recorder room where the personnel were stationed. Radioactive washdown water was collected starting at U+1.2 hr. The rate of collection was approximately 200 ml/hr. The first 50 ml measured 10 r/hr at the surface of the container; it was diluted and aliquoted for decay measurements. On U+1.6 days, the bottles on YAG 39 were received at the field laboratory. Their average reading was 69 ± 5 mr/hr; the funnels measured 24 ± 4 mr/hr. Six of the 12 bottles were sent to USNRDL.

TABLE 3.3 - Samples from Shot 3

Station	Volume (ml)	Total Count at K+7.3 days (c/m x 10 ⁻⁷)		Description	Comments
		Gamma	Beta		
3-250.05	1365	30.6	48.0	Liquid and solid	Buoy - TC(a)
3-250.05	1822	31.4	48.5	Liquid and solid	Raft - TC
3-250.07	1650	15.6	23.8	Liquid and solid	Raft - TC
3-250.07	1065	26.3	42.3	Liquid and solid	Raft - TC
3-250.08	1020	35.7	56.6	Liquid and solid	Raft - TC
3-Coca	355	53.1	82.1	Liquid and solid	TC
3-Coca	166	3.33	5.33	Liquid and solid	3C ^(b) (1 bottle)
3-251.02	1160	36.8	57.8	Liquid and solid	TC (island)

- (a) Project 2.5a total collector
(b) Project 2.6a triple bottle collector

On the YAG 40, significant differences were found in the sample collected on each side of the bridge. Considerable rain had fallen before the samples were recovered. Bottles from the port side read 24 ± 3 mr/hr on U+4 days; the funnels averaged 6 ± 1 mr/hr; and the average water volume was 376 ± 68 ml. Bottles from the starboard side read 28 ± 8 mr/hr; the funnels averaged 10 ± 3 mr/hr; and the liquid volume was 911 ± 80 ml. On that day, the average total gamma count was 4.67×10^7 c/m per bottle for port side collectors and 13.2×10^7 c/m per bottle for starboard collectors or 2.8 times as much activity for the collectors which had been directly exposed to the drifting fallout.

In addition, on U-day wipe samples were taken from an F-34 which had flown through the cloud. These read as high as 35 r/hr at about U + 6 hr. The early decay of these wipe samples was much slower than that of the fallout collected on the YAG 39. Since considerable fractionation would be possible during contamination and decontamination of the aircraft, these samples were not considered to be truly representative of the material in the cloud. Although these samples were given rather extensive treatment, only the data for iodine analysis will be reported.

TABLE 3.4 - Samples from Shot 4

Station	Volume (ml)	Total Count (c/m x 10 ⁻⁷)		Description	Comments
		Gamma	Beta		
4-Y39(a)	9.2(b)	32.4(c)	58.0	Liquid	Top of No. 1 king-post ave. of 6 bottles
4-Y40-P1	385	5.62(d)	-	Liquid	Port side of bridge
4-Y40-P2	280	4.08	-	Liquid	Port side of bridge
4-Y40-P3	340	2.89	-	Liquid	Port side of bridge
4-Y40-P4	374	4.92	-	Liquid	Port side of bridge
4-Y40-P5	393	4.26	-	Liquid	Port side of bridge
4-Y40-P6	485	6.26	-	Liquid	Port side of bridge
4-Y40-S1	987	24.5	-	Liquid	Starboard side of bridge
4-Y40-S2	937	10.9	-	Liquid	Starboard side of bridge
4-Y40-S3	1006	11.6	-	Liquid	Starboard side of bridge
4-Y40-S4	818	8.75	-	Liquid	Starboard side of bridge
4-Y40-S5	840	7.36	-	Liquid	Starboard side of bridge
4-Y40-S6	878	15.9	-	Liquid	Starboard side of bridge

- (a) Y - Project 6.4 YAG
- (b) Total volume of 7 bottles was 64.4 ml
- (c) Count at U+2.6 days
- (d) Count for YAG 40 samples at U+4 days

3.1.5 Evaluation of Samples

Since the primary purpose of the investigation was to characterize the fallout material, with the ultimate aim of obtaining information which could be used to predict its contamination-decontamination behavior, it was originally considered essential that the fallout be collected under carefully specified conditions. Requirements were that no extraneous materials be collected before the detonation or after the fallout had stopped. No loss of material could be allowed after the collection of the fallout material had been made. Ideally, the samples should have been collected and examined as soon as possible after the cessation of fallout so that, in addition to meeting the above conditions, the samples would have been analyzed before extensive physical or chemical changes could occur. However, because of a combination of such factors as failure of the automatic sampling apparatus, changes in the recovery scheme, and incomplete recovery of station arrays these conditions were not attained. The result was that some samples were diluted by rain water and others by sea water (spray and/or waves). Still others were

concentrated by evaporation. Furthermore, for three of the shots the samples were not received until 3 to 6 days after detonation and even on the fourth shot the fallout sample was not received at the site laboratory until late in the day after the detonation.

For these reasons, the characterization of the fallout itself in many respects was not achieved. However, it is doubtful whether a complete characterization of fallout material from some of the shots would have been feasible even with satisfactory collection methods. According to some eyewitness reports, it would appear that the fallout from Shot 1 (at least at distances of the order of 30 to 50 miles from ground zero) consisted of dry particles, while that from Shot 2, at the same distances appeared to consist of a fine aerosol which in itself would produce practically negligible volume in the collector bottles (some collector bottles were, in fact, dry). For Shot 4 early, invisible fallout arrived on the YAG 39.

In summary, it should be borne in mind that the results of some of the following analyses and experiments do not apply to material as it actually fell at the collection sites, but rather to the total sampled material as received at the site laboratory and which in the majority of cases underwent important changes before it could be examined. This applies especially to the physical state separations and chemical states of Np and I.

3.2 PHYSICAL STATE SEPARATIONS

This part of the investigation sought to separate the fallout material recovered as an aqueous suspension into three fractions: ionic, colloidal, and solid, and then to determine the distribution of the gamma emitting activity and also the distribution of inactive elements among the three fractions.

The solid fraction was defined as that material which was removed by centrifugation for 15 min at 2500 RPM (980 g). The ionic fraction was defined as that part of the supernatant which passed through a cellophane ultrafilter membrane of pore size 12 to 40 Å; the colloidal fraction was that part which was stopped by the membrane.

3.2.1 Physical Treatment of Samples

A 10 to 15 ml aliquot was taken from the original sample with rapid stirring. A volumetric pipette with its tip broken off to sample the suspended particles was used in this sampling. The slurry aliquot was placed directly in a weighed, graduated cone-point centrifuge tube, which was then reweighed to obtain both the weight and the volume of the sample. In addition, an aliquot of the original slurry was taken with a micropipet whenever possible for gamma counting; for samples with appreciable quantities of suspended solids the aliquot for gamma counting was taken from the acidified material used in the neptunium procedure.

The slurry sample was centrifuged for 10 min at 2500 RPM. The pH of the supernatant was measured immediately. A small aliquot of the supernatant was taken for a gamma count and a 5- or 10-ml aliquot was placed in an ultrafilter. The ultrafilter was a modification of one

used in earlier work in this laboratory.¹¹ Its medium was a cellophane dialysis membrane previously found to have a pore size of 12 to 40 Å. One thickness of cellophane at a pressure of 400 psig (under nitrogen) gave a flow rate of 3.5 to 4.0 ml/hr. After the whole supernatant aliquot had passed the filter, a gamma counting aliquot of the effluent was taken. Upon disassembly of the ultrafilter, the membrane was counted to determine the gamma activity in the colloidal fraction.

The solid fraction separated by centrifugation was transferred quantitatively to a weighed fritted glass filter using anhydrous methanol and after drying the filter was weighed again. Then the solid on the filter was dissolved with 6N-HCl and washed through. After several washings, the combined filtrates were transferred to a 100-ml volumetric flask and made up to volume. An aliquot of this dissolved solid fraction was taken from this solution for gamma counting.

Thus, for each sample five gamma counts were taken, (1) original slurry, (2) supernatant, (3) ultrafiltrate, (4) colloidal fraction, and (5) solid fraction. This procedure allowed the calculation of an activity balance for the two separation steps. The last three counts gave the breakdown of the gamma activity into ionic, colloidal, and solid fractions. These samples were also used to follow the gamma decay of the fractions for all the shots. For the fractions of the samples from Shots 1 and 2 lead absorption data were taken; for the fractions of the samples from Shots 2,3, and 4 gamma analyzer data were taken. Finally, portions of the fractions of samples from Shots 2,3, and 4 were returned to USNRDL for quantitative analysis of their major and minor constituents.

3.2.2 Results

The results of these studies are given in the following sections.

3.2.2.1 Gamma Activity Distribution Among Physical State Fractions

In general, good activity balances were obtained for the separation steps. The sum of the total gamma counts of the liquid (supernatant) and the solid fractions was 94 to 103 per cent of the total gamma count for all samples, except one, as determined by the assay of the original sample. Similarly, recoveries in the ultrafiltration step (sum of colloidal and ultrafiltered fractions) ran about 86 to 96 per cent of the total liquid activity. Totals were normalized to 100 per cent by taking account of the known sources of loss. In the solid-liquid separation the main source of loss was in the transfer of the solid to the frit and in the residue left on the frit after the acid wash. In the ultrafiltration separation the main source of loss was in adsorption on the metal surfaces of the ultrafilter below the membrane. Separate experiments showed that the extent of these losses was sufficient to account for an occasional low recovery. Tables 3.5 and 3.6 summarize the gamma activity fractionation results together with pH values and percentage of solids by weight. Table 3.5 gives the results for the individual samples while Table 3.6 gives ranges of values for all samples analyzed in each shot, and groups these results by type of shot. Some pertinent observations based on Table 3.6 are:

TABLE 3.5 - Physical State Fractionation of Gamma Activity

Sample	Time After Detonation (days)	Wt. of Solid (%)	pH	Gamma Count			Amount Ionic ^(a) in Liquid Phase (%)
				Solid (%)	Ionic (%)	Colloidal (%)	
1-251.03	6.5	9.2	11.9	96.33	3.56	0.11	97.0
1-251.02	8.1	0.94	12.3	92.08	7.72	0.20	97.5
1-250.05	8.3	0.85	9.0	98.05	1.89	0.06	97.0
2-A4	3.4	< 0.01	7.5	24.70	72.90	2.40	96.8
3-Coca TC	4.2	0.18	10.5	92.44	7.33	0.23	97.0
3-251.02	5.5	0.23	11.2	94.17	5.60	0.23	96.1
4-Y39	1.8	< 0.01	7.7	40.20	57.91	1.89	96.8

(a) Percentage of gamma count in the liquid phase found in the ionic fraction

TABLE 3.6 - Summary, Physical State Fractionation of Gamma Activity

Shot Type	Number	Number of Samples	Time After Detonation (days)	Wt. of Solid (%)	pH	Gamma Count			Amt. Ionic ^(a) in Lqd. Phase (%)
						Solid (%)	Ionic (%)	Colloidal (%)	
Island	1	3	6.5-8.3	0.85-9.2	9.0-12.3	92.1-98.1	1.9-7.7	0.06-0.2	97.0-97.5
	3	2	4.2-5.5	0.18-0.23	10.5-11.2	92.4-94.2	5.6-7.3	0.23-0.23	96.1-97.0
Barge	2	1	3.4	< 0.01	7.5	24.7	72.9	2.4	96.8
	4	1	1.8	< 0.01	7.7	40.2	57.9	1.9	96.8

(a) Percentage of gamma count in the liquid phase found in the ionic fraction

(1) Percentage of solids by weight - Island shot samples show a much higher percentage of solids than do barge shots, with Shot 1 samples having a higher percentage than Shot 3. No quantitative correlations based on per cent solids can be made because of the variable volume of water.

(2) pH - Island shot samples had the high pH characteristic of suspensions of alkaline earth hydroxides. CaO or Ca(OH)_2 was present in the fallout as a product of the pyrolyzation of CaCO_3 , from the island coral which had been drawn up into the fireball. The fallout samples from the island shots consisting of both solid and liquid usually contained enough of the hydroxide to maintain a solid-liquid equilibrium. The pH of the liquid from barge shots was fairly close to the pH of sea water itself.

(3) Gamma Activity Fractionation - Where the solids were present in large percentages (island shots), most of the gamma activity was found in the solid fraction. On the other hand, for barge shots most of the activity was in the ionic fraction.

It should be noted that for every sample treated (both island and barge shots) the liquid fraction itself was 96.1 to 97.5 per cent ionic. The constancy of this figure suggests that the material held by the filter membrane was not colloidal since the percentage of colloids in the liquid samples should depend on when the samples were treated and should also vary from sample to sample and shot to shot. It is more likely that a constant percentage of the liquid activity is adsorbed by the membrane. Whatever constituted the so-called colloidal fraction, it was never very important in the samples as analyzed, for the gamma activity in this fraction was never higher than 2.4 per cent of the total sample. The small percentage found, however, does not necessarily mean that there was originally such small amounts of gamma activity associated with a colloidal fraction in the fallout itself. Disappearance of a colloid which may have occurred originally in the fallout could be explained by: either (1) agglomeration of colloidal particles with time in the presence of rather high concentrations of electrolyte, or (2) adsorption of colloidal particles on crystalline materials or on the walls of the sample bottle. The centrifugation separation would not distinguish between particles which were large enough to settle in a centrifugal field and colloidal-sized particles which were associated with crystalline solids. A very early collection and analysis of liquid fallout material for detonations which might produce a liquid phase fallout would serve to determine whether colloidal particles are present and whether they do indeed agglomerate at appreciable rates. In terms of particle size, the colloid cannot be disregarded in estimating contamination potential of the fallout unless it can be conclusively shown that they do not exist at the time the fallout contacts a surface.

3.2.2.2 Gamma Decay of Physical State Fractions

Decay for the three fractions and the original slurry are given in Figs. 3.1 through 3.4 for some of the samples separated. To aid in the comparison of the fractions for a given sample, all counts were normalized to .1000 at the earliest possible time. Where a decay curve was

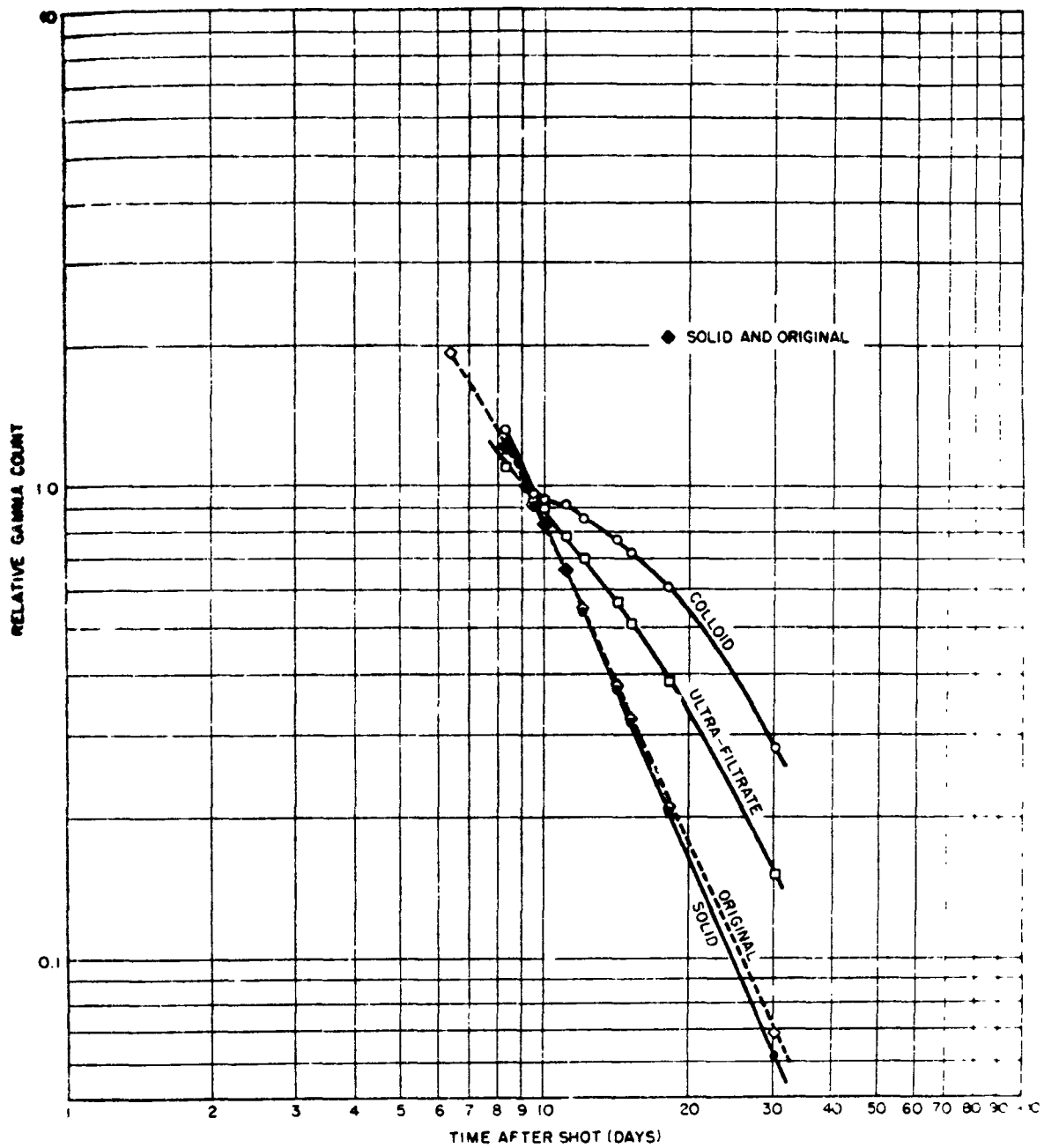


Fig. 3.1 Gamma Decay of Physical State Fractions of Sample 1-251.03

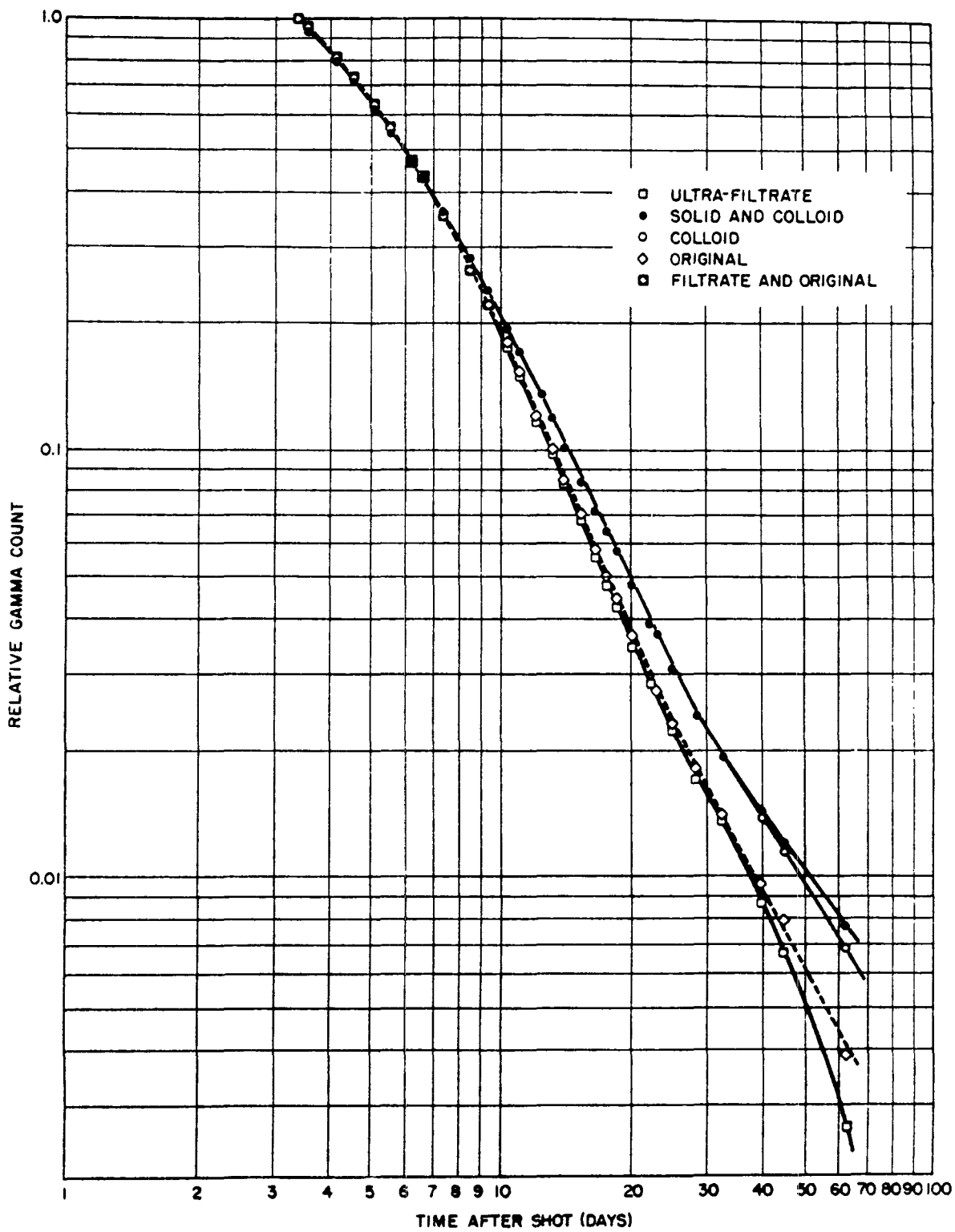


Fig. 3.2 Gamma Decay of Physical State Fractions of Sample 2-A4

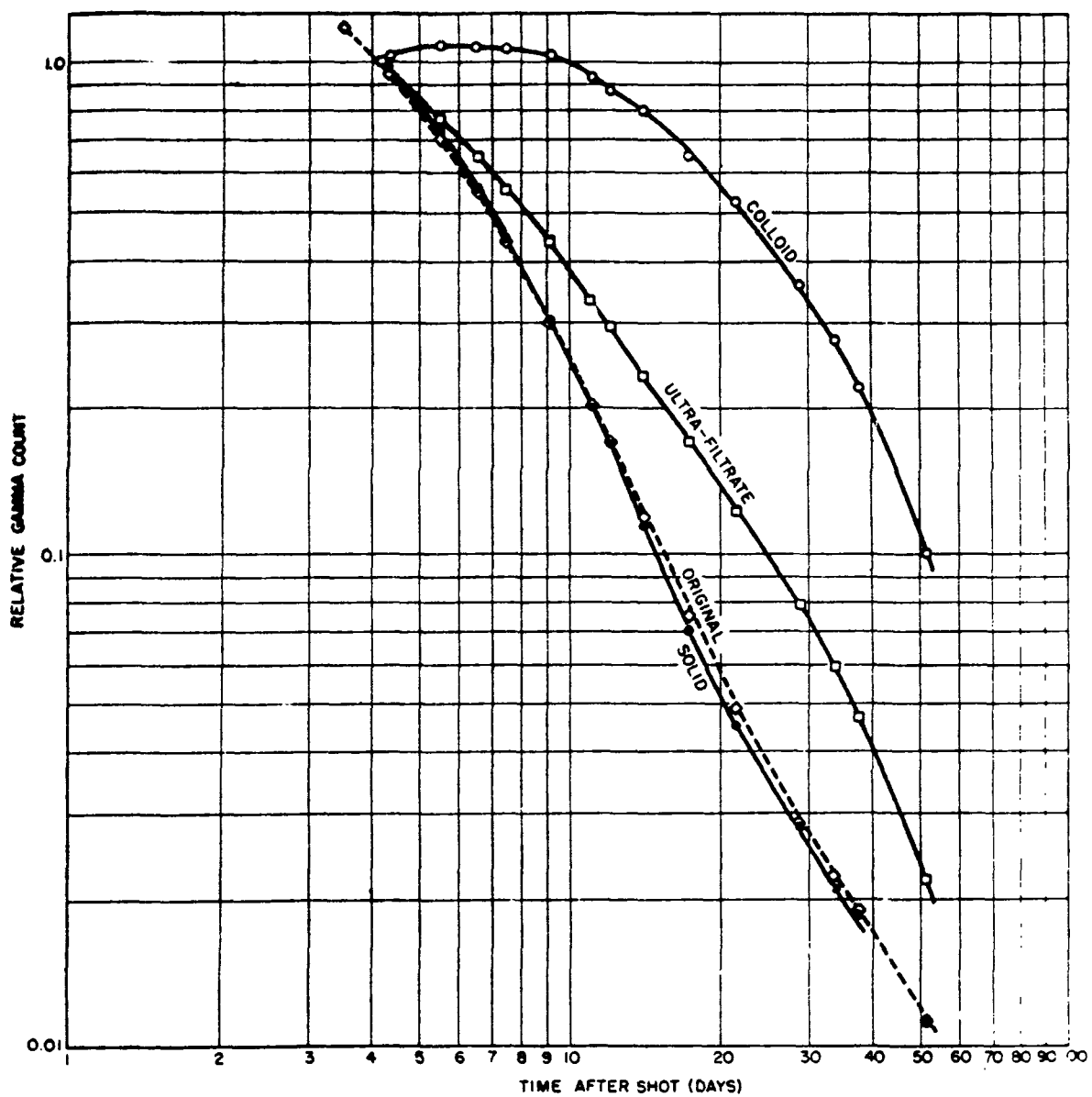


Fig. 3.3 Gamma Decay of Physical State Fractions of Sample 3-Coca TC

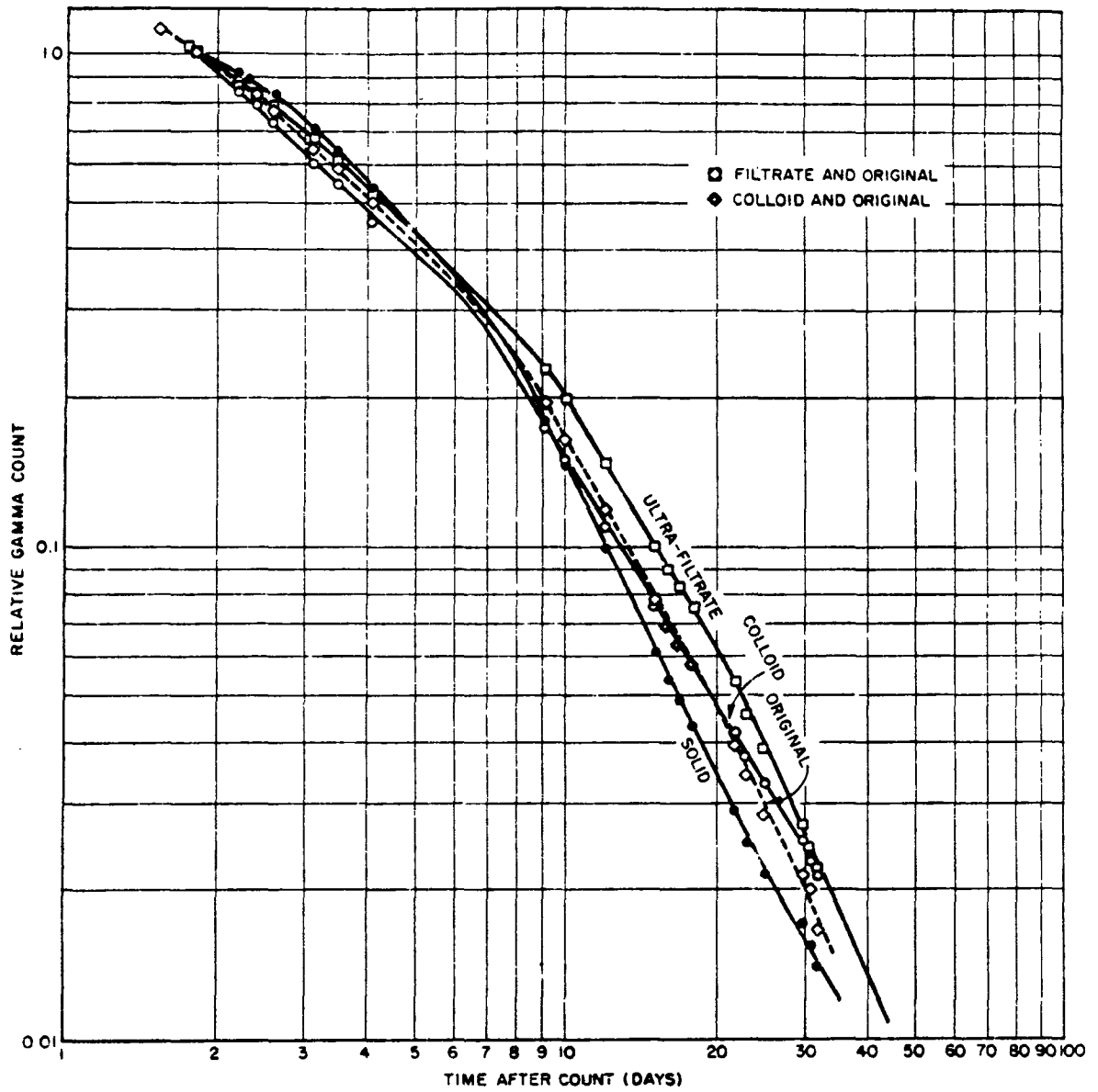


Fig. 3.4 Gamma Decay of Physical State Fractions of Sample 4-Y39

straight for an appreciable time the log-log decay slope was determined graphically. The decay slopes for all of the samples are summarized in Table 3.7. They are tabulated for three time ranges: early times are up to 4 days after detonation; medium times are 4 to 9 days; and late times are after 9 days.

In the 9 to 30-day period the solid fraction decay was generally more rapid than the original sample. The ultrafiltrate decayed more slowly than the original. The colloidal fraction usually decayed more slowly than the ultrafiltrate.

The decay curves of the various fractions diverged more for island shot samples than those for the barge shot samples. The solid fraction from island shot samples decayed at about the same rate as the original slurry, while with the barge shot samples the ultrafiltrate decayed like the original slurry. These results are logical in view of the gross distribution of the gamma activity between the liquid and solid phases for the two types of shot.

3.2.2.3 Gamma Energy Distribution of Physical State Fractions

Lead absorption curves were taken on samples for Shots 1 and 2. The curve for the 2-A4 sample on Shot 2 was taken at two times. Some of the curves are shown in Figs. 3.5 through 3.7. All fractions were normalized to a count of .1000 at zero thickness of lead absorber for better comparison. The absorption curve of each fraction was analyzed into three component energies and the percentage of each component was determined by weighting the "zero-absorber" count rate of each component energy by the relative photon efficiency as taken from Fig. 2.1. The results are tabulated in Table 3.8. It may be noted that the average gamma energy of the "colloidal" fraction was consistently higher for both surface island and surface water shot samples, whereas the solid and ionic fractions show large differences in relative amount of each component and average energy. This again lends support to the argument that selective absorption occurred on the ultrafiltrate. The low energy components range from 145 to 180 kev, the medium from 320 to 485 kev, and the high from 1020 to 1620 kev.

The fractions of the three "apparent" gamma energies from the solid fraction of Shot 1 sample (1-251.03) were similar to those for the original sample. In addition, the ultrafiltrate (ionic) fraction had a higher percentage of the highest energy gammas than did the solid fraction, while the colloidal fraction had a still higher percentage of high energy gammas. The order of average energy was colloidal > ionic > solid. The 1-251.02 sample fractions were somewhat different; both the decay and the lead absorption show very little fractionation of gamma emitting isotopes between the solid and the ionic fractions. However, the comparison of average energies among the physical state fractions of any sample is not as reliable an indicator of fractionation as is the comparison of the percentage of the high energy component among the fractions. The latter depends upon the observed count at high absorber thicknesses while the former depends upon slopes extrapolated from 2 or 3 points.

For the Shot 2 sample (2-A4) absorption curve of the solid

TABLE 3.7 - Summary of Log-Log Decay Slopes

Sample(a)		Times					
		Early		Medium		Later	
		Slope	Days	Slope	Days	Slope	Days
1-251.03	F	-	-	-	-	-1.32	9.-15.
	S	-	-	-	-	-2.33	9.-30.
	C	-	-	-	-	curved	
	O	-	-	-1.79	6.-9.	-2.25	9.-30.
1-251.02	F	-	-	-	-	-1.83	9.-13.
	S	-	-	-	-	-2.27	13.-25.
	C	-	-	-	-	-2.23	9.-30.
	O	-	-	-	-	-0.76	9.-15.
1-250.05	F	-	-	-	-	-2.23	9.-30.
	S	-	-	-	-	-1.05	9.-14.5
	C	-	-	-	-	-1.49	14.5-30.
	O	-	-	-	-	-2.34	9.-30.
2-A4	F	-	-	-	-	-1.94	9.-17.
	S	-	-	-	-	-2.21	9.-30.
	C	-	-	-1.06	3.8-4.6	-2.44	9.7-20.
	O	-	-	-1.07	3.8-4.6	-2.10	10.-25.
3-Coca TC	F	-	-	-	-	-2.10	10.-25.
	S	-	-	-	-	-2.10	10.-25.
	C	-	-	-	-	-1.94	9.-17.
	O	-	-	-	-	-2.21	9.-30.
3-251.02	F	-	-	0.97	4.2-7.0	-1.50	9.-30.
	S	-	-	curved		-2.27	9.-22.
	C	-	-	curved		curved	
	O	-	-	-1.34	4.2-6.6	-2.12	9.-22.
4-Y39	F	-	-	-1.71	5.5-9.	-2.23	9.-35.
	S	-	-	curved		-2.23	9.-22.
	C	-	-	curved		-1.15	10.-22.
	O	-	-	curved		-2.23	9.-22.
4-Y39	F	-0.70	1.7-2.9	-	-	-1.70	9.-22.
	S	-0.52	1.8-2.6	-	-	-2.11	9.-25.
	C	-0.93	1.8-4.0	-	-	-1.65	9.-32.
	O	-0.70	1.7-2.5	-	-	-1.82	9.-32.
		-0.94	2.4-4.1	-	-		

(a) State of sample indicated by following symbols:
 F = ultrafiltrate; S = solid; C = colloid; O = original sample

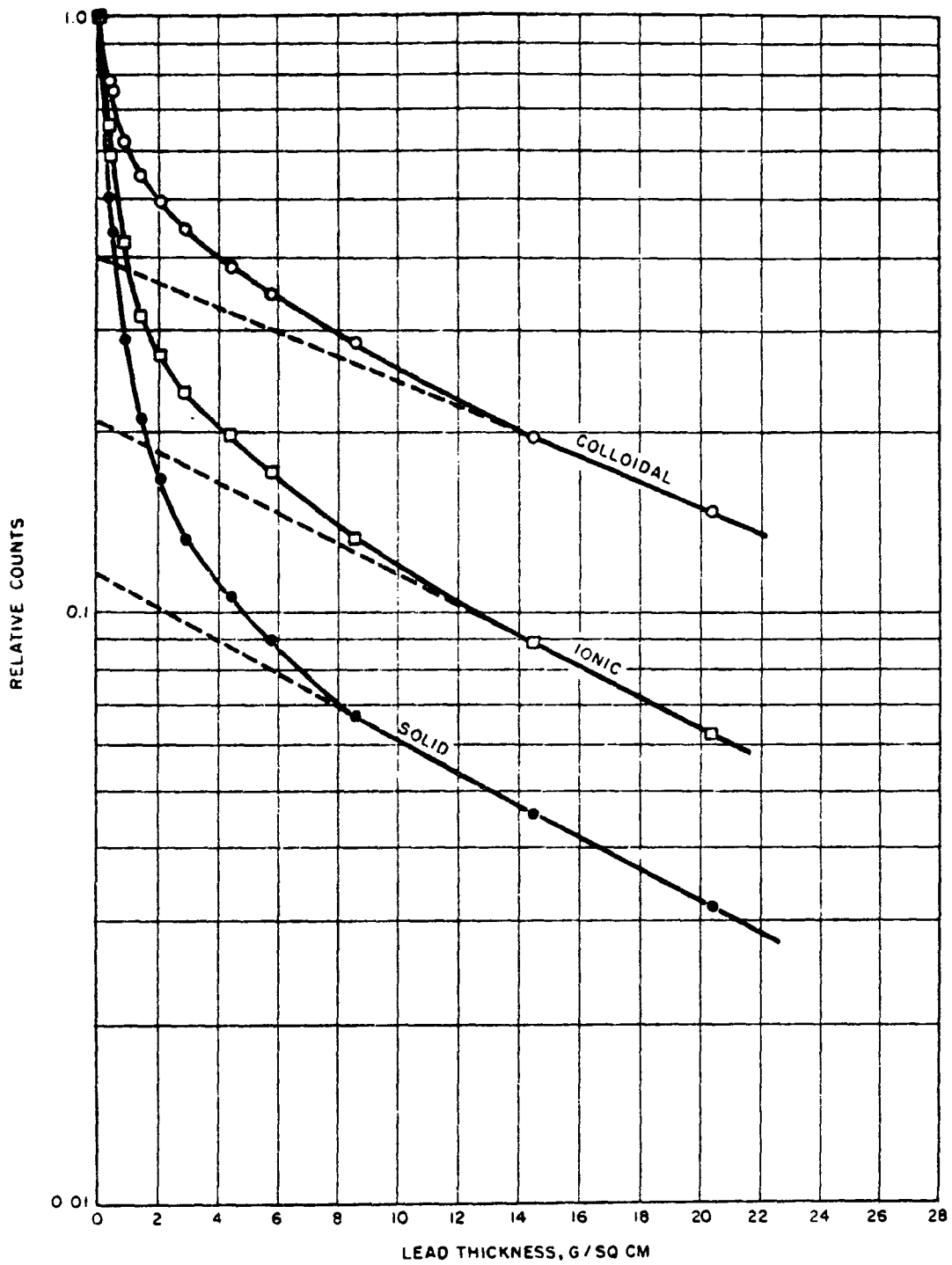


Fig. 3.5 Lead Absorption Curves at 8.3 days for Sample 251.03, Shot 1

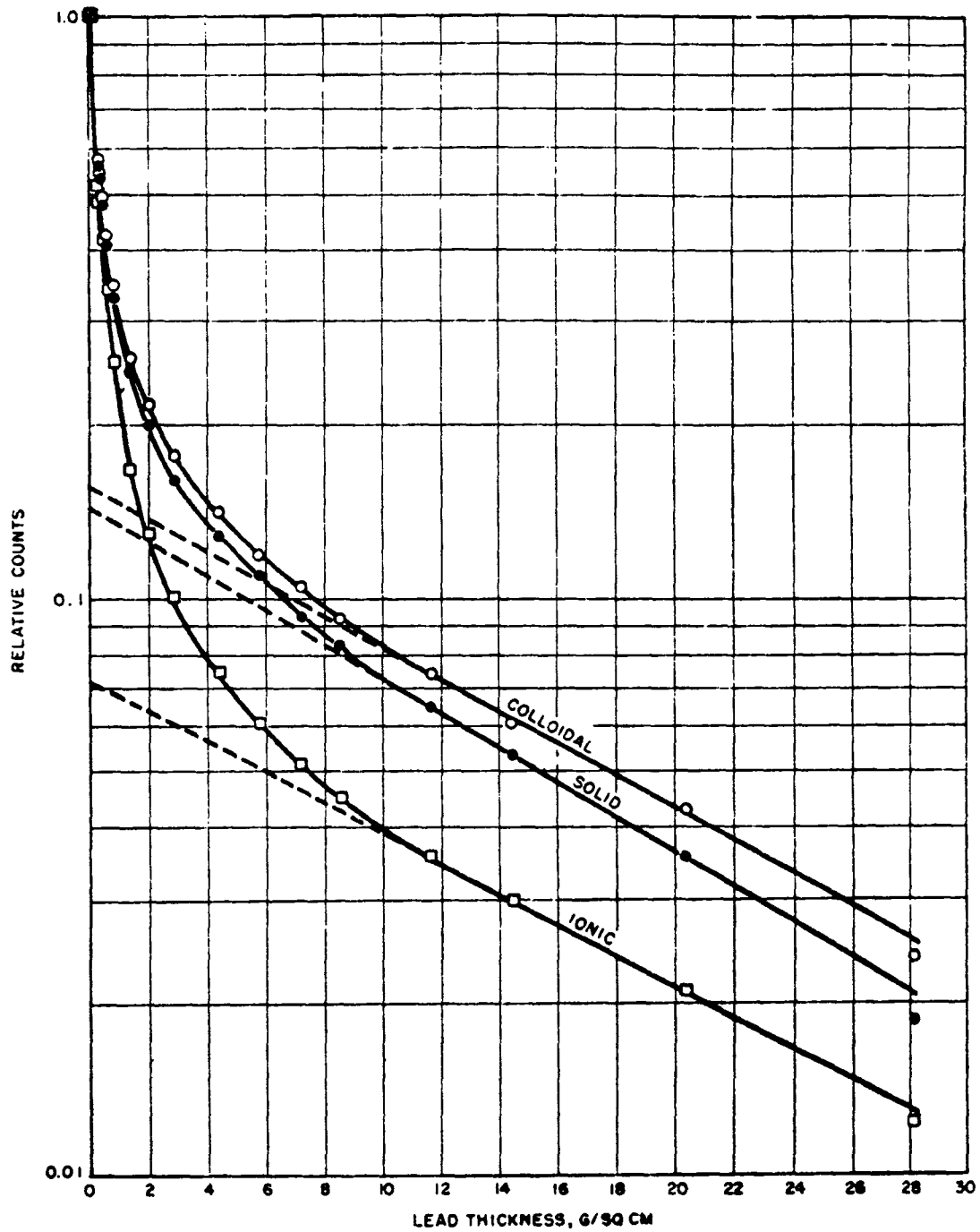


Fig. 3.6 Lead Absorption Curves at 3.6 days
for Sample 2-A4, Shot 2

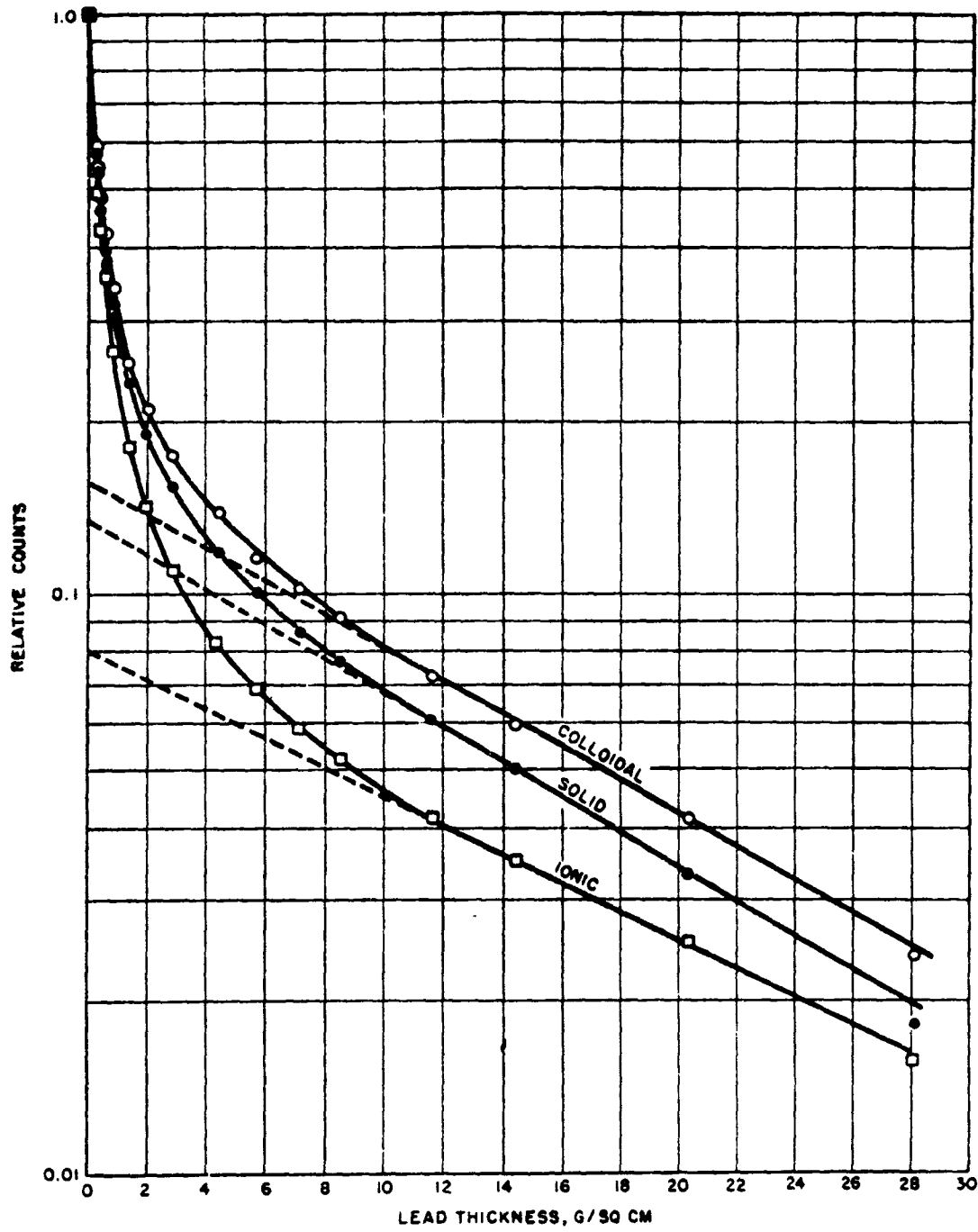


Fig. 3.7 Lead Absorption Curves at 5.3 days for Sample 2-A4, Shot 2

TABLE 3.8 - Gamma Energy Distribution of Physical State Fractions Determined by Lead Absorption

Sample(b)	Time (days)	Half-thickness (gm of Pb/sq cm)	Fraction of Total Count			Average Energy (kev)
			Energy (kev)	(Uncorrected) (%)	(Corrected) ^(a) (%)	
1-251.03 S	8.3	0.27	150.	71.7	50.1	466.
		1.42	340.	16.8	21.5	
		11.0	1120.	11.5	28.4	
1-251.03 F	8.3	0.27	150.	60.8	36.3	669.
		1.85	380.	18.5	19.35	
		11.7	1220.	20.7	44.35	
1-251.03 C	8.3	0.38	180.	41.2	18.25	1153.
		2.90	480.	18.8	17.95	
		14.1	1620.	40.0	63.8	
1-251.02 S	9.1	0.25	145.	69.9	47.0	527.
		1.52	350.	17.3	21.9	
		11.8	1230.	12.8	31.1	
1-251.02 F	9.1	0.30	160.	73.4	50.25	508.
		1.73	375.	13.0	17.35	
		11.0	1120.	13.6	32.4	
1-251.02 C	9.1	0.38	180.	44.7	21.8	880.
		2.04	400.	20.5	19.6	
		12.3	1300.	34.8	58.6	
1-250.05 S	9.2	0.27	150.	73.2	53.7	429.
		1.32	325.	18.0	23.2	
		11.5	1180.	8.8	23.1	

(a) Corrected for counter efficiency as function of energy

(b) State of sample indicated by following symbols:

S = solid; F = ultrafiltrate (ionic); C = colloid

TABLE 3.8 - Gamma Energy Distribution of Physical State Fractions Determined by Lead Absorption (Contd.)

Sample ^(b)	Time (days)	Half-thickness (gm of Pb/sq cm)	Fraction of Total Count			Average Energy (kev)
			Energy (kev)	(Uncorrected) (%)	(Corrected) ^(a) (%)	
1-250.05 F	9.2	0.34	170.	70.6	46.1	573.
		2.96	485.	15.4	22.15	
		11.7	1220.	14.0	31.75	
1-250.05 C	9.2	0.32	163.	48.5	26.1	723.
		1.27	320.	24.2	22.3	
		11.5	1180.	27.3	51.6	
2-A4 S	3.6	0.27	150.	66.2	44.0	478.
		1.40	340.	19.4	23.5	
		10.1	1020.	14.4	32.5	
2-A4 F	3.6	0.27	150.	75.9	57.25	390.
		1.40	340.	16.9	23.3	
		11.3	1160.	7.25	19.45	
2-A4 C	3.6	0.27	150.	63.4	40.5	529.
		1.40	340.	21.0	24.5	
		10.8	1100.	15.6	35.0	
2-A4 S	5.3	0.25	145.	68.0	46.0	463.
		1.40	340.	18.7	23.2	
		10.2	1030.	13.3	30.8	
2-A4 F	5.3	0.25	145.	73.3	53.6	433.
		1.40	340.	18.7	25.15	
		12.1	1270.	8.0	21.25	
2-A4 C	5.3	0.25	145.	65.7	42.5	514.5
		1.40	340.	18.7	22.25	
		10.6	1070.	15.6	35.25	

47

fraction was higher than that of the ionic fraction so that the average energy for the solid fraction was higher than for the Shot 1 samples. The absorption curve of the colloidal fraction was again the highest of the three resulting in a highest average energy for the colloidal fractions.

Gamma spectra were taken of samples for Shots 2,3, and 4, but because of low resolution and other limitations, it was not possible to use the gamma-spectra to obtain important information about the constituents of the physical state fractions.

In general, the spectra only support what was already obvious, such as the fact that Np^{239} , which was the most important single contributor to the activity in the time range 2 to 10 days, became less important at later times.

Figure 3.8 is a gamma analyzer plot for pure neptunium separated from the fallout sample 3-251.02. It was taken 7 days after detonation. In the range 0 to 0.7 Mev, it shows the reported Np^{239} peaks at 0.065, 0.105, 0.230, and 0.295 Mev.

Figures 3.9 through 3.11 are gamma analyzer spectra (low energy region) for the physical state fraction of the same sample at the same time. The solid fraction spectrum, which contained 94 per cent of the activity was a fair reproduction of the neptunium spectrum with an additional peak at 0.51 Mev due to an unknown constituent. The ultrafiltrate fraction, however, did not reproduce the neptunium spectrum; the spectrum had peaks at 0.14, 0.39, and 0.49 Mev. The peaks at about 0.5 Mev are undoubtedly due largely to annihilation gammas, indicating the presence of gamma radiation with energies greater than 1 Mev. The colloidal fraction spectrum appeared to contain portions of the neptunium spectrum, as well as peaks found in the other fractions. Spectra of fractions taken at other times show other peaks, but it was not possible to identify these in the absence of other information about important species present.

3.2.2.4 Quantitative Analysis of Physical State Fractions

The concentration analysis of the solid and ionic fractions (as separated in the field) is given in Table 3.9. Aliquots of the solid and the ionic fractions of samples 2-A4, 3-Coca TC, 3-251.02 and 4-Y39 were returned to the laboratory as liquids (the solid fraction had been dissolved in HCl and made up to 100 ml). The concentrations are given in micrograms per milliliter (ppm). The colloidal fraction was not returned for analysis because it was used in its entirety as a counting sample and because of the difficulty of recovering the small quantities from the ultrafilter membrane. There were no visible deposits on the membrane.

Table 3.10 gives the mass in milligrams of each element in the liquid and solid fractions of the total sample recovered in the field. It also gives the total mass of each element in the total original sample as well as the percentage distribution of each element between the liquid and the solid fractions. For sample 2-A4, the liquid fraction data are taken as the average of the supernatant and ultrafilter data. For the other samples the ultrafiltrate represents the liquid; supernatant was not returned for analysis.

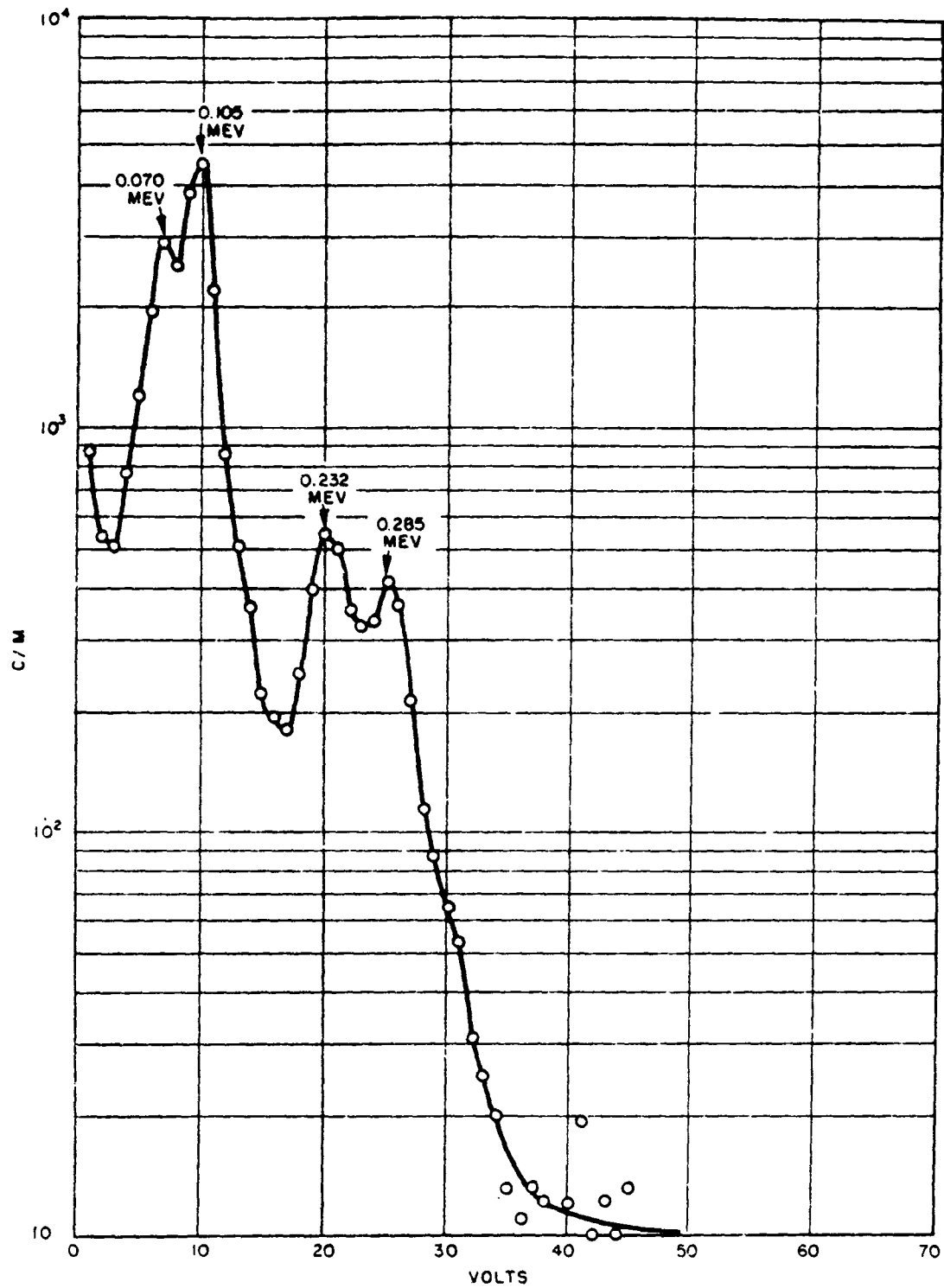


Fig. 3.8 Gamma Spectra of NpV-VI,
Sample 3-251.02 at + 7 days

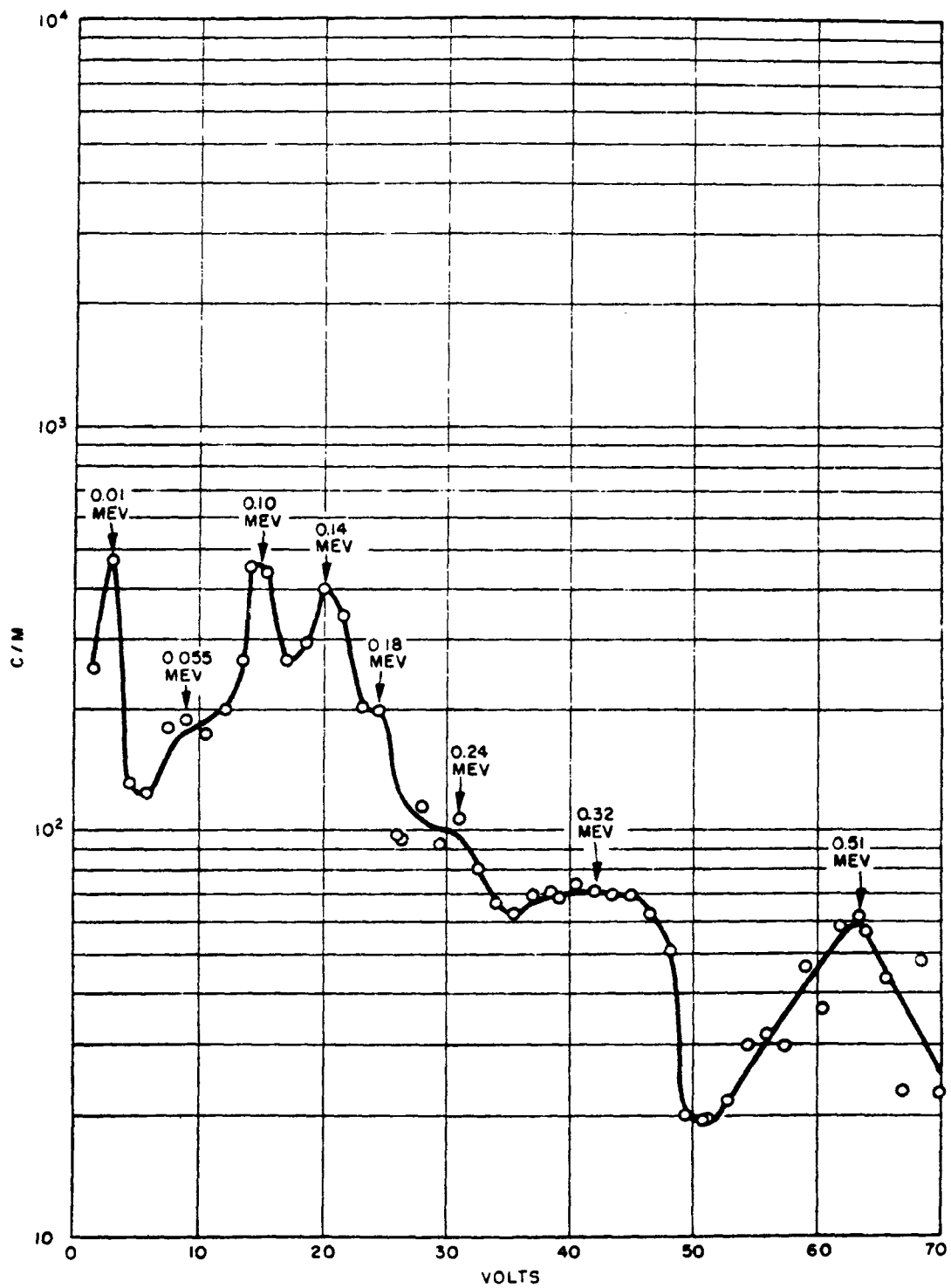


Fig. 3.9 Gamma Spectra of Solid,
Sample 3-251.02 at + 7 days

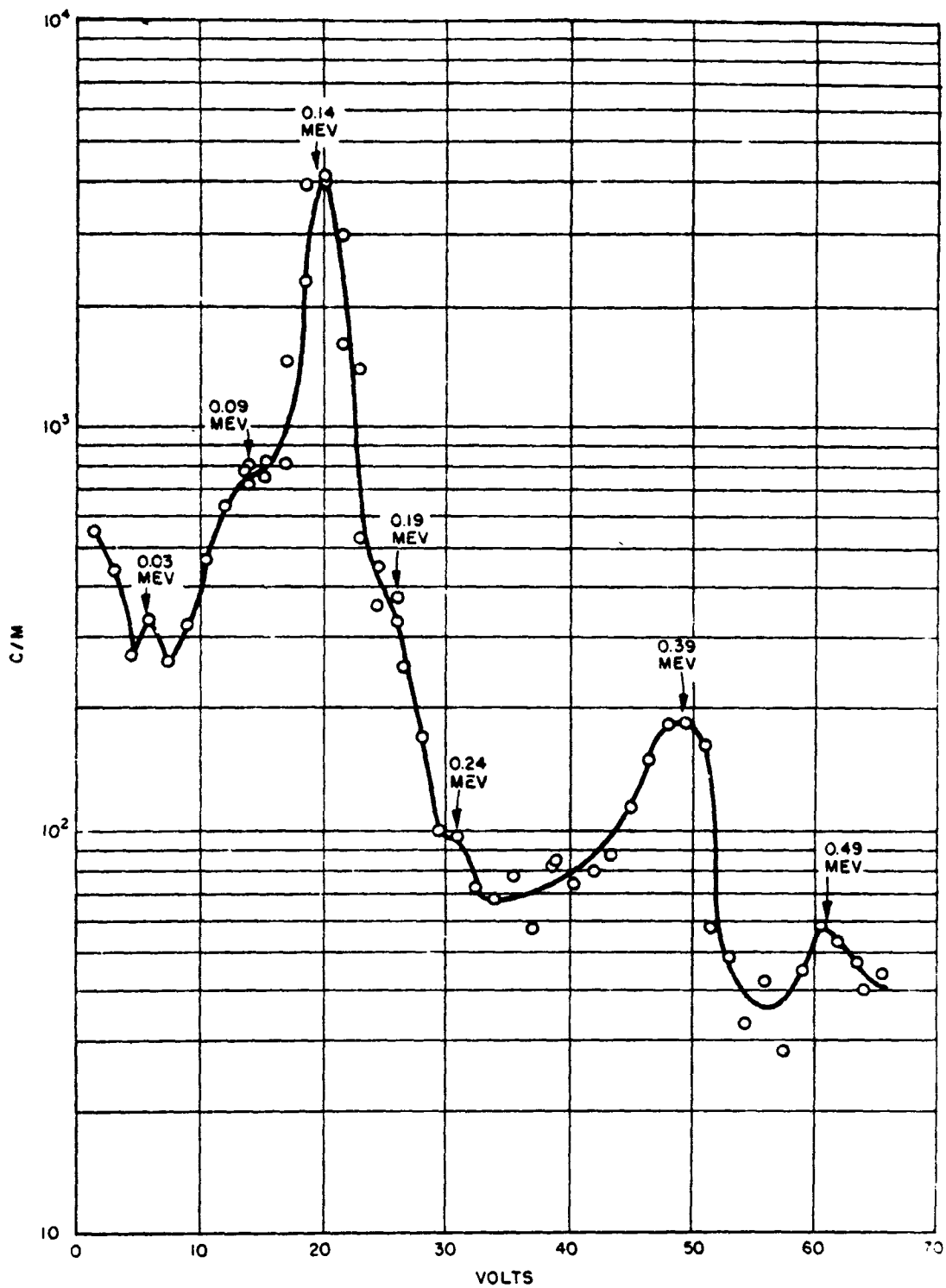


Fig. 3.10 Gamma Spectra of Ultrafiltrate,
Sample 3-251.02 at + 7 days

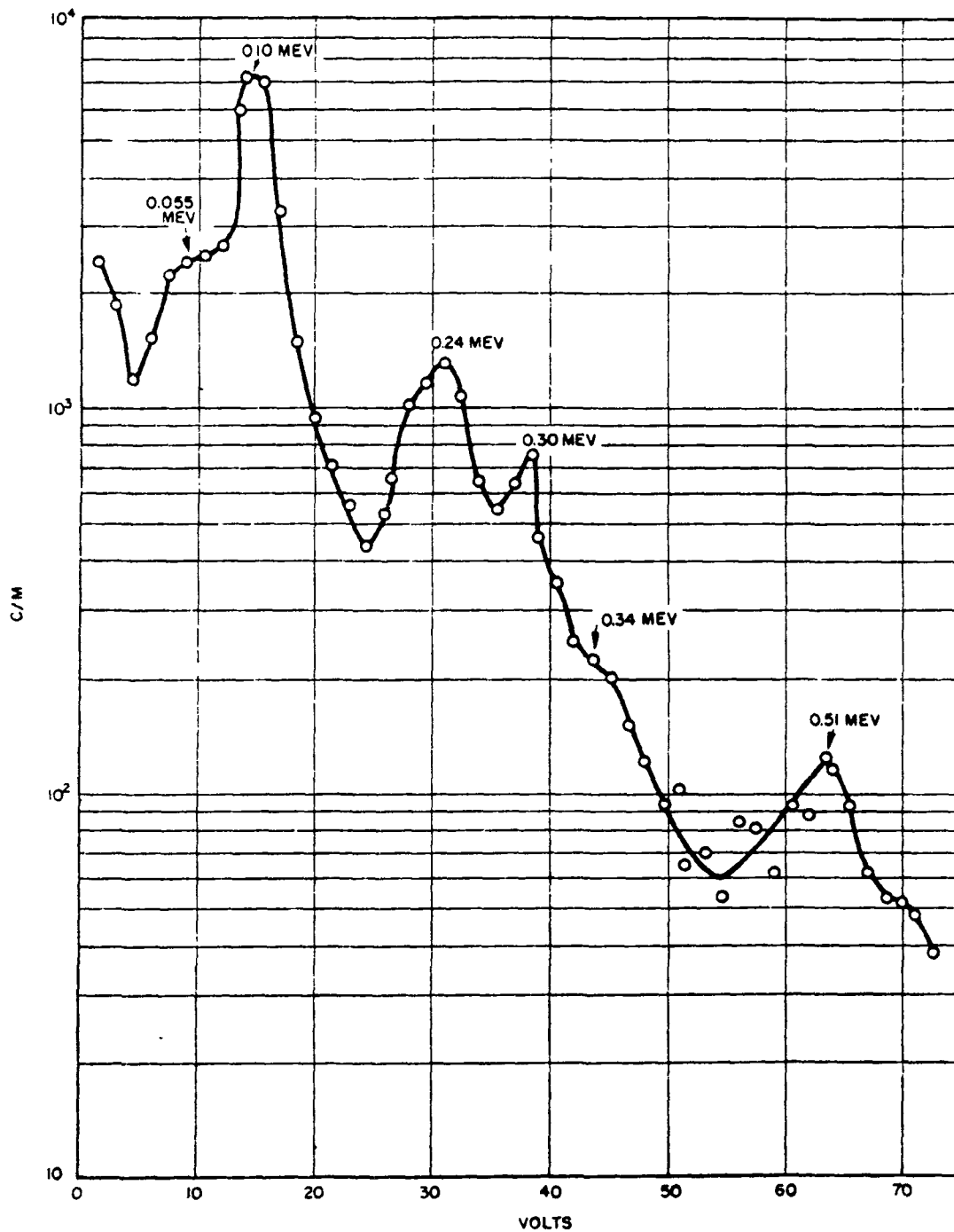


Fig. 3.11 Gamma Spectra of Colloid Fraction,
Sample 3-251.02 at + 7 days

TABLE 3.9 - Concentration of Elements of Interest in Solutions of Physical State Fractions

Sample	Vol. of Sample separated in field, (ml)	Vol. of Sample as analysed, (ml)	Concentration ($\mu\text{g/ml}$)								
			Cl(a)	Na	K	Mg	Ca	Fe	Al	Cu	Si
2-A4 Supernate Ultrafiltrate Solid	19.3	8.2	1,595.	840.	37.0	104.	58.6	0.78	<0.40	<0.40	0.97
		3.5	355.	574.	39.6	151.	105.	<0.4	<0.8	<7.6	<2.0
		100.4	-	1.5	1.8	0.0	7.6	2.74	0.40	0.22	0.03
3-Coca TC Ultrafiltrate Solid	12.1	2.7	1,170.	227.	11.5	28.0	428.	<0.3	<0.67	<0.43	<0.40
		99.0	-	0.8	0.0	4.8	79.	1.50	0.30	<0.08	0.02
3-251.02 Ultrafiltrate Solid	27.0	7.4	35.5	37.3	1.7	0.0	15.8	0.67	0.02	<0.38	1.10
		98.4	-	1.6	0.0	15.2	158.	1.09	0.30	<0.08	0.05
4-Y39 Ultrafiltrate Solid	15.0	4.0	25,100.	12,680.	496.	1,870.	574.	<0.05	1.15	<0.76	1.84
		99.0	-	0.0	0.0	0.0	4.8	0.55	0.02	<0.08	0.03

(a) Chloride concentrations given originally as normality; for <400 $\mu\text{g/ml}$, only 1 significant figure
 400 - 4000 $\mu\text{g/ml}$ 2 significant figures
 >4000 $\mu\text{g/ml}$ 3 significant figures

Table 3.10 - Mass Distribution of Elements of Interest in Liquid and Solid Fractions

Sample		Cl		Na		K		Mg		Ca	
		mg	%	mg	%	mg	%	mg	%	mg	%
2-A4 (39.5 ml)	Liquid	63.0	100	28.0	98.9	1.49	80.1	5.04	100.	3.23	67.6
	Solid	-	-	0.31	1.1	0.37	19.9	0.00	0.	1.55	32.4
	Total	63.0		28.3		1.86		5.04		4.78	
3-Coca TC (355. ml)	Liquid	419.	100	81.1	97.1	4.10	100.	10.0	41.4	153.0	39.7
	Solid	-	-	2.4	2.9	0.00	0.	14.2	58.6	233.0	60.3
	Total	419.		83.5		4.10		24.2		386.0	
3-251.02 (1160 ml)	Liquid	43.	100	43.4	86.3	1.97	100.	0.00	0.	18.3	2.6
	Solid	-	-	6.9	13.7	0.00	0.	64.0	100.	679.	97.4
	Total	43.		50.3		1.97		64.0		697.	
4-Y39 (64.4 ml)	Liquid	1,615.	100	815.	100.	31.9	100.	120.0	100.	36.9	94.6
	Solid	-	-	0.00	0.	0.00	0.	0.00	0.	2.06	5.4
	Total	1,615		815.		31.9		120.0		39.0	

TABLE 3.10 - Mass Distribution of Elements of Interest in Liquid and Solid Fractions (Continued)

Sample		Fe		Al		Cu		Si	
		mg	%	mg	%	mg	%	mg	%
2-A4 (39.5 ml)	Liquid	< 0.047	< 8.	< 0.047	< 36.	< 0.016	< 26.	0.038	86.
	Solid	0.560	> 92.	0.082	> 64.	0.045	> 74	0.006	14.
	Total	0.560		0.082		0.045		0.044	
3-Coca TC (355. ml)	Liquid	< 0.11	< 2.	< 0.24	< 21.	< 0.15	-	< 0.14	< 70.
	Solid	4.40	> 98.	0.88	> 79.	< 0.24	-	0.06	> 30.
	Total	4.40		0.88		< 0.39		0.06	
3-251.02 (1160. ml)	Liquid	0.776	14.4	0.0232	1.8	< 0.44	-	1.16	84.0
	Solid	4.60	85.6	1.3	98.2	< 0.34	-	0.22	16.0
	Total	5.38		1.32		< 0.78		1.38	
4-Y39 (64.4 ml)	Liquid	< 0.003	< 1.	0.0741	89.3	< 0.049	-	0.119	90.2
	Solid	0.236	> 99.	0.0086	10.7	< 0.034	-	0.013	9.8
	Total	0.236		0.083		< 0.083		0.0132	

Since the concentrations for many of the elements were extremely low and the volumes of the ultrafiltrate were small, some of the analyses had to be made near or below their lower limit of reliability. Thus, the results for iron, aluminum, and copper, which are the important detonation products, are very much in doubt. However, some conclusions can be drawn. Sodium and potassium, as expected, are predominantly in the liquid fraction. Magnesium and calcium, derived from both sea water and coral, are predominantly in the liquid fraction in the barge shot samples and predominantly in the solid fraction in the island shot samples. Calcium hydroxide being more insoluble than magnesium as well as constituting a larger percentage of coral had a greater tendency to be in the solid fraction than does magnesium.

More than 85 per cent of the iron was always found in the solid fraction. Aluminum also was found predominantly in the solid fraction; however, lower total concentrations of aluminum and lower pH tend to reverse this behavior.

3.3 CHEMICAL STATE OF NEPTUNIUM AND IODINE

Experiments were carried out to determine the oxidation states of Np and I in the fallout material. These two elements contribute significantly to the gamma radiation of the fallout from nuclear detonations, and accordingly, their contamination-decontamination behavior is important. Furthermore, the decontamination of these two elements depends on their oxidation states since the sorption and solubility and chemical reactivity of each are dependent on it. Knowledge of the chemical behavior of a few of the important radionuclides in the fallout together with that of some of the stable elements could lead to a realistic and practical approach to the preparation of synthetic contaminants.

3.3.1 Oxidation State of Neptunium

The oxidation state of Np in fallout samples was determined for Shots 1 through 4. In order to carry out the determination, a fairly large amount of activity was required (sample reading of 20 to 30 mr/hr at surface of container).

3.3.1.1 Chemical Treatment of Samples

The procedure for separating Np(IV) from Np(V) and Np(VI) was based on the extraction of Np(IV) into a 0.4 M TTA solution in benzene from a 2N-HCl aqueous phase. The Np(IV) back-extracts into an aqueous phase of 8N-HCl. The chemical procedure is given in Appendix A.

3.3.1.2 Neptunium Results

The experimental results for Shots 1,2,3, and 4 are tabulated in Table 3.11.

Two Shot 1 samples not listed in Table 3.11 were processed but the results were not considered satisfactory for the reasons given below.

Shot 1 sample 251.02 (land station) was the first processed. As a result of the observations from that experiment, significant improvements were made in the procedure. Therefore, the results of that run, which gave 10 per cent Np(IV) and 90 per cent Np(V-VI), were not considered significant. On sample 251.04, Shot 1, an attempt was made to shorten the neptunium procedure considerably by eliminating some of the purification steps. However, decay curves of the product indicated impure neptunium which invalidated the results.

TABLE 3.11 - Summary of Analysis of Neptunium Oxidation States

Shot	Station	Np(IV) (%)	Np(V-VI) (%)	Sample Source
1	1-250.05	58	42	Lagoon station
2	2-T4	44	56	Free floating buoy
3	3-Coca TC	66	34	Center of lagoon
3	3-251.02	80	20	Island station
4	4-Y39	77	23	YAG-39
	Average	65 ± 11	35 ± 11	

The decay of the various neptunium fractions for all samples was followed for at least three half-lives. In every case, except those specified above, the neptunium showed no indication of any impurities. Decay was followed with a gamma scintillation counter. Gamma ray spectrometer data were also used to help identify the Np samples.

3.3.2 Chemical State of Iodine

The chemical state of iodine in the fallout samples was determined for Shots 1 through 4. The procedures and results are given in the following sections.

3.3.2.1 Chemical Treatment of Samples

Several procedures were used to investigate the oxidation and phase state of iodine in the fallout material. In the first procedure, BaCl₂ was added to the original sample to precipitate the sea water sulfate and any iodate present as BaIO₃. The sample was centrifuged to separate the solid and liquid phases. Iodide and iodate carriers were added to the supernatant and precipitate, respectively, and the iodine oxidized and reduced with NaNO₂ and Na₂SO₃ alternately while in contact with a CCl₄ phase to extract the iodine as I₂. This procedure actually gave the amount of iodine in the liquid and solid phases when the two were initially present (as was the case in the samples as received for Shots 1 and 3).

In another procedure, the sample was dissolved in a minimum amount of HCl, divided into two aliquots. Iodide carrier was added to

one fraction and iodate carrier to the other. The iodide carrier was oxidized with NaNO_2 in contact with a CCl_4 phase to extract iodine as I_2 . The iodate carrier was reduced carefully with an equivalent amount of Na_2SO_3 in contact with a CCl_4 phase; after separating the phases, more iodate carrier and then Na_2SO_3 were added to the aqueous phase; both fractions were then oxidized with NaNO_2 in contact with a CCl_4 phase. The iodine was back-extracted from the three CCl_4 solutions into the aqueous phase with Na_2SO_3 . Comparison of the iodine activity in the three fractions was used as an indication of the oxidation state of iodine.

A third procedure incorporated the use of ion exchange resins. For this procedure the original sample was placed on a cation resin column at a pH of 5 to 6. Iodine along with other anions and uncharged particles was washed out with de-ionized water. The wash-through was analyzed for iodine. Procedures for the separation of iodide and iodate on an anion resin column resulted in a good elution of iodide from Dowex 1 resin with 3N-HCl. A number of reagents were tried for an elution of iodate but no satisfactory reagent was found at that time; iodate was not removed by 50 column volumes of 3N-HCl.

3.3.2.2 Results

The results for the analysis of iodine are summarized in Table 3.12. The values showing the distribution of total iodine activity in the solid and liquid phase are accurate to within a few per cent. The growth in and decay of the different isotopes of iodine complicate the procedures and the interpretation of the data. The procedures were not as sensitive nor as satisfactory as those for neptunium to show the presence of the several oxidation states. Furthermore, the oxidation state of iodine in the original fallout probably changed before the samples were recovered. The presence of organic bodies, the susceptibility of iodine to air oxidation, possibilities of self-oxidation reduction, and exchange with sea water carrier would contribute to the formation of the resultant oxidation state of iodine in the samples at the time of analysis.

The gamma spectra of the iodine fractions for Shots 2,3, and 4 showed the presence of I^{131} , I^{132} , and I^{133} . The decay of the early sample on Shot 4 indicated a large amount of I^{132} while the gamma spectra showed also the presence of I^{131} and I^{133} .

3.4 COMPOSITION OF THE FALLOUT MATERIAL

The samples analyzed quantitatively consisted of materials collected from the environment of the shot points prior to detonation and the fallout samples. Three coral samples each from sites Charlie and Tare, two surface lagoon sea water samples, one bottom lagoon sea water sample, and one bottom lagoon coral sample were analyzed. Within the limits of variation of the major elements in these samples their chemical analysis was used to determine the amount of environmental or background constituents in the fallout samples. Then, if it is assumed that no great variation in the constituent elements occurred due to fractionation

subsequent to a detonation, the fallout material can be considered as being composed of one or more of the following three components: (1) coral, (2) sea water, and (3) device products (DP). By proper choice of elements, the chemical changes of the constituent compounds of the background components need not be considered. The radioactive device products are treated in other sections.

TABLE 3.12 - Summary of Results for State of Iodine

Shot	Station	Time After Shot	Percentage of Iodine in Solid Phase	Percentage of Total Gamma Count	Apparent Oxidation State
1	250.05, 250.06, 251.02	+ 6 to 7 days	50-80	ca 5	-1
2	2-A6	+ 2.5 to + 3.5 days	ca 0	ca 6	-1
3	Coca Head	+ 3 days	93	5	-1
4	airplane wipe	+ 16 hr	ca 0	0.7	-1

3.4.1 Physical Treatment of Samples

The activity of each sample was first measured with a laboratory survey meter. The liquid fraction, if any, was then separated from the solid phase by filtration through a weighed sintered glass frit. The activity of each phase was again measured. The volume and pH of each liquid fraction was then measured and the weight of solid was determined.

In general, the samples treated were portions from the fallout collectors aliquoted at the site laboratory.

3.4.2 Chemical Treatment of Samples

The liquid samples were processed without chemical pre-treatment whenever possible. The solid fractions were dissolved in nitric acid which usually dissolved most of the material. Remaining organic residues were oxidized by the wet ashing method using perchloric acid as the oxidizing agent. Two such perchloric acid treatments usually gave a clear colorless solution. Chemical analysis of the solid fractions was done whenever the total solids were greater than 5 mg.

In general, the chemical treatments of the samples were restricted to a minimum of reagents to prevent as far as possible the addition of elements as impurities which were being determined.

The analytical methods for the various elements are summarized in Tables 3.13 and 3.14. The Beckman flame photometer was specially designed to permit analysis of radioactive samples without hazard to the analysts. The elements Cl, Na, K, Mg, Ca, and Sr were designated as

major constituents; the elements Fe, Al, Cu, Si and Br were designated as minor constituents on the basis of analysis of the background components (coral and lagoon sea water).

TABLE 3.13 - Summary of Analytical Methods

Element	Method(a)	Reagent
Cl	Mohr Titration Method	Silver nitrate
Na	Beckman Flame Photometer	-
K	Beckman Flame Photometer	-
Mg	Beckman Flame Photometer	-
Ca	Beckman Flame Photometer	-
Sr	Beckman Flame Photometer	-
Fe	Beckman Spectrophotometer	Dipyridyl
Al	Beckman Spectrophotometer	Aluminon
Cu	Beckman Spectrophotometer	Diethyldithiocarbamate
Si	Beckman Spectrophotometer	Reduced Silicomolybdate
Br	Beckman Spectrophotometer	Fluorescien-eosin

(a) Application of Analytical Methods to the Analysis of Fallout Material, USNRDL Technical Report in preparation

TABLE 3.14 - Spectrophotometric Analysis of Minor Constituents

Element	Solvent Medium	pH		Wave Length of Max. Absorption (m μ)	Optimum Amount of Sample	
		Permissible Range	Used		Liquid (ml)	Solid (mg)
Fe	H ₂ O	3.0 - 9.0	5.7	520	>100	10 - 50
Al	H ₂ O	4.0 - 7.5	4.2	535	10	10 - 25
Cu	CCl ₄	5.0 - 9.0 (for extraction)	5.7	435 (in CCl ₄)	>100	100-500
Si	H ₂ O	4.2 - 6.8	4.5-6.0	820 (used 700)	10 - 100	10
Br	H ₂ O	-	5.7	517	<1	-

The elements Fe, Cu, and Si were characterized by very stable complexes ideally suited for analytical purposes. However, the Si procedure gave soluble Si only. The Al and Br procedures were sensitive to pH and salt concentration. Solutions of Al and Cu could be concentrated without increasing interferences from other elements to any great extent - the Al being carried on Fe(OH)₃ and Cu being extracted into CCl₄ as the diethyldithiocarbamate complex.

3.4.3 Results

Analyses of the background components, sea water and coral, are summarized in Table 3.15. The sea water analysis is compared to that given by Sverdrup.^{30/} The ratio of Cl to the other elements given by Sverdrup was used as the sea water component composition in reducing the data. Ratio values of 1.05×10^{-6} for Fe and 5.3×10^{-7} for Cu were used in the calculations. The coral analyses for sites Charlie and Tare are averages of three samples each of surface coral furnished by Holmes and Narver, Inc. All samples did not give identical analyses; and since they were surface samples, further differences in the ratio of Ca to other elements could have occurred in the fallout coral itself. These analyses, however, were taken as being the best estimate available of the coral component composition.

The physical measurements made on the fallout samples are given in Table 3.16. The fraction of a sampler bottle analyzed was occasionally greater than one when the fallout from more than one bottle was combined. In other cases funnel rinsings were added to the sample so that the fraction is not always the direct ratio of column 1 in Table 3.16 to the total sample as given in Section 3.1.

The concentration analyses of the liquid and solid fractions are given in Tables 3.17 and 3.18. In the cases where the samples were slurries or mixtures of liquid and solid, the comparison of the concentration of the various elements in each phase with those in Table 3.15 for the sea water and coral elements were used to show something about the history of the samples. For example, the consistent high values for 1-250.25 (liquid fraction) indicate evaporation of sea water. This was the case for other samples from Shot 1 where the sample bottles could not be securely sealed, the caps having been destroyed by fire on site Tare.

The concentration analyses of the two fractions were combined for a component analysis of each sample as shown in Table 3.19. The usual procedure was to use the Na and Cl analyses as a basis for the sea water component; when small amounts of Cl were found the Na value was used. After correcting for coral Na, the sea water Na and Cl were recalculated. The ratio values of Table 3.15 were then used to estimate the remaining elements in the sample contributed by sea water. Using the remaining Ca as coral Ca, the ratio values of Table 3.15 for coral were used to estimate the remaining elements as contributed to the fallout from coral. The remainders are attributed as being the contribution of the device-products to the fallout. In most cases positive amounts of Mg remained; this may be due to poor sampling of the background coral (surface coral may not be representative of all the coral thrown up by the detonation). In all cases, excepting one, positive remainders for Fe, Al, and Cu were found. For Shot 1, the island station samples (1-251 series) which contained no liquid were used as a qualitative guide for determining the nature of the fallout. None of these samples show the presence of sea water; the Na remainder after taking out the coral is negative more often than it is positive. The high coral content of many of the island station samples was undoubtedly due to drifting of coral particles into the surface-level pits. The lagoon samples were known to be rinsed together

TABLE 3.15 - Analysis of Background Components

Element	Sea Water (pH = 7.8)			Coral (weight basis)					
	ppm (mg/l)	Ratio		Site Charlie		Site Tare		Lagoon Bottom	
		NRDL	Sverdrup	(%)	Ratio	(%)	Ratio	(%)	Ratio
Cl	19,570	1	1	0.24	6.7×10^{-3}	0.10	2.8×10^{-3}	-	-
Na	10,610	0.542	0.556	0.31	8.7×10^{-3}	0.31	8.8×10^{-3}	0.69	2.9×10^{-2}
K	390	0.0199	0.0200	0.01	3×10^{-4}	0.01	3×10^{-4}	0.03	1×10^{-3}
Mg	1,313	0.0671	0.0670	2.02	5.68×10^{-2}	3.00	8.46×10^{-2}	0.64	2.7×10^{-2}
Ca	405	0.0207	0.0211	35.6	1	35.4	1	23.7	1
Sr	-	-	6.8×10^{-4}	0.33	9.3×10^{-3}	0.34	9.6×10^{-3}	0.37	1.6×10^{-2}
Fe	< 0.05	$< 3 \times 10^{-6}$	1×10^{-6}	0.0041	1.1×10^{-4}	0.0043	1.2×10^{-4}	0.0193	8.14×10^{-4}
			1×10^{-7}						
Al	< 0.01	$< 0.5 \times 10^{-6}$	2.6×10^{-6}	0.00010	2.9×10^{-6}	0.00016	4.6×10^{-6}	0.000058	2.4×10^{-6}
Cu	< 0.08	$< 4 \times 10^{-6}$	5.3×10^{-7}	0.00013	3.5×10^{-6}	0.00018	5.2×10^{-6}	0.00016	6.8×10^{-6}
			5.3×10^{-8}						
Si	1.82	9.3×10^{-5}	2×10^{-4}	0.132	3.7×10^{-3}	0.074	2.1×10^{-3}	0.044	1.9×10^{-3}
			1×10^{-6}						
Br	-	-	3.4×10^{-3}	-	-	-	-	-	-

TABLE 3.16 - Physical Measurements of the Fallout Samples

Sample	Total Analytical Sample	Fraction of One Sampler Bottle	Wt. Solid(a) Fraction (mg)	Vol. Liquid Fraction (ml)	pH of Liquid Fraction
	(g)				
1-250.04	26.77	1.80	1,204	24.4	11.7
1-250.05	23.39	0.377	394	21.7	7.2
1-250.06	24.12	1.04	398	22.0	7.8
1-250.17	24.36	1.63	34.6	22.0	8.1
1-250.22	4.06	1.41	53.0	3.4	7.6
1-250.24	52.03	1.39	206	49.0	7.5
1-250.25	7.90	2.05	131	6.6	8.1
1-251.02	14.41	0.114	254	14.1	12.0
1-251.03	3.83	0.248	206	3.6	12.2
1-251.04	0.814	0.0250	814	0	-
1-251.05	41.17	0.385	13.9	41.1	7.2
1-251.06	2.78	1.82	2,782	0	-
1-251.07	0.430	0.536	430	0	-
1-251.08	0.608	1.63	608	0	-
1-251.10	0.826	0.549	826	0	-
	(ml)				
2-A4	18.0	0.456	4.1	18.0	7.5
2-A5	5.8	0.126	2.4	5.8	7.9
2-Q4	18.2	0.700	1.8	18.2	-
2-R4	53.6	0.958	5.2	53.6	-
2-T4	9.0	0.300	2.1	9.0	-
3-250.05B(b)	517	0.379	289	517	10.4
3-250.05R(c)	515	0.273	782	515	10.7
3-250.07A	355	0.215	230	355	7.9
3-250.07B	126	0.0764	124	126	8.3
3-250.07C	128	0.120	151	128	8.1
3-251.02	128	0.110	1,033	128	11.5
3-Coca (TC)	128	0.360	326	128	11.9
3-Coca (3C)	128	0.771	45.9	128	7.8
4-Y39	28	1.70	12.5	28	7.4

(a) Density of coral was approximately 2.4

(b) B - Buoy TC

(c) R - Raft TC

TABLE 3.17 - Concentration Analyses of Liquid Fractions from Fallout Samples

Sample	Element (ppm)									
	Cl	Na	K	Mg	Ca	Fe	Al	Cu	Si ^(a)	Br
1-250.04	15,880	9,000	290	270	1,610	< 0.05	0.72	0.67	0.10	59.2
1-250.05	20,450	11,300	385	1,680	660	< 0.05	0.69	< 0.08	1.43	95.0
1-250.06	25,630	14,800	530	2,350	570	0.07	0.15	0.12	0.94	117
1-250.17	38,640	20,000	845	5,200	796	< 0.05	0.58	0.38	1.07	110
1-250.22	62,760	34,000	1,320	6,400	1,740	0.10	0.15	0.025	0.046	-
1-250.24	19,610	10,700	360	1,930	426	< 0.05	0.29	0.14	0.59	95.0
1-250.25	60,260	33,500	1,200	6,960	1,340	0.73	0.73	0.38	0.39	-
1-251.02	780	680	31	77	237	0.56	0.43	0.90	0.56	-
1-251.03	1,910	1,348	46	115	224	< 0.3	1.48	< 0.26	0.30	-
1-251.04	0	0	0	0	0	0	0	0	0	0
1-251.05	920	198	8.0	43	30.8	< 0.05	0.27	0.11	1.13	0.80
1-251.06	0	0	0	0	0	0	0	0	0	0
1-251.07	0	0	0	0	0	0	0	0	0	0
1-251.08	0	0	0	0	0	0	0	0	0	0
1-251.10	0	0	0	0	0	0	0	0	0	0
2-A4	2,700	760	34.0	119	38.9	7.98	0.38	3.03	2.50	-
2-A5	5,600	404	16.3	80.8	48.4	3.84	0.76	5.61	0.05	-
2-Q4	-	250	6.7	97.6	26.8	19.8	2.70	7.20	0.10	-
2-R4	-	200	2.5	52.8	19.4	21.5	2.48	2.06	0.10	-
2-T4	-	552	9.2	120	40.4	23.9	4.21	4.26	0.30	-
3-250.05B	142	52.2	2.0	10.6	17.2	< 0.05	0.04	< 0.08	0.15	-
3-250.05R	100	50.1	2.8	11.6	18.2	0.03	0.04	< 0.08	0.18	-
3-250.07a	75.4	50.4	0.8	19.0	18.9	0.01	0.02	< 0.08	0.23	-
3-250.07b	83.7	47.2	2.8	6.4	17.2	0.01	0.14	< 0.08	0.28	-
3-250.07c	109	25.8	0.8	2.1	12.2	< 0.05	0.10	< 0.08	1.03	-
3-251.02	58.6	16.1	3.0	9.5	20.5	< 0.05	0.06	< 0.08	0.43	-
3-Coca (TC)	259	120	6.6	8.5	41.6	0.16	< 0.06	< 0.08	7.72	-
3-Coca (3C)	276	34.0	2.6	8.5	111	< 0.05	0.19	< 0.08	0.23	-
4-Y39	21,130	12,620	374	1,690	412	1.88	0.27	0.27	0.74	21.0

(a) As soluble silica

TABLE 3.18 - Concentration Analyses of Solid Fractions from Fallout Samples

Sample	Element (Wt. %)								
	Na	K	Mg	Ca	Sr	Fe	Al	Cu	Si(a)
1-250.04	0.509	0.020	3.79	38.1	0.50	0.0282	0.0121	<0.0034	0.0009
1-250.05	0.990	0.050	9.82	28.6	0.45	0.0147	0.0234	<0.0037	0.0069
1-250.06	0.980	0.039	7.74	34.7	0.40	0.0250	0.0143	<0.0037	0.0011
1-250.17	3.80	0.18	4.34	19.9	-	0.0872	0.0737	0.0268	0.0157
1-250.22	12.1	0.34	1.42	15.1	0.034	0.171	0.116	0.0131	0.0051
1-250.24	0.396	0.019	7.44	36.5	0.32	0.0667	0.0125	0.0189	0.0003
1-250.25	1.00	0.036	5.87	33.5	0.18	0.0910	0.0213	0.0285	0.0007
1-251.02	0.239	0.013	2.62	43.6	0.47	0.0338	0.0139	0.0078	0.0014
1-251.03	0.181	0.0028	2.33	44.0	0.41	0.0433	0.0142	<0.0036	0.0019
1-251.04	0.102	0.0073	2.31	37.4	0.46	0.0044	0.0354	0.0022	0.0024
1-251.05	0.105	0.0	1.27	24.4	-	0.0834	0.0176	0.0192	0.0211
1-251.06	0.243	0.0090	2.78	38.9	0.54	0.0200	0.0444	0.0021	0.0150
1-251.07	0.258	0.0075	2.26	37.7	0.62	0.0617	0.0097	0.0057	0.0002
1-251.08	0.372	0.024	2.62	37.7	0.50	0.0095	0.0062	<0.0034	0.0006
1-251.10	0.263	0.0089	2.08	36.9	0.72	0.0223	0.0112	0.0153	0.0006
2-A4	-	-	-	-	-	-	-	-	-
2-A5	-	-	-	-	-	-	-	-	-
2-Q4	-	-	-	-	-	-	-	-	-
2-R4	-	-	-	-	-	-	-	-	-
2-T4	-	-	-	-	-	-	-	-	-
3-250.05B	0.134	0.006	4.06	38.1	0.36	0.180	0.0494	0.0266	<0.0011
3-250.05R	0.154	0.006	3.23	37.0	0.43	0.099	0.0134	0.0042	0.0046
3-250.07a	0.164	0.025	2.90	35.1	0.47	0.336	0.0418	0.0086	<0.0012
3-250.07b	0.171	0.038	0.80	35.5	0.39	0.189	0.0254	0.0089	0.00025
3-250.07c	0.203	0.008	2.29	39.1	0.42	0.687	0.0105	<0.0089	0.00075
3-251.02	0.205	0.008	2.99	35.6	0.31	0.0309	0.00726	0.0080	<0.0010
3-Coca (TC)	0.170	0.003	3.84	36.5	0.36	0.403	0.0199	0.0224	0.00038
3-Coca (3C)	0.159	0.007	2.04	28.3	0.037	0.959	1.29	0.0477	0.00074
4-Y39	20.6	0.662	2.89	2.46	-	1.05	0.194	0.0719	<0.020

(a) As soluble silica

65

TABLE 3.19 - Component Analysis of Fallout Samples

Sample	Component	Element (mg)									
		Cl	Na	K	Mg	Ca	Sr	Fe	Al	Cu	
1-250.04	Total	388	226	7.24	52.2	498	6.0	0.339	0.164	0.016	<0.057
	Sea Water	393	219	7.86	26.3	8	.3	0.0004	0.001	0.0002	
	Coral	3	4	0.14	27.8	490	4.5	0.056	0.001	0.0017	
	D.P. (a)	-8	+3	-0.76	-1.9	0	+1.2	+0.283	+0.162	0.014	<0.055
1-250.05	Total	444	249	8.55	75.2	127	1.8	0.0580	0.107	<0.017	
	Sea Water	445	247	8.90	29.8	9	0.3	0.0005	0.001	0.0002	
	Coral	1	1	0.03	6.7	118	1.1	0.0134	0.0003	0.0004	
	D.P.	-2	+1	-0.38	+38.7	0	+0.4	+0.0241	+0.106	<0.016	
1-250.06	Total	564	330	11.8	82.5	151	1.6	0.101	0.0602	0.0026	<0.0176
	Sea Water	577	321	11.5	38.6	12	0.4	0.0006	0.0015	0.0003	
	Coral	1	1	0.04	7.9	139	1.2	0.0158	0.0004	0.0005	
	D.P.	-14	+8	+0.3	+36.0	0	0	+0.085	+0.0583	0.0018	<0.0168
1-250.17	Total	850	441	18.6	116	24.4	-	0.0302	0.0383	0.101	
	Sea Water	822	457	16.4	55	17.3	0.6	0.0009	0.0022	0.0004	
	Coral	0.05	0.06	0.002	0.4	7.1	0.07	0.0008	0.00002	0.00002	
	D.P.	+28	-16	+2.2	+61	0	-	+0.0285	+0.0361	+0.101	
1-250.22	Total	213	122	4.67	22.5	13.9	0.016	0.0909	0.0621	0.00702	
	Sea Water	216	120	4.33	14.5	4.5	0.15	0.0002	0.0006	0.00011	
	Coral	0.1	0.1	0.003	0.5	9.4	0.09	0.0011	0.00003	0.00003	
	D.P.	-3	+2	+0.34	+7.5	0	-0.22	+0.0896	+0.0615	+0.00688	
1-250.24	Total	961	525	17.7	110	96.0	0.66	0.137	0.0399	0.0458	
	Sea Water	952	529	19.0	64	20.0	0.65	0.001	0.0025	0.0005	
	Coral	0.5	0.7	0.02	4	76.0	0.004	0.009	0.0002	0.0003	
	D.P.	+9	-5	-1.3	+42	0	+0.01	+0.127	+0.0372	+0.0450	
1-250.25	Total	398	222	7.97	53.6	52.8	0.24	0.0167	0.0327	0.0399	
	Sea Water	398	222	7.97	26.7	8.4	0.27	0.0004	0.0010	0.0002	
	Coral	0.3	0.4	0.01	2.5	44.4	0.41	0.0051	0.0001	0.0002	
	D.P.	0	0	-0.01	+24.4	0	-0.44	+0.0112	+0.0316	+0.0395	

g

TABLE 3.19 - Component Analysis of Fallout Samples (Continued)

Sample	Component	Element (mg)								
		Cl	Na	K	Mg	Ca	Sr	Fe	Al	Cu
1-251.02	Total	11.0	10.2	0.47	7.7	114	1.2	0.0936	0.0412	0.0324
	Sea Water	16.6	9.2	0.33	1.1	0.3	0.01	0.00002	0.00004	0.00009
	Coral	0.8	1.0	0.03	6.4	114	1.2	0.0130	0.0004	0.0004
	D.P.	-6.4	0	+0.11	+0.2	0	0	+0.0806	+0.0408	+0.0320
1-251.03	Total	6.89	5.22	0.17	5.20	91.5	0.84	0.0898	0.0345	<0.0168
	Sea Water	7.96	4.43	0.16	0.53	0.2	0.005	0.000008	0.00002	0.000004
	Coral	0.62	0.79	0.03	5.18	91.3	0.84	0.0104	0.0003	0.0003
	D.P.	-1.69	0	-0.02	-0.51	0	0	+0.0794	+0.0342	<0.0165
1-251.04	Total	-	0.83	0.059	18.8	304	3.7	0.0357	0.118	0.0181
	Coral	-	2.65	0.086	17.3	304	2.8	0.0347	0.0009	0.0011
	D.P.	-	-1.82	-0.027	+1.5	0	+0.9	+0.0010	+0.117	+0.0170
1-251.05	Total	37.8	8.15	0.33	1.96	4.66	-	0.0116	0.0135	0.00719
	Sea Water	14.6	8.11	0.29	0.98	0.31	0.01	0.00002	0.00004	0.000008
	Coral	0.03	0.04	0.001	0.25	4.35	0.04	0.0005	0.00001	0.00002
	D.P.	+23.3	0	+0.04	+0.73	0	-	+0.0111	+0.0135	+0.00716
1-251.06	Total	-	6.76	0.25	77.3	1,080	15	0.0557	0.373	0.0175
	Coral	-	9.43	0.30	61.4	1,080	10	0.1234	0.003	0.0038
	D.P.	-	-2.67	-0.05	+15.9	0	+5	-0.0677	+0.370	+0.0137
1-251.07	Total	-	1.11	0.032	9.71	162	2.7	0.0265	0.0416	0.0244
	Coral	-	1.41	0.045	9.18	162	1.5	0.0184	0.0005	0.0006
	D.P.	-	-0.30	-0.013	+0.53	0	+1.2	+0.0081	+0.0411	+0.0238
1-251.08	Total	-	2.26	0.15	15.9	229	3.0	0.0578	0.0376	<0.021
	Coral	-	2.00	0.06	13.0	229	2.1	0.0262	0.0007	0.0008
	D.P.	-	+0.26	+0.09	+2.9	0	+0.9	+0.0316	+0.0369	<0.020
1-251.10	Total	-	2.17	0.074	17.2	305	5.9	0.184	0.0924	0.0126
	Coral	-	2.66	0.086	17.3	305	2.8	0.035	0.0009	0.001
	D.P.	-	-0.49	-0.012	-0.1	-	+3.1	+0.149	+0.0915	+0.125

TABLE 3.19 - Component Analysis of Fallout Samples (Continued)

Sample	Component	Element (mg)									
		Cl	Na	K	Mg	Ca	Sr	Fe	Al	Cu	
2-A4	Total	49	13.7	0.61	2.14	0.700	-	0.144	0.0068	0.0545	
	Sea Water	25	13.7	0.49	1.65	0.518	-	0.00003	0.00006	0.000001	
	Coral	0.001	0.001	0.00005	0.001	0.182	-	0.00002	-	-	
	D.P.	+24	0	+0.12	+0.49	0	-	+0.144	+0.0067	+0.0545	
2-A5	Total	32	2.34	0.094	0.469	0.281	-	0.0208	0.0043	0.0326	
	Sea Water	4.2	2.34	0.084	0.282	0.089	-	0.000005	0.00001	0.000002	
	Coral	0.001	0.002	0.00005	0.001	0.192	-	0.00002	-	-	
	D.P.	+28	0	+0.010	+0.186	0	-	+0.0208	+0.0043	+0.0326	
2-Q4	Total	-	4.55	0.12	1.78	0.488	-	0.360	0.0491	0.131	
	Sea Water	-	4.55	0.16	0.55	0.172	-	0.000009	0.00002	0.000004	
	Coral	-	0.003	0.00009	0.002	0.316	-	0.00004	-	-	
	D.P.	-	0	-0.04	+1.23	-	-	+0.360	+0.0491	+0.131	
2-P4	Total	-	10.7	0.13	2.83	1.04	-	1.15	0.133	0.110	
	Sea Water	-	10.7	0.38	1.29	0.40	-	0.00002	0.00005	0.00001	
	Coral	-	0.006	0.0002	0.004	0.64	-	0.00007	-	-	
	D.P.	-	0	-0.25	+1.54	0	-	+1.15	+0.133	+0.110	
2-T4	Total	-	4.97	0.083	1.08	0.364	-	0.215	0.0379	0.0383	
	Sea Water	-	4.97	0.179	0.60	0.188	-	0.00009	0.0002	0.000005	
	Coral	-	0.002	0.00005	0.001	0.176	-	0.00002	-	-	
	D.P.	-	0	-0.096	+0.48	0	-	+0.215	+0.0377	+0.0383	
3-250.05B	Total	73.4	27.4	1.0	17.2	119	1.0	0.521	0.164	0.077	< 0.118
	Sea Water	47.4	26.4	0.9	3.2	1	0.03	0.00005	0.00001	0.00002	
	Coral	0.3	1.0	0.03	10.0	118	1.0	0.014	0.0005	0.0006	
	D.P.	+25.7	0	+0.1	+4.0	0	0	+0.507	+0.164	0.076	< 0.117
3-250.05R	Total	51.5	27.0	1.5	31.2	299	3.4	0.789	0.125	0.033	< 0.074
	Sea Water	43.8	24.4	0.9	2.9	1	0.03	0.00004	0.0001	0.00002	
	Coral	0.8	2.5	0.08	25.2	298	2.9	0.036	0.0014	0.002	
	D.P.	+ 6.9	0	+0.5	+3.1	0	+0.5	+0.753	+0.124	0.031	< 0.072

TABLE 3.19 - Component Analysis of Fallout Samples (Concluded)

Sample	Component	Element (mg)									
		Cl	Na	K	Mg	Ca	Sr	Fe	Al	Cu	
3-250.07a	Total	26.8	18.3	0.34	13.4	87.4	1.1	0.776	0.0968	0.20	<0.048
	Sea Water	31.4	17.5	0.63	2.1	0.7	0.02	0.00003	0.00008	0.00002	
	Coral	0.3	0.8	0.02	7.3	86.7	0.8	0.011	0.0004	0.0004	
	D.P.	-4.9	0	-0.31	+4.0	0	+0.2	+0.765	+0.0963	0.020	<0.048
3-250.07b	Total	10.5	6.16	0.40	1.80	46.1	0.48	0.234	0.0490	0.011	<0.021
	Sea Water	10.4	5.76	0.21	0.69	0.2	0.007	0.00001	0.00003	0.000006	
	Coral	0.1	0.40	0.01	3.88	45.9	0.44	0.006	0.0002	0.0002	
	D.P.	0	0	+0.18	-2.77	0	+0.03	+0.228	+0.0488	0.011	<0.021
3-250.07c	Total	14.0	3.61	0.11	3.73	60.6	0.63	1.04	0.0287	<0.0235	
	Sea Water	5.5	3.08	0.11	0.37	0.1	0.003	0.000005	0.00002	0.000003	
	Coral	0.2	0.53	0.017	5.12	60.5	0.58	0.007	0.0003	0.0003	
	D.P.	+8.3	0	0	-1.46	0	+0.05	+1.03	+0.0284	<0.0232	
3-251.02	Total	7.50	4.18	0.47	32.1	391	3.2	0.319	0.0827	0.083	<0.093
	Sea Water	1.35	0.75	0.03	0.1	0.03	0.001	0.000001	0.000004	0.0000007	
	Coral	1.10	3.43	0.11	33.1	391	3.8	0.048	0.0018	0.002	
	D.P.	+5.05	0	+0.33	-1.1	0	-0.6	+0.271	+0.0809	0.081	<0.091
3-Coca TC	Total	33.1	15.9	0.86	13.5	124	1.2	1.33	0.0649	0.073	<0.083
	Sea Water	26.6	14.8	0.53	1.8	0.6	0.02	0.00003	0.00007	0.00001	
	Coral	0.4	1.1	0.04	10.5	123	1.2	0.02	0.0006	0.0006	
	D.P.	+6.1	0	+0.29	+1.2	123	0	+1.31	+0.0642	0.072	<0.083
3-Coca 3C	Total	35.3	4.42	0.34	2.02	27.2	0.18	0.443	0.617	0.022	<0.032
	Sea Water	7.5	4.19	0.15	0.50	0.2	0.005	0.000008	0.00002	0.000004	
	Coral	0.1	0.24	0.008	2.29	27.0	0.26	0.003	0.0001	0.0001	
	D.P.	+27.7	0	+0.20	-0.77	0	-0.08	+0.440	+0.617	0.022	<0.032
4-T39	Total	592	353	10.6	47.7	11.6	-	0.184	0.0318	0.0166	
	Sea Water	613	341	12.3	41.1	12.9	-	0.0006	0.0016	0.0003	
	D.P.	-21	+12	-1.7	+6.6	-1.3	-	+0.183	+0.0302	+0.0163	
	Sea Water (b)	93.2	51.8	1.9	6.2	2.0					

(a) Device Product

(b) 15.2% of total sea water elements as fallout material

with the aid of lagoon sea water. Although the analyses for a number of these samples indicated various stages of evaporation, the amount of the various sea water constituents was generally in the correct order. On the other hand, the sea water rinsing of two bottles into the third provided samples in which the recovery of the total fallout was far greater than when the dry material was collected without rinsing. For this reason, the amounts of fallout material as coral or device-products from the lagoon stations (1-250 series) were considered the most valid. Hence, the fallout material from Shot 1 consisted of coral and the device-product components. The material from Shot 2 showed the presence of all three components. Three of the samples were combined acid (HCl) washes of funnel and bottle so the Cl analysis was not included. Small amounts of residue (carbonaceous) were not analyzed. The fallout from Shot 3 also contained significant amounts of all three components in addition to large volumes of rain water. The rain washed down the funnels. Only one sample from Shot 4 was analyzed; the analysis of this sample gave a 15.2 per cent excess concentration (based on Cl, Na, and Mg analysis) of sea water but no remainder as coral; however, the sample was known to have been exposed too short a time for evaporation of that extent to occur so that the excess was attributed to fallout.

The field teams of Project 2.5a inspected the collectors periodically to remove extraneous material from the bottle collectors; however, it was not always possible to make such an inspection immediately prior to shot time at all stations. Therefore, when analyses indicate, the island station samples may be assumed to be high in coral while the raft or buoy (or YAG) station collectors high in sea water constituents. For any shot, the best estimate of the amount of coral would accordingly be obtained from a collector stationed in the lagoon while the best estimate of the amount of sea water in the fallout would be obtained from a sampler stationed on an island. Any departure of sea water constituents from the lagoon water concentration would indicate either evaporation or collection of rain water. Samplers mounted on buoys were further from the water than those mounted on rafts; hence the amount of spray collected by buoy samplers would be less than that collected by raft samplers and should give a better estimate of sea water in the fallout as well as a better estimate for the radioactive material. These considerations, along with those given in the preceding paragraph, are used in the following discussion of the data.

The surface density of the three components, coral, sea water, and device products are tabulated in Table 3.20. The density distributions are plotted in Figs. 3.12 through 3.14. The surface densities are calculated for the 7-in. diameter funnel in terms of the original (unchanged) component material. Due to limitations of time and manpower as well as considerations of application of the data, analyses to determine the amounts of pyrolyzed and non-pyrolyzed coral were not attempted. If they had been, estimates of extraneous material (as drift-in) might have been made. From appearances of the samples, however, the coral component from Shots 1 and 2 was essentially all pyrolyzed coral while that from Shot 3 appeared to contain large amounts of unchanged coral.

The surface density of equivalent coral on Shot 1 ranged from about 50 to 3000 mg/sq ft for the lagoon station samples. On Shot 2 (buoy

TABLE 3.20 - Surface Density of Fallout Components

Sample	Coral		Sea Water		Device	
	Total Ca (mg)	Density ^(a) (mg/sq ft)	Total Na (mg)	Density ^(b) (ml/sq ft)	Total Fe (mg)	Density ^(c) (fraction/sq ft) x 10 ¹²
1-250.04	272	2,860	0	0	0.157	10.6 ^(d)
1-250.05	313	3,290	0	0	0.064	4.30
1-250.06	134	1,410	0	0	0.082	5.50
1-250.17	4.4	46	0	0	0.018	1.20
1-250.22	6.7	70	0	0	0.064	4.30
1-250.24	55	580	0	0	0.091	6.12
1-250.25	22	230	0	0	0.0055	0.37
1-251.02	1,000	10,700	0	0	0.707	4.76
1-251.03	368	3,870	0	0	0.320	21.5
1-251.04	12,200	128,000	0	0	0.040	2.69
1-251.05	11	120	0	0	0.029	1.95
1-251.06	594	6,240	0	0	-	-
1-251.07	302	3,170	0	0	0.015	1.01
1-251.08	140	1,470	0	0	0.019	1.28
1-251.10	556	5,840	0	0	0.272	18.3
2-A4	0.40	4.2	30.0	10.6	0.315	5.01
2-A5	1.52	16.0	18.6	6.56	0.165	2.62
2-Q4	0.45	4.7	6.5	2.29	0.514	8.18
2-R4	0.67	7.0	11.2	3.95	1.20	19.1
2-T4	0.59	6.2	16.6	5.86	0.717	11.4
3-250.05B	312	3,300	69.7	24.6	1.34	98.2
3-250.05R	1,090	11,500	89.4	31.5	2.76	202
3-250.07a	403	4,260	81.4	28.7	3.56	261
3-250.07b	601	6,350	75.4	26.6	2.98	218
3-250.07c	504	5,320	25.7	9.06	8.59	629
3-251.02	3,550	37,500	6.82	2.40	2.46	180
3-Coca TC	342	3,610	41.1	14.5	3.64	267
3-Coca 3C	35	370	5.44	1.92	0.570	41.7
4-Y39	0	0	30.5	10.8	0.108	1.52

(a) In terms of original coral composition

(b) In terms of original sea water composition

(c) From total steel in device and device-site construction

(d) Values for Shot 1 for above grade materials only

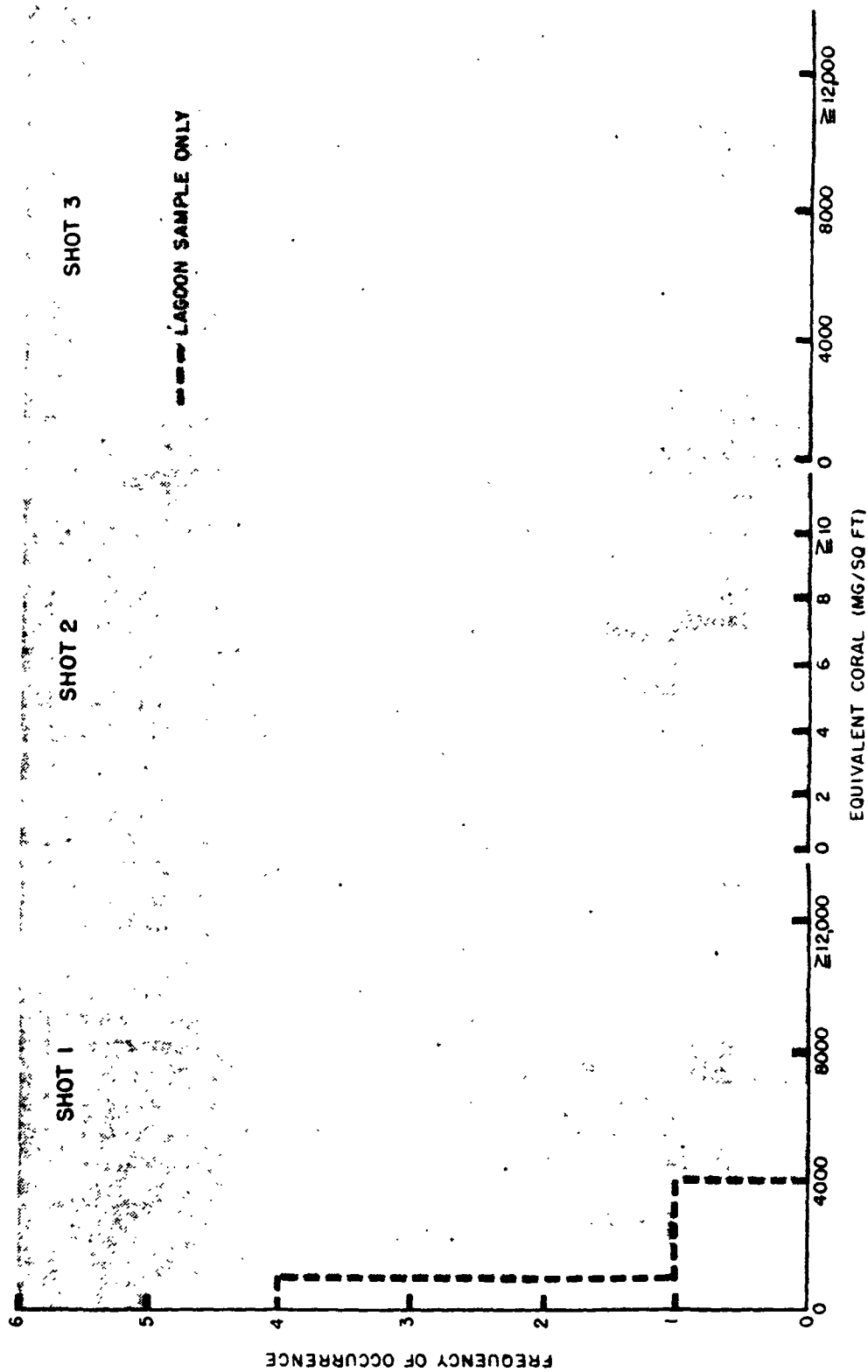


Fig. 3.12 Density Distribution of Equivalent Coral for Shots 1, 2, and 3

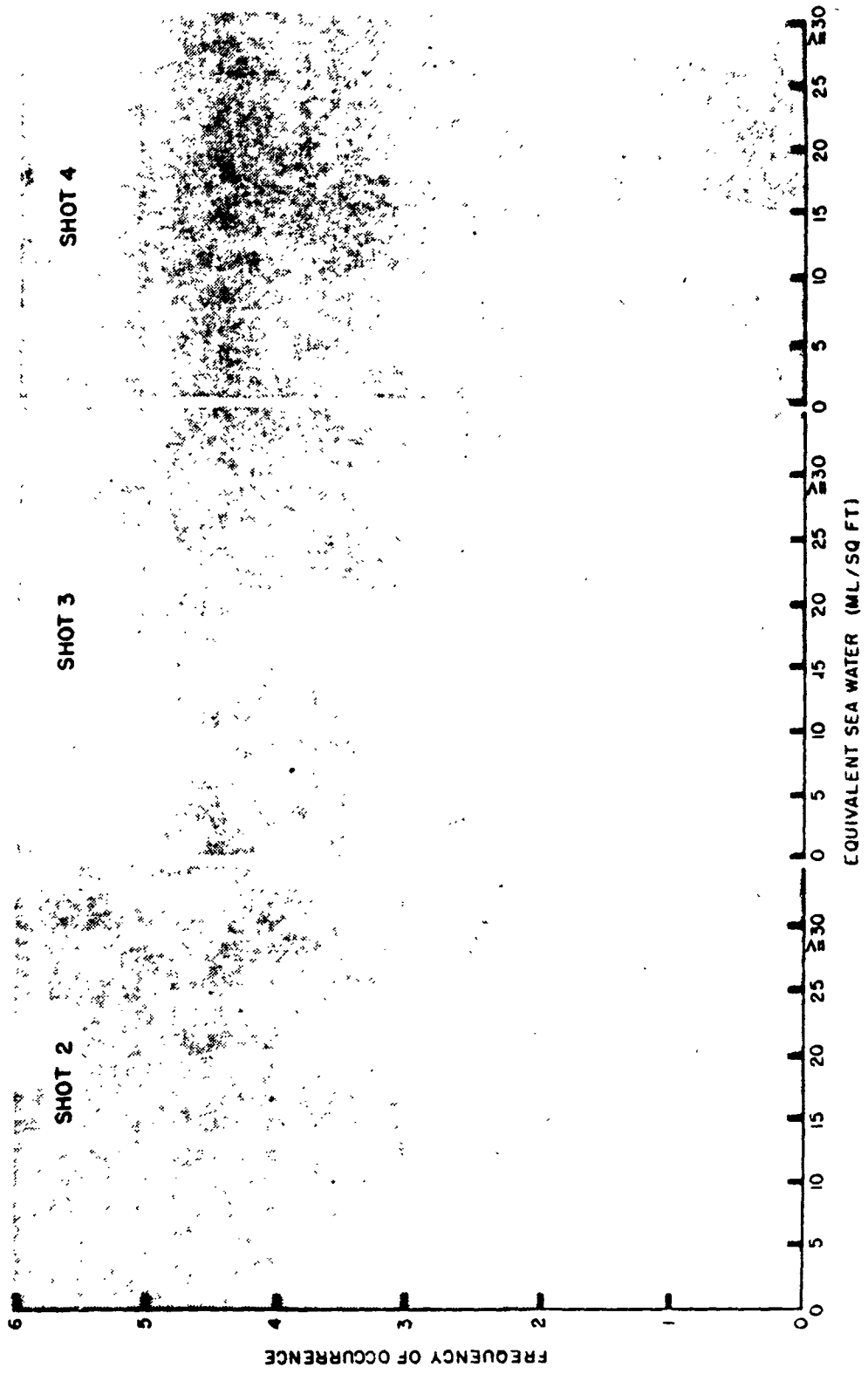


Fig. 3.13 Density Distribution of Equivalent Sea Water for Shots 2,3, and 4

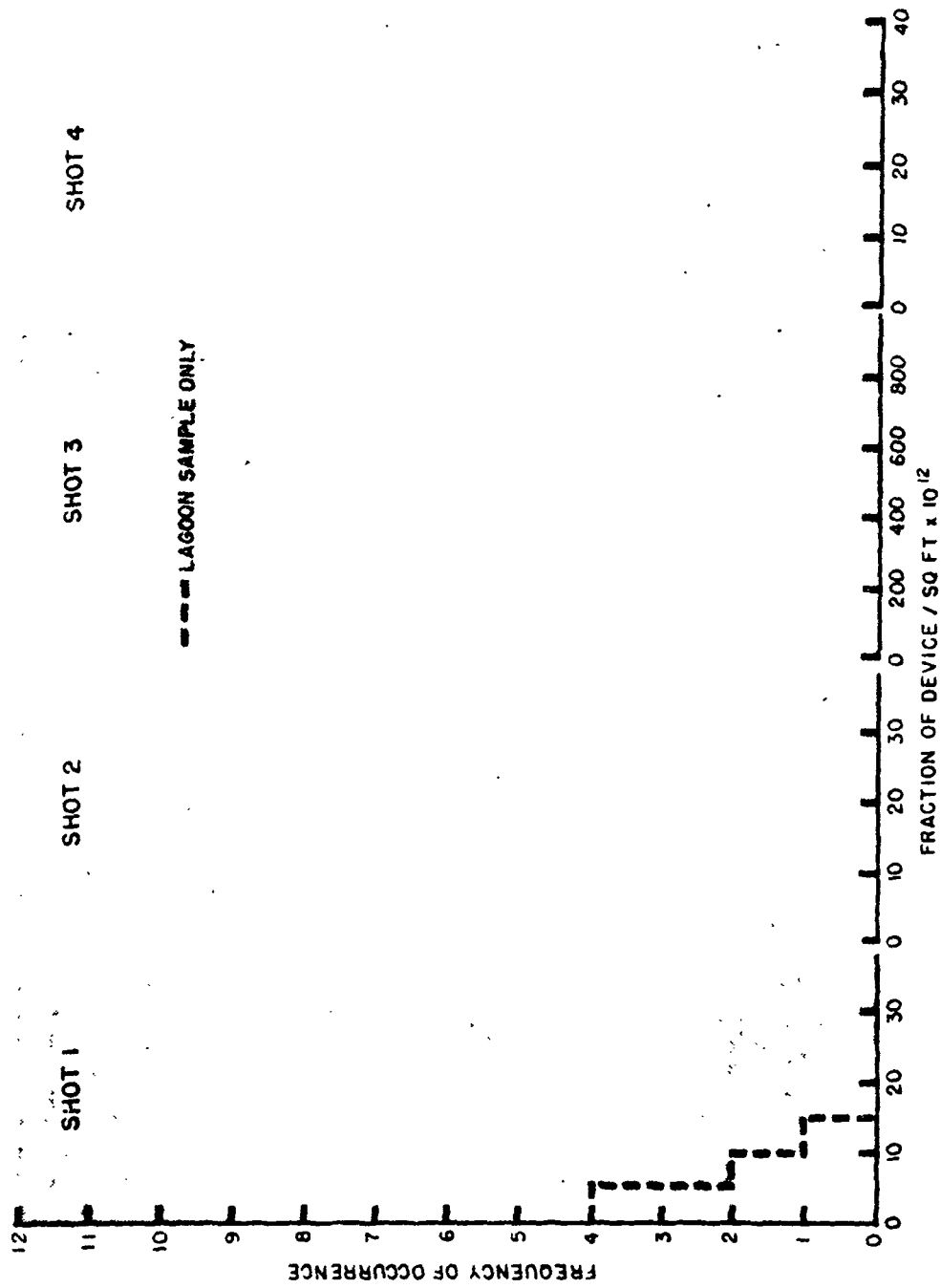


Fig. 3.14 Density Distribution of Device Fraction for Shots 1, 2, 3, and 4

samples), the surface density ranged from 4 to 7 mg/sq ft (with one sample at 16). On Shot 3, the surface density of coral ranged from 3000 to 7000 mg/sq ft (with one sample at 12,000).

The surface density of equivalent sea water on Shot 2 ranged from 2 to 11 ml/sq ft. The samples collected were both dry and wet. For those containing liquid, the concentration analyses gave too low values to indicate a pure sea water splash-in. Some rain was experienced during recovery of these samples. Hence, Shot 2 fallout was probably essentially a dry material when it arrived at the collectors. On Shot 3, the surface density of sea water ranged from 2 to 30 ml/sq ft. The island station and 3-bottle sampler values were near the lower end of the range; the total collector on Coca Head gave a mid-range value; the total collectors on the lagoon rafts and buoys generally gave values at the high end of the range as shown by the split distribution plot. No definite information is available as to when the sample bottles were last checked for splash-in prior to shot time. It seems likely, however, from the analyses alone that the higher distribution was due to splash-in and that the 2 to 15 ml/sq ft surface density is the more reliable distribution. On Shot 4, the single sample gave a value of 11 ml/sq ft for the equivalent surface density of the sea water component.

The surface density of the device is given for Fe in terms of fraction of the device which fell on each square foot range from about 1×10^{-12} to 10×10^{-12} on Shot 1 for the lagoon station samples. A mid-range fractional density of 4.3×10^{-12} per sq ft would give (as a minimum) a coverage of about 8000 sq mi for a 100 per cent fallout. On Shot 2, the fractional surface density for the device ranged from about 3×10^{-12} to 20×10^{-12} per sq ft. On Shot 3, the fractional surface density ranged from about 100×10^{-12} to 300×10^{-12} for the majority of samples. A mid-range fractional density of 230×10^{-12} per sq ft would give a coverage of about 160 sq mi for a 100 per cent fallout. The areas for a 100 per cent fallout are given only for a qualitative check on the analytical data and do not indicate the actual coverage such as do the fallout distributions as given in the CASTLE report of Project 2.5a. If it would have been possible to analyze the fallout samples at more stations, fallout contours of surface density of coral, sea water, and device products could have been determined for comparison with the dosage contours. On Shot 4, the one value at 1.5×10^{-12} per sq ft was about a factor of 3 less than the mid-range value for Shot 1 and roughly a factor of 5 or 6 less than that for Shot 2.

A comparison of an estimated radiation field to the surface density of each component is made in Table 3.21, with the corresponding distributions given by Figs. 3.15 through 3.17. The total gamma counts for each fallout collector bottle (taken in the same geometry) were corrected back to 1 hr from a calculated beta decay scheme (see Chapter 5). For Shot 1, the estimated radiation field reading at 1 hr given by Project 2.5a was used. On Shots 2 and 4, preliminary estimates of the field were made using uncorrected data taken from recorded data on a 50 x 50 ft section of flight deck of the YAG 40 at as early a time as possible (5 to 16 hr). These readings were compared to the total gamma count in the Project 2.5a total collectors. On Shot 2, the ratio of r/hr to c/m ranged from 0.026×10^{-7} to 0.051×10^{-7} while on Shot 4, the ratio

TABLE 3.21 - Comparison of Radiation Field with Surface Density of Fallout Components

Sample	Total Gamma Count per bottle (c/m x 10 ⁻⁷ at 1 hr)	Estimated Equiva- lent Field (r/hr at 1 hr)	Ratio of Field to Coral Sur- face Density (r/hr:mg/sq ft)	Ratio of Field to Sea Water Surface Density (r/hr:ml/sq ft)	Ratio of Field to Device Fractional Density (r/hr:fraction/sq ft) x 10 ⁻¹²
1-250.04	2,400	100(a)	0.035	0	9
1-250.05	4,800	80(a)	0.024	0	19
1-250.06	1,500	80(a)	0.057	0	15
1-250.17	15	50(a)	1	0	25
1-250.22	150	26(a)	0.4	0	6
1-250.24	2,100	28(a)	0.048	0	5
1-250.25	50	30(a)	0.13	0	80
1-251.02	89,000	1,650(a)	0.15	0	350
1-251.03	11,000	600(a)	0.15	0	28
1-251.04	6,900	350(a)	0.003	0	130
1-251.05	200	210(a)	1.7	0	110
1-251.06	2,900	60(a)	0.01	0	-
1-251.07	10	22(a)	0.007	0	22
1-251.08	-	19(a)	0.01	0	15
1-251.10	20	30(a)	0.005	0	2
2-A4	2,200	120	29	11	24
2-A5	1,700	90	6	14	34
2-Q4	40	2	-	-	-
2-P4	2	0.1	-	-	-
2-Q4	2,000	110	23	48	13
2-R4	9,000	480	69	120	25
2-T4	1,700	90	15	15	?
2-Y39	310	20	-	-	-
2-Y40	2,600	140(b)	-	-	-
3-250.05B	8,300	440	0.14	18	4.5
3-250.05R	8,500	450	0.039	14	2.2
3-250.07a	4,500	240	0.056	8	0.9
3-250.07b	4,500	240	0.038	9	1.1

76

TABLE 3.21 - Comparison of Radiation Field with Surface Density of Fallout Components (Concluded)

Sample	Total Gamma Count per bottle (c/m x 10 ⁻⁷ at 1 hr)	Estimated Equiva- lent Field (r/hr at 1 hr)	Ratio of Field to Coral Sur- face Density (r/hr:mg/sq ft)	Ratio of Field to Sea Water Surface Density (r/hr:ral/sq ft)	Ratio of Field to Device Fractional Density (r/hr:fraction/sq ft. x 10 ⁻¹²)
3-250.07c	7,100	380	0.071	42	0.6
3-251.02	9,900	520	0.014	220	2.9
3-Coca TC	14,400	770	0.21	53	2.9
3-Coca 3C	900	50	0.14	26	1.2
3-250.08	9,600	510	-	-	-
4-Y39	2,300	120	0	11	79
4-Y40P	660	40	-	-	-
4-Y40S	2,000	110 ^(b)	-	-	-

(a) Average of Rad Safe and/or Project 2.5a surveys (see Project 2.5a report)

(b) Estimate from Project 6.4 preliminary uncorrected data (see text)

TABLE 3.21 - Comparison of Radiation Field with Surface Density of Fallout Components (Concluded)

Sample	Total Gamma Count per bottle (c/m x 10 ⁻⁷ at 1 hr)	Estimated Equiva- lent Field (r/hr at 1 hr)	Ratio of Field to Coral Sur- face Density (r/hr:mg/sq ft)	Ratio of Field to Sea Water Surface Density (r/hr:ml/sq ft)	Ratio of Field to Device Fractional Density (r/hr:fraction/sq ft. x 10 ⁻¹²)
3-250.07c	7,100	380	0.071	42	0.6
3-251.02	9,900	520	0.014	220	2.9
3-Coca TC	14,400	770	0.21	53	2.9
3-Coca 3C	900	50	0.14	26	1.2
3-250.08	9,600	510	-	-	-
4-Y39	2,300	120	0	11	79
4-Y40P	660	40	-	-	-
4-Y40S	2,000	110(b)	-	-	-

(a) Average of Rad Safe and/or Project 2.5a surveys (see Project 2.5a report)

(b) Estimate from Project 6.4 preliminary uncorrected data (see text)

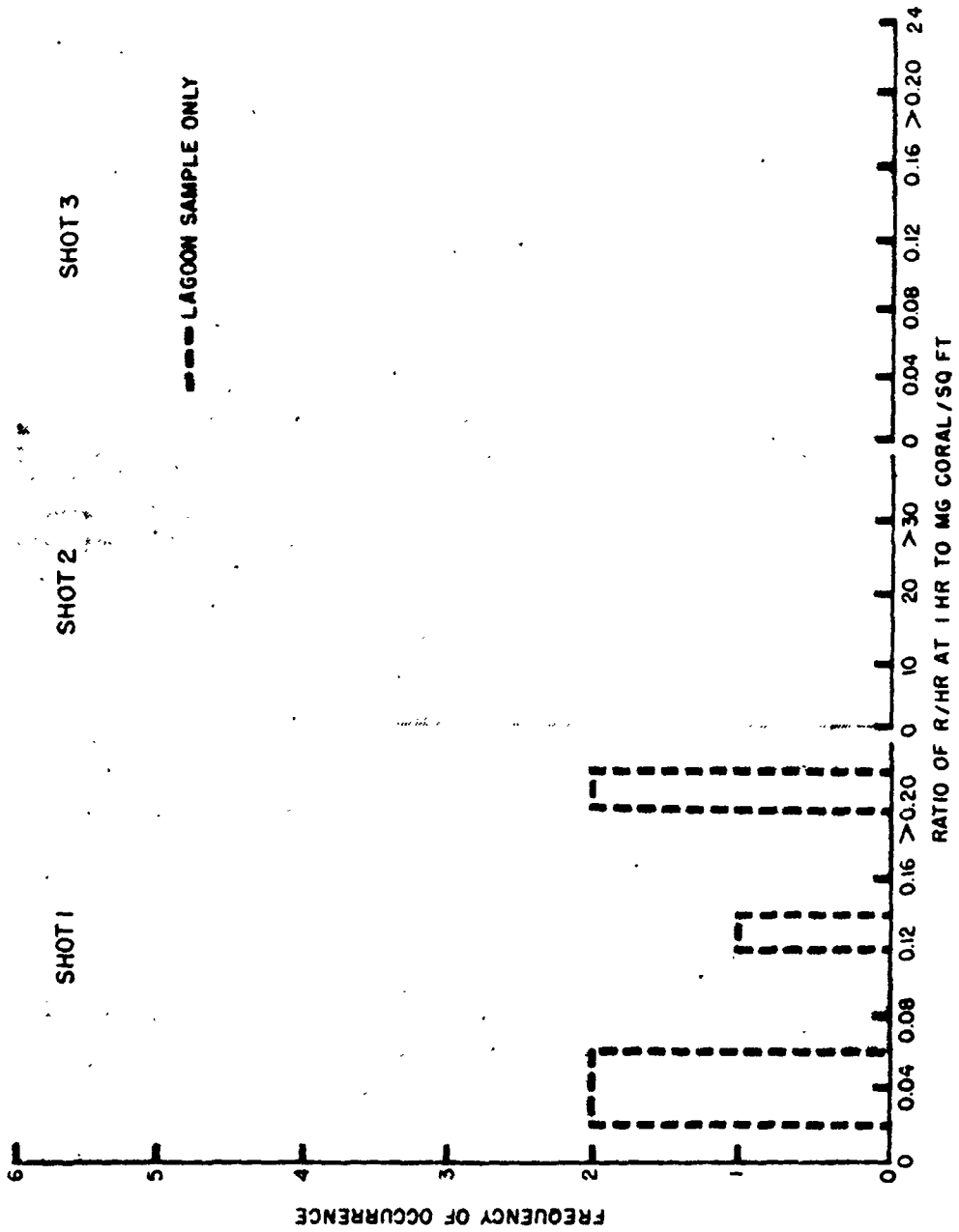


Fig. 3.15 Distribution of the Ratio of the Radiation Field to the Surface Density of the Coral Component

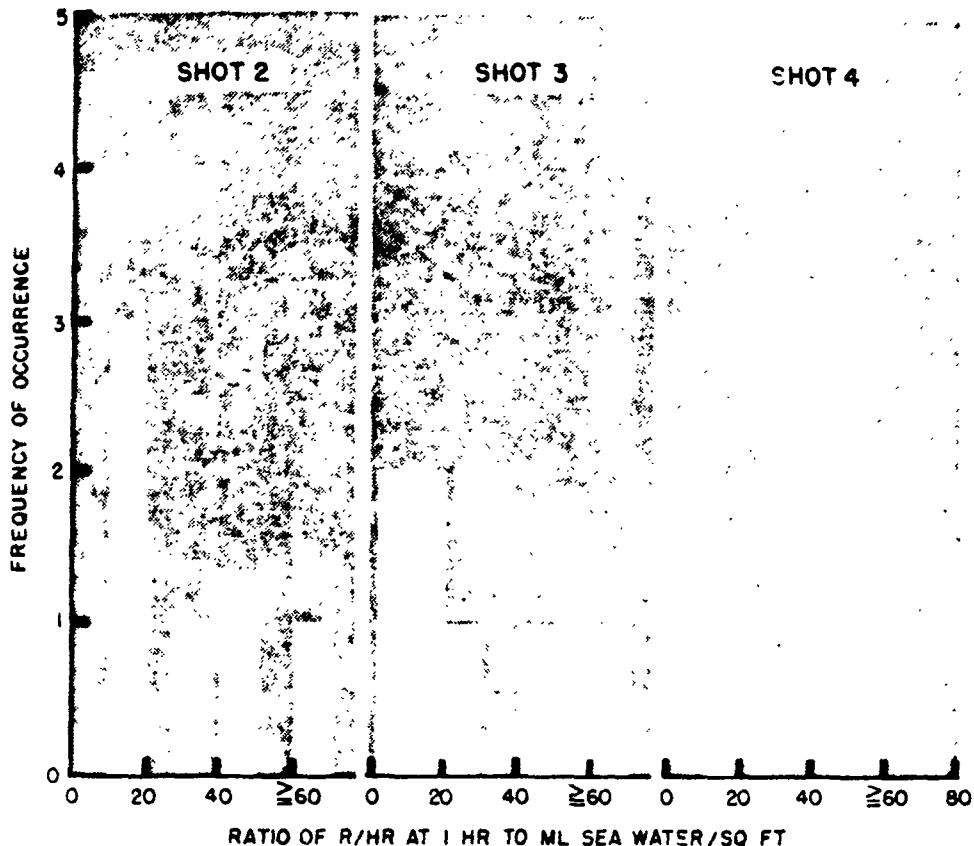


Fig. 3.16 Distribution of the Ratio of the Radiation Field to the Surface Density of the Sea Water Component

varied from 0.045×10^{-7} to 0.070×10^{-7} . For samples 251.03 and 251.04 on Shot 1, using only the island survey data (as corrected to 1 hr by Project 2.5a) gave a ratio of 0.045×10^{-7} to 0.064×10^{-7} and 0.043×10^{-7} to 0.058×10^{-7} while other island station samples gave ratios varying from 0.01×10^{-7} to 1.0×10^{-7} when similarly compared. Excepting for those noted in Table 3.21, a factor 0.053×10^{-7} was used to estimate the field reading from the total gamma count. If the assumption of complete mixing of the three components with the radioactive device components is valid and if the sampling techniques are sound so that the sample is a representation of the over-all fallout in the particular area, then the ratio of the field radiation to the surface density of the tracer fallout components should be a constant for each shot. The comparisons as given in Table 3.21 show large variations instead of constancy. Actual field readings were available only for Shot 1 island stations where the sample recovery was actually the most questionable. The extent of error in the

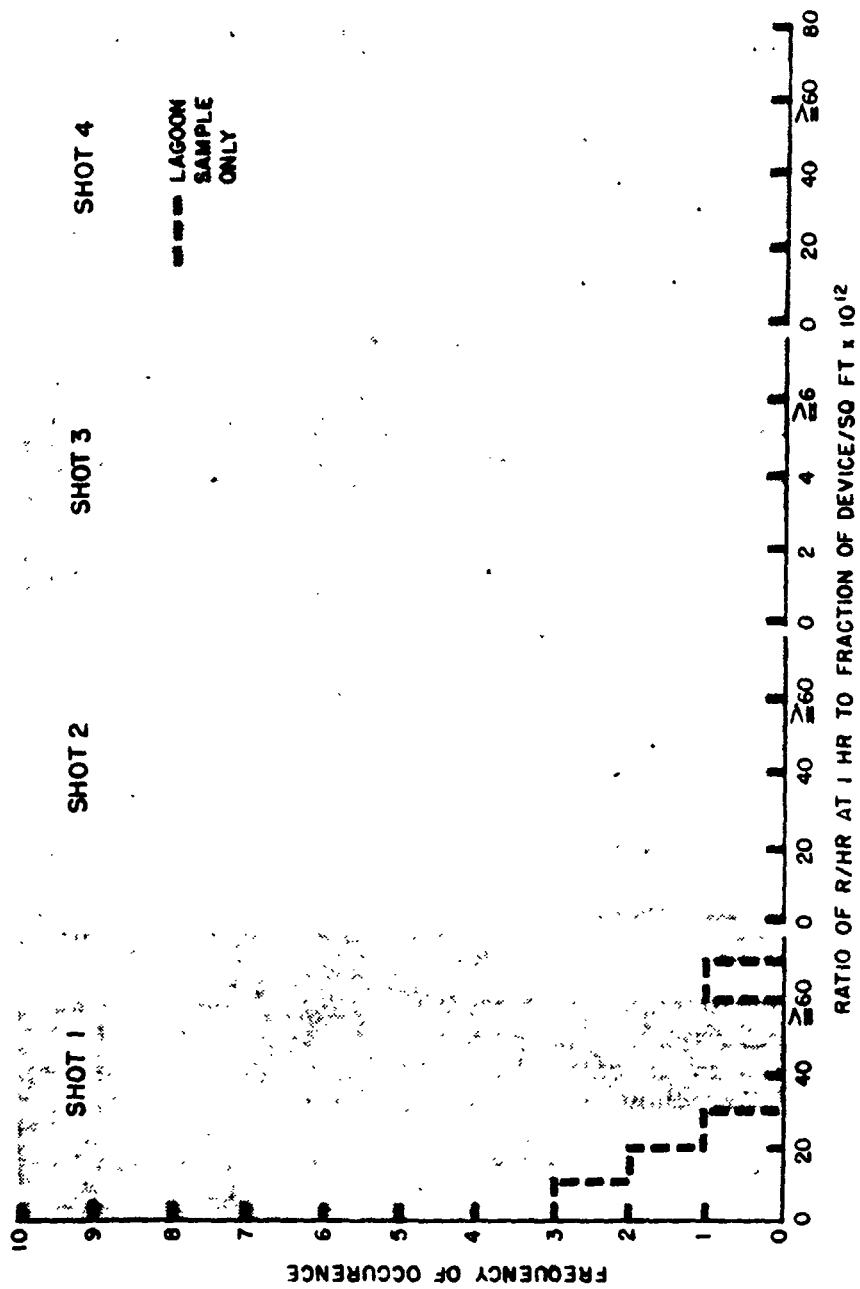


Fig. 3.17 Distribution of the Ratio of the Radiation Field to the Surface Density of the Device Fraction Component

given field reading corresponding to the sample area for all other samples is entirely unknown. With the available data and in view of the sample treatment from recovery to analysis, the following values were selected as a set of reasonable values for the radiation field to surface density ratio: (1) Coral (ratio of r/hr at 1 hr to mg coral per sq ft); Shot 1 - 0.04, Shot 2 - 25, Shot 3 - 0.05, (2) Sea water (ratio of r/hr at 1 hr to ml sea water per sq ft); Shot 2 - 20, Shot 3 - 200, Shot 4 - 10, (3) Device Components (ratio of r/hr at 1 hr to fraction of device per sq ft); Shot 1 - 20×10^{12} , Shot 2 - 25×10^{12} , Shot 3 - 3×10^{12} , Shot 4 - 50×10^{12} . The constancy of these values should serve as a means of testing the reliability of sampling methods, testing the reliability of the component analysis for tracing fallout components, and, in the absence of a radioactive component (fission product surface density data), to furnish a guide as to the radiation field associated with a given surface density of debris material.

CHAPTER 4

PHYSICAL MEASUREMENTS

The aerosol and fallout sampling devices discussed in this chapter were placed in the field primarily to obtain representative samples of active airborne material for measurements of particle size and concentration, activities, and the physical and chemical nature of individual particles. These objectives were only partially fulfilled.

In this chapter, aerosols are taken as dispersions of solid or liquid particles in air which are so small that they readily follow the streamlines of air set in motion by air-suction devices of various types. Fallout is that material which happens to deposit in or on various containers and surfaces. It is clear that the distinction is purely for instrumental convenience and that no actual dividing line exists.

4.1 PROPERTIES OF AEROSOLS

Efforts were made to determine the properties of the ambient aerosols sampled at three island stations, William, Yoke, and Zebra, and on the Project 6.4 YAG's.

4.1.1 Operational Record

Many unanticipated difficulties were experienced in the field. The unexpected size of Shot 1 and the fire on Tare destroyed all but two of the air filter heads, greatly curtailing the filter sampling effort subsequent to Shot 1. The millipore filters from Shot 1, though torn or punctured, collected a considerable amount of activity and were useful for some purposes. After exposing electrostatic precipitators on island stations for Shots 1, 2, and 3, with virtually no airborne activity arriving within the preset 6-hr sampling period, the island stations were abandoned and one ESP was installed on each of the Project 6.4 test ships, YAG 39 and YAG 40. The two salvaged air filter heads (DMT) were mounted on the flying bridge of YAG 40. Successful collections were obtained with these instruments from Shots 4 and 5, with the exception of the ESP on YAG 39, Shot 4. In this instance the plug to the aerosol inlet was inadvertently left in place during the sampling run.

4.1.2 Observations and Results

Results of the investigations of the properties of aerosols are summarized in a series of general observations on Shots 1, 2, 4, and 5, by a consideration of the physical state of the activity on the air filters and in measurement of the specific gravity of the settled active aerosols.

4.1.2.1 General Observations, Shot 1

Millipore filters were examined with the optical microscope by reflected and transmitted light. The general deposit consisted of large friable aggregations white in color, and frequently exhibiting black specks of adherent material. Autoradiographs of thin sections of the larger fallout particles (Section 4.3) show very little correlation between particle size and activity. Two general types of active particles were found; (1) surface-active, with some diffusion toward interior if the particle was exposed to water, and (2) approximately spherical, with the activity distributed throughout the particle volume.

In an effort to determine the physical nature of the radioactive components of these particles, DMT filter samples were leached in water and weak acetic acid, and filtered with the hydrosol type millipore filter. It was found that after the water leach, 76 per cent of the activity was retained on the filter, whereas after a weak acetic acid leach only 4 per cent was retained.

The active particles from the water leach, as disclosed by autoradiograph, were red-brown, red-gray, gray, and black, with some smooth and white (type 2, above). The white particles frequently presented black surface-occluded particles.

The active solids surviving the acetic acid leach were red-orange to black in color, irregular in shape, and generally lumpy in appearance. Small black specks were generally distributed about the surfaces. Other faint autographs were found for which no source could be located under 600X magnification.

Figure 4.1 comprises photomicrographs of the original, water leach, and acid leach active particles, while Fig. 4.2 gives their size distributions.

All MP filters recovered from Shot 1 were damaged to some extent by blast and large coral fragments tearing through the paper; consequently, the total airflow through the filters is unknown.

4.1.2.2 General Observations, Shot 2

The aerosol from this shot was fundamentally different from Shot 1, the explosion having taken place over water. Much of the information obtained was derived from MP filter samples from Project 6,4 with additional information sometimes available from ESP film samples⁹ and DMT filters.

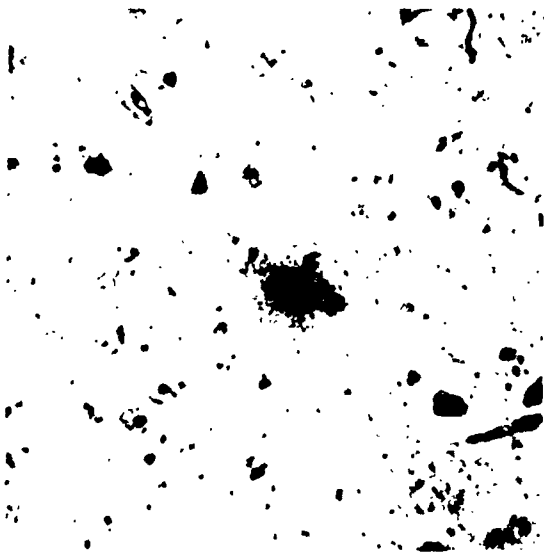
The millipore filters exposed topside on the washdown ship YAG 39 were intensely radioactive. The major portion of the radioactivity



a. Untreated



1 division = 100 μ



c. Acetic Acid Leach



b. Water Leach

Fig. 4.1 Photomicrographs of Aerosol Samples From Shot 1. Dark areas surrounding radioactive particles are autoradiographs on NTB nuclear emulsion

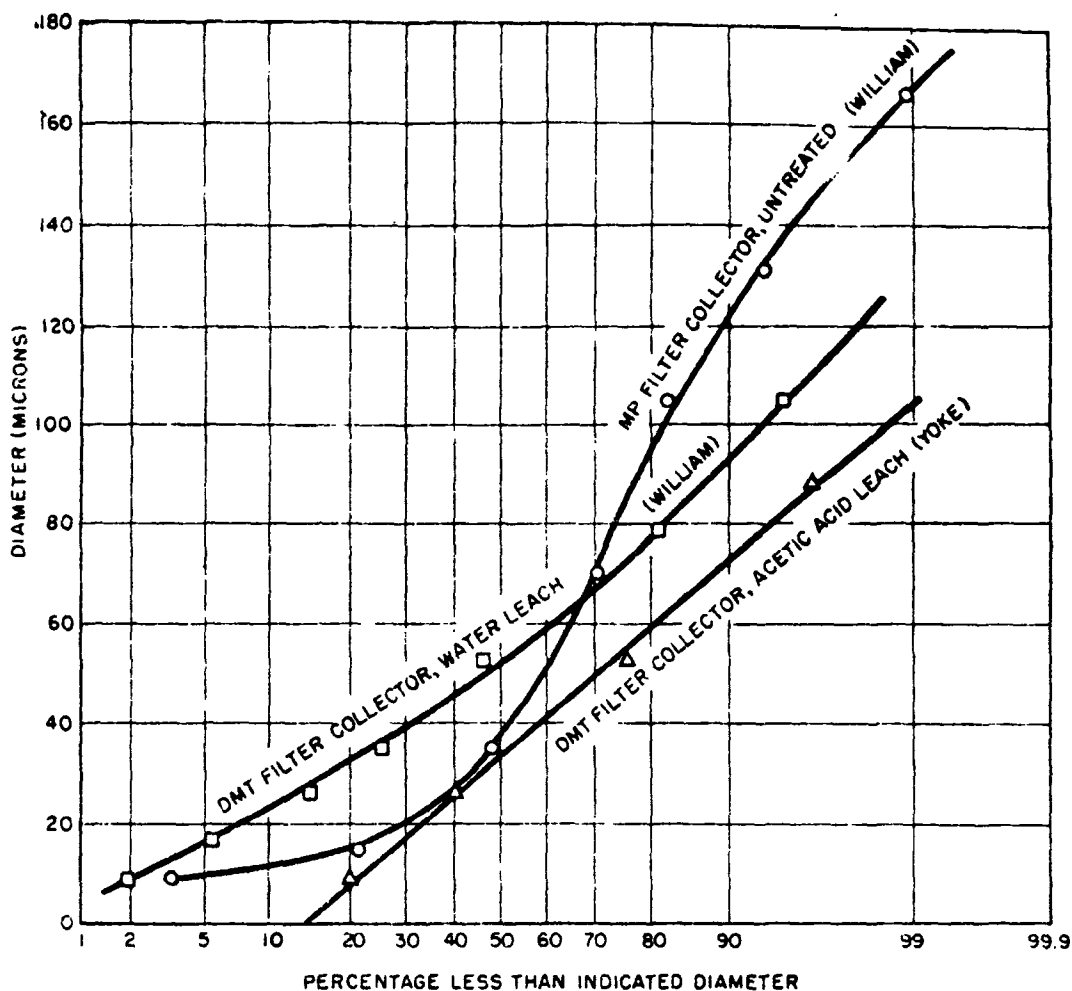


Fig. 4.2 Size Distribution of Active Aerosol Particles from Shot 1

appeared to have arrived at the filter in the form of liquid droplets, as shown by Fig. 4.3, a reproduction of an autograph of the filter on type K X-ray film. Examination of these active areas of the filter under the optical microscope revealed simply a deep tangled deposit of crystalline forms, with no specific resolvable source of activity other than the whole generalized mass covering the autograph. On the other hand, millipores exposed topside on YAG 40 were free from radioactive drop indications, as shown by the X-ray autograph also reproduced in Fig. 4.3

Microscopic examination of these filters autoradiographed with Eastman type NTB stripping film by a slightly modified technique developed at this Laboratory¹⁶ definitely associated the activity with material hardly describable as particles or crystals. They were flaky or ash-like, quite large ($\sim 10 \mu$ to 70μ) and generally distributed or smeared out in nebulous patches, as illustrated in Fig. 4.4. There were a few coral grains. In some areas of high concentration, the active material



a. Kingpost, YAG 39 (washdown)



b. Flying Bridge, IAG 40

Fig. 4.3 Autoradiographs of Millipore Filters, Shot 2
(Type K X-ray film Actual Size)



1 division = 1 μ

Fig. 4.4 Photomicrograph of Radioactive Aggregate, Shot 2. This sample was collected on a millipore filter mounted on flying bridge of YAG 40. Autoradiograph on NTB Nuclear emulsion surrounds activity.

was spread out in very large chains and clumps of crystalline aggregates, for which the term "particle size" becomes quite meaningless. It appears that the active aerosol material when collected was in the solid state, carrying no more water than the normal temperature-humidity equilibrium amount.

4.1.2.3 General Observations, Shot 4

Millipores exposed topside on YAG 40 appear to have collected a mixture of dry and liquid active aerosol material, as evidenced by the X-ray film autoradiographs in Fig. 4.5. A sample autograph of a topside MP filter from the washdown ship (YAG 39) is included for comparison. So far as is known, the MP filters on YAG 40 were not subjected to spray from other experimental equipment on the ship, or to natural rainfall before recovery. Again, NTB autoradiographs and microscopy identified the active centers as crystalline aggregates in the heavy deposits, and sometimes resolvable crystals arranged in a ring in the areas which obviously were struck by radioactive liquid droplets. The droplet autographs ranged from 1 to 2 mm in diameter. There was an almost continuous background blackening of the film due to very small low-activity crystals dispersed more or less uniformly over the face of the filter. Free NaCl crystals were generally present in low concentrations, with no associated radioactivity. Figure 4.6 comprises photomicrographs of two active centers and their autographs from the MP filter samples collected on the YAG 40 at deckhouse and flying bridge positions.

The ESP on YAG 40 functioned on Shot 4, collecting the most concentrated samples at zero plus 2 hr, and zero plus 5 1/2 hr. Qualitatively, the active deposits were identical to those on the MP filters. It was observed that in every case the activity was associated with a halide-reacted spot on the film. The active spot diameters were generally greater than 0.1 mm (the upper useful limit of the film); consequently, most of the impinging liquid droplets were smeared as the film wound onto the take-up reel. The active drop residue, distributed or aggregated within the spot boundary had the same appearance as the heavy active deposits on the MP filters, described above. The occurrence of active spots to inactive salt and fresh water drops was about 1 to 100.

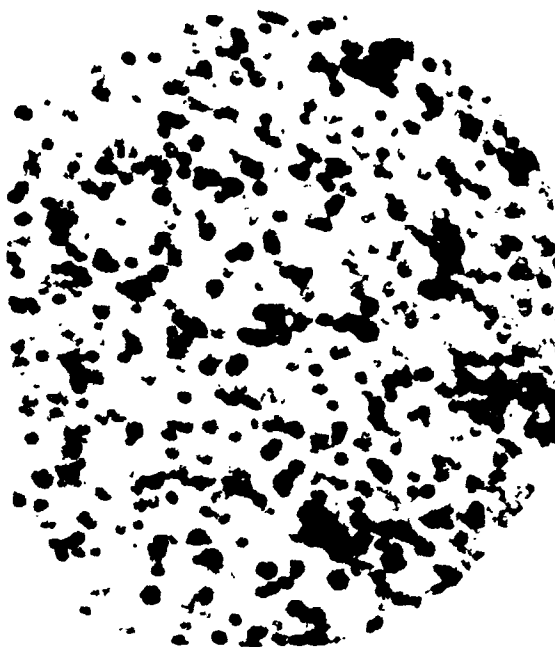
4.1.2.4 General Observations, Shot 5

On this shot MP filters exposed topside on the YAG's were badly damaged, apparently due to exposure to heavy rains following the period of active aerosol sampling.* The filters were in fragments, as shown by the X-ray film autographs of Fig. 4.7. The filter material was very

* Deduced from the recorded pressure drop across the venturi system of the MP filter pumps. The records from the topside samplers on YAG 39 and YAG 40 show three periods of simultaneous relief valve operation, which occurs only with excessive filter resistance.



a. Flying Bridge, YAG 40



b. Deck House, YAG 40



c. Kingpost, YAG 39 (washdown)

Fig. 4.5 Autoradiographs of Millipore Filters, Shot 4
(Type K I-ray film actual size)



a. Flying Bridge, YAG 40



b. Deckhouse, YAG 40

Fig. 4.6 Photomicrographs of Radioactive Areas of Millipore Filters, Shot 4. Black areas are autoradiographs on NTB nuclear emulsion.



a. Deckhouse, YAG 40



b. Kingpost, YAG 39 (washdown)

Fig. 4.7 Autoradiographs of Fragments of Millipore Filters, Shot 5.
(Type K X-ray film, actual size)

brittle, and would not dissolve in the usual solvents for millipores, suggesting possible radiation damage.

The ESP fared little better, some 70 ft of film at the start of the run being permanently glued together on the reel. Usable portions of the film, however, showed active deposits very similar to those of Shot 4, except that the spots were on the order of 1 or 2 mm in diameter. The active spots contained densely aggregated crystals containing Na, Ca, and Mg. It is believed that the aerosol from this shot was identical to that of Shot 4, with the possible exception of having a slightly higher liquid-solid ratio.

4.1.2.5 Physical State of Activity on Air Filters

DMT and MP filters were also used as a source of activity for physical state studies. MP samples were dissolved in a suitable solvent, and thoroughly dispersed by ultrasonic agitation. The specific activity was then determined, after which an aliquot was centrifuged* and the specific activity of the supernatant again measured, yielding fractions of activity associated with the insoluble residue and liquid portions.

TABLE 4.1 - Physical State of Activity

Shot	Sample	Solvent	Per Cent Total Activity		
			Insoluble Solids ^(a)	Ionic	Colloidal
1	Yoke (DMT)	Weak Acetic Acid	4	96	0
	William (DMT)	Water	76	23	1
2	Kingpost YAG 39 (MP)	Ethyl Acetate	95	-	-
	"	Acetone	95	4.9 ^(b)	0.1
4	Flying bridge YAG 39 (DMT)	Water	89	10	1
	Deckhouse YAG 40 (MP)	Acetone	98	-	-
5	Flying bridge YAG 40 (DMT)	Water	49	47	4
	Kingpost YAG 39 (MP)	Ethyl Acetate	97	-	-

(a) Values for MP samples include colloidal.

(b) Acetone decanted after centrifugation, water added to centrifugate and electro dialysed.

* Air-driven, capable of settling 0.01 to 0.1 μ diameter gold sol at approximately 20,000 RPM.

DMT samples, free of the filter after sublimation, were leached directly in water, and filtered through the hydrosol type MP filter for the insoluble residue fraction. The filtrate was electro-dialyzed for the colloidal and ionic fractions. Results of these measurements appear in Table 4.1.

The various fractions reported above do not refer to the state of the active aerosol as it existed in the field, as all filter samples were of course in the solid state when received at the Laboratory. The purpose was to determine if any significant amount of activity were associated with colloidal particles in the aerosol. The results indicate a negative conclusion.

4.1.2.6 Specific Gravity of Settled Radioactive Aerosol

A number of shallow trays containing a thin layer of salicylic acid crystals were placed on the floors of test compartments in the ships YAG 39 and YAG 40. The active material settling out on the crystal bed was transferred with the crystals to a small container, where the salicylic acid was sublimed off, resulting in a concentrated sample.

The distribution of activity with respect to specific gravity was determined by counting the precipitate following successive centrifugations of the sample in bromobenzene-bromoform mixtures of increasing density. Results appear in Table 4.2

It should be emphasized that these measurements apply only to that portion of the radioactive fallout and aerosol material which reached the ships, penetrated a curtain of exhaust smoke (and washdown spray, in some cases), entered the vent system, traversed some 50 ft of duct, and settled to the compartment floor. It is possible, if not probable, that the modal specific gravity of ~2.0 is due to carbon (Sp. gr. = 1.8 to 2.25) and oil droplets acting as carriers. The Shot 5 sample was particularly black and oily in appearance.

4.2 PROPERTIES OF FALLOUT (SHOT 1)

The flour-tray drop sampling instruments³³ were designed to sample liquid fallout over the size range of natural raindrops. Trays of flour (exposed area = 14 sq in) were serially exposed to the fallout, liquid drops forming pellets in the flour and solid particles retaining their identity. The flour trays were shipped to USNRDL, the flour sieved, weighed, counted, and in some cases, thin-sectioned. In the event of mixed liquid-solid fallout, the presumption was that the drop-formed flour pellets could be easily distinguished from solid fallout material by means of a water-soluble dye (in powder form) mixed with the flour. Water produced pellets would then be distinctively colored, in contrast to solid fallout particles which would retain their natural appearance or at most be coated with the dry, white, flour-dye mixture.

TABLE 4.2 - Specific Gravity of Active Material Settling on Decks of Ships Compartments

A. Shots 2 and 4

Specific Gravity	Per Cent Total Beta Activity in Fraction				
	Shot 2(a)	Shot 2(b)	Shot 2(c)	Shot 4(a)	Shot 4(b)
≤ 1.50	9.7	8.9	19	5.5	7.3
1.50 - 1.98	42	56	67	13	44
1.98 - 2.30	24	4.9	9.4	70	42
2.30 - 2.45	4.6	9.4	2.2	0.9	2.1
2.45 - 2.58	1.2	9.3	1.2	1.4	1.5
2.58 - 2.77	0.4	1.1	0.3	0.7	0.7
2.77 - 2.85	0.2	1.5	0.3	1.6	0.4
> 2.85	18	8.5	0.3	6.8	1.9

B. Shot 5

Specific Gravity	Per Cent Total Beta Activity in Fraction(a)
≤ 1.50	9.2
1.50 - 2.10	52
2.10 - 2.37	28
2.37 - 2.51	3.2
2.51 - 2.52	1.5
2.62 - 2.80	2.0
2.80 - 2.85	0.7
> 2.85	3.2

- (a) Unprotected Ventilation System, 670 cfm, YAG 40
 (b) Unprotected Ventilation System, 1000 cfm, YAG 39 (washdown)
 (c) Unprotected Ventilation System, 1000 cfm YAG 40

Due to procurement difficulties, no proper dye could be obtained in time for Shot 1, which produced great quantities of white coral fallout. Attempts at separation of flour pellets and coral grains have proved to be unreliable, making it impossible to determine the water-coral ratio of the fallout.

4.2.1 Distribution of Activity with Particle Size

Gross samples, therefore, were sieved,* weighed and counted, with the resulting size-activity data of the mixture reported in Table 4.3.

The size fractions indicated in the table were analyzed for Na by the wet ash method, capable of detecting $0.20 \pm 0.05 \mu\text{g}$ of Na. Only background amounts of Na were found.

Following the sieving runs, fallout samples from other collection devices were received, from which it was learned that most of the active coral particles, altered by heat and water to $\text{Ca}(\text{OH})_2$, were friable, a development casting doubt on the validity of the sieve-determined size distributions.

A total of nine collection devices were exposed on Shot 1, of which Love cycled two trays (combined in Table 4.3), with one cycling at Oboe, Uncle, William, and Zebra. The remaining instruments, positioned at Fox, How, Nan, and Yoke, suffered various combinations of malfunction due to blast damage and flooding. Spare parts, stock flour, and pre-loaded trays stored on Tare were destroyed by fire. Further drop sampling was abandoned.

4.3 INDIVIDUAL PARTICLE COMPOSITION AND CHARACTERISTICS

The work reported in this section was undertaken to obtain a description of the internal structure, chemical composition, and distribution of radioactivity within the radioactive fallout particles collected following Shot 1. A description of a likely mechanism of formation of the fallout particles is given.

4.3.1 General Description

Most of the particles studied were collected in sampling devices which were distributed in a comprehensive array over the lagoon and islands of Bikini atoll. The wind directions at shot time were such that the main path of the fallout passed over many of the collecting stations. The particles selected for study were chosen from stations over as great an area as possible. The greatest number of particles were, however, chosen from stations in or near the path of heaviest fallout.

Two techniques were used in studying the particles: X-ray diffraction analyses of individual particles and the observation under the petrographic microscope of thin sections ground from individual particles. 3,2/

* Mechanical agitation was employed for about 1 min, followed by manual sieving and brushing on the 50- and 60-mesh screens.

TABLE 4.3 - Distribution of Fallout Activity^(a) with Particle Size
Shot 1

Sampler Location		Size Range, mm.						
		>1.9 ^(b)	1.9-0.93	0.93-0.57	0.57-0.42	0.42-0.29	0.29-0.26	< 0.26
Love	Activity(mv)	135.0	33.06	33.67	19.69	14.58	4.08	89.23
	Wt(g)	4.542	0.662(c)	0.414(c)	0.217	0.108	0.0598	-
	Specific Activity(mv/g)	29.7	49.9	81.3	90.7	135.	68.2	-
Oboe	Activity(mv)	1.84	4.17	1.94	0.656	1.79	0.005	6.50
	Wt(g)	0.132	0.292	0.150(c)	0.0915	0.0669	0.0016	-
	Sp. Activity (mv/g)	13.9	14.3	12.9	7.17	26.8	3.13	-
Uncle	Activity(mv)	0.121	2.57	1.79	3.30	1.12	0.0814	12.46
	Weight(g)	0.083	0.188	0.715(c)	1.410	0.961	0.057	-
	Sp. Activity (mv/g)	1.47	13.7	2.50	2.34	1.16	1.43	-
William	Activity(mv)	4.70	1.12	1.31	1.12	1.65	0.024	8.19
	Weight(g)	1.704	0.106	0.198(c)	0.174	0.150	0.002	-
	Sp. Activity (mv/g)	2.76	2.76	6.60	6.45	11.0	11.80	-
Zebra	Activity(mv)	0.307	2.09	3.73	1.12	1.16	0.016	11.64
	Weight(g)	0.068	0.394(c)	0.661	0.432	0.252	0.009	-
	Sp. Activity (mv/g)	4.53	5.30	5.64	2.59	4.60	1.72	-

(a) Measured by 4 π gamma chamber, 9 March 1954. 0.1 mg radium produces a reading of 78 mv.

(b) The fraction >1.9mm generally contained pieces of flour crust, mold, organic debris, etc.

(c) Analysis made for sodium content. Background amounts only detected.

The radioactive fallout particles were white, opaque, irregularly shaped grains. Some of them were fluffy and very fragile while others appeared hard and dense. They varied in size from about 25 μ to 1 or 2 mm. in diameter. X-ray diffraction analyses showed that they were composed primarily of calcium hydroxide and calcium carbonate (calcite structure). Other compounds occurring in minor amounts were calcium oxide, calcium carbonate (aragonite structure), sodium chloride and magnesium carbonate tri-hydrate. Tentatively identified as present in several particles were calcium nitrate tetra-hydrate and calcium sulfate dihydrate and hemihydrate.

Studying the thin sections of the fallout particles with the petrographic microscope gave a detailed picture of the distribution of the hydroxide and carbonate. Most of the particles were composed largely of calcium hydroxide in the central part with an outer layer of calcium carbonate. The thickness of the outer layer of carbonate varied from a few microns up to about 100 μ . While the areas of the two compounds were distinct, the transition between them was sufficiently gradual to indicate that the outer carbonate layer had been formed by the carbonation of the calcium hydroxide.

Occasionally, a particle was found with an inner core of unaltered calcium carbonate and an outer zone of calcium hydroxide.

A few particles were found with cores of calcium oxide the outer layer of which had been hydrated to calcium hydroxide.

Some radioactive particles consisting of unaltered coral grains were found.

4.3.2 Distribution of Activity

By making radioautographs of the thin sections with Eastman NTB stripping film, a knowledge of the distribution of the radioactivity within the particles was obtained. In practically all of the thin sections studied, the radioactivity was located on the exterior of the particle. The activity was most intense on the surface and diminished fairly abruptly to very low levels at depths of 50 to 150 μ . The graded appearance of the boundary suggested that the penetration of the activity into the particle was by solution and deposition. The distribution of the activity was independent of the compositional structure of the particle.

In a few instances, the radioactivity was distributed irregularly in patches throughout the particles. In these cases, the particles themselves usually had spherical or spheroidal shapes as contrasted with the angular shapes of the particles in which the activity was found on the exterior.

4.3.3 Solubility Studies

Four samples of fallout material from Shot 1 were leached in water for varying times. An initial separation was then made into soluble and insoluble fractions by filtering the suspensions through millipore filters. According to the manufacturer's description, millipore filters are completely retentive for particles one-half micron and larger in diameter. The filtrate was then subdivided into ionic and colloidal fractions by treatment in an electrodialysis cell. The results are tabulated below:

	Sample 1	Sample 2	Sample 3	Sample 4
Activity remaining in the insoluble residue	76%	82%	96%	98%
Soluble activity in ionic form	23%	8%	4%	2%
Activity in colloidal form	1%	Trace	Trace	Trace

The percentages refer to the comparative counting rates of each fraction as measured with an end-window GM tube under the same geometrical conditions. These results are consistent with those found in similar studies on fallout performed at the site (see Tables 3.5 and 3.6).

Sample 1 was obtained from a DMT filter. The sample was leached in water for 3 days and was 20 days old at the beginning of the experiment.

Sample 2 was obtained from a DMT filter. The sample was leached in water for 4 weeks and was 25 days old at the beginning of the experiment.

Sample 3 consisted of several fallout particles obtained from a belt sampler.^{29/} The sample was leached in water for 2 weeks and was 6 1/2 months old at the beginning of the experiment.

Sample 4 consisted of several fallout particles obtained from a belt sampler. The sample was leached in water for 3 weeks and was 6 1/2 months old at the beginning of the experiment.

4.3.4 Mechanism of Formation

The processes by which the fallout particles originated can be described as follows. The material constituting the non-active body of the fallout particle was derived from the coral atoll. Modern reef building corals are composed mostly of the calcium carbonate chiefly in the form of aragonite. The effect of the bomb detonation was to heat and throw aloft a huge amount of coral dust. Most of the coral dust which was close enough to the explosion to become contaminated with radioactivity was heated sufficiently to drive off carbon dioxide and to form calcium oxide. These calcium oxide particles swept off the condensing fission products which were probably in the form of very small metallic or metallic oxide particles. At some subsequent time, as the cloud cooled, the calcium oxide hydrated to calcium hydroxide. This could easily have occurred while the particles were still in the air since large amounts of sea water were evaporated and blown into the air by the explosion. In some cases, the hydration was not complete as shown by the examples of several particles still retaining cores of unaltered calcium oxide.

Probably during the hydration process a part of the soluble fraction of the radioactive material went into solution and diffused into the particle leaving a zone of radioactivity which was most intense on the surface and diminished gradually to very low levels within a distance of about 100 μ .

At about the same time, the outer surfaces of the calcium hydroxide particles must have been carbonated by the carbon dioxide of the atmosphere. It is well known from observations on the hardening of plaster (calcium hydroxide) that the outer layer of the plaster is slowly converted to calcium carbonate in the presence of moist air. The fallout particles were exposed to moist tropical air several days before their shipment to this Laboratory. A study of the thin sections plainly showed the progressive carbonation of the calcium hydroxide which was, however, confined to a surface layer usually not exceeding 100 μ in thickness. Any calcium carbonate formed in this manner would probably have the calcite structure as this is the stable form at low temperatures. The X-ray diffraction analyses showed the presence of both calcite and aragonite (unaltered coral) in the fallout particles. However, the amount of calcite was much greater than the amount of aragonite indicating that most of the calcium carbonate in the fallout particles was of this secondary origin.

It seems probable that most of the fallout particles were formed from discrete grains of coral rather than by the agglomeration of pulverized materials. This is evidenced by the homogeneity of the particle in texture and composition, by the angular shape of the particle and by the occurrence in some particles of a central core of unaltered coral surrounded by a layer of calcium hydroxide.

A few of the particles, however, showed definite signs of being formed by accretion. They had spherical or sub-spherical shapes and were not homogeneous but were formed of agglomerations of crystalline grains and the radioactivity was distributed irregularly throughout the particle.

Some of the particles were not close enough to the fireball to be decarbonated and remained unaltered except for collecting a surface coating of radioactivity.

CHAPTER 5

RADIOCHEMICAL MEASUREMENTS

Gross decay, energy spectra, and radiochemical composition of material resulting from the various detonations were determined. Fission product yields and neutron induced radionuclides were measured. From this information computations were made of the extent of fractionation of the bomb constituents and also the fraction of the bomb per unit area collected at several fallout stations.

5.1 RADIATION CHARACTERISTICS OF GROSS FALLOUT SAMPLES

Beta and gamma decay were observed at the site as well as at USNRDL with geiger counters, proportional gas-flow counters, and scintillation counters. Gamma ionization decay was observed on a single sample from Shot 4 in cooperation with Project 6.4. Both absorption and gamma spectra measurements were made.

5.1.1 Preparation of Counting Samples

Counting sources for decay and absorption measurements were made by taking a measured amount of the fallout material from various collectors. These fallout samples were carefully aliquoted so that the total beta and gamma count of the fallout in the collector could be determined. Fallout in the form of solids, or slurries containing coral was dissolved with a minimum amount of HCl before the counting sample was taken. Liquid fallout was sampled directly. The source for the beta counting was prepared by pipetting an aliquot of the solution onto a piece of rubber hydrochloride plastic (2 x 2 x 0.00094 in.) which had been loosely spread over a glass planchet (1 in. o.d. x 1/4 in. deep). This arrangement confined the solution to an area about 2 cm in diameter. The solution was then evaporated under an infrared lamp placed at sufficient distance to prevent the rubber hydrochloride from melting. When the solution had completely evaporated, the sheet containing the dried contaminant was mounted on a stiff piece of cellulose acetate (3-5/16 x 2-1/2 x 1/32 in.) with a 1-3/8 in. hole in the center. The rubber hydrochloride sheet was sealed to the back of the cellulose acetate with scotch tape so that the contaminated area was centered in the hole. Krylon plastic was sprayed over the top of the counting sample. The Krylon tended to

contract the rubber hydrochloride to a smooth, taut surface. The backing and cover for the counting sample which were made of a very thin film of low atomic weight materials reduced self-absorption and back-scattering of the beta rays to a minimum. On Shot 1 the beta counting samples were prepared in glass planchets because of the large amount of solids; these samples were quite thick so that those beta decay data for Shot 1 were subject to considerable self-absorption of the soft components.

Gamma counting samples were prepared in glass planchets 1 in. o.d. from the same solutions as the beta sources. After drying, the sample was coated lightly with Krylon.

5.1.2 Gross Decay

Beta and gamma decay measurements were taken of all fallout samples received and processed by the field laboratory for Shots 1 through 4 to check for gross fractionation in the fallout.

The gross beta decay of the fallout samples from Shots 1 through 4 are given in Table 5.1 and are plotted in Fig. 5.1. The gross gamma decay data are given in Table 5.2, and are plotted in Fig. 5.2. The relative count in each case was normalized to the number given in parentheses at + 10 days.

5.1.2.1 Shot 1

The gross beta and gamma decay data are average values of all the fallout samples received at the site laboratory (Chapter 3). In addition, some values for the gamma decay (later than 10 days) were obtained from Project 2.5a as an average decay of five active particles from gummed paper samples.

5.1.2.2 Shot 2

The early gamma decay was taken on a gummed paper collector exposed to fallout at Parry Island on shot day. Fallout arrived at about 1800 to 1830 hr or + 12 hr after shot time. The sample, consisting of a one sq ft folded paper did not prove suitable for beta decay measurements. The beta decay and gamma decay data from 3 days are an averaged decay of all the fallout samples received at the site laboratory.

5.1.2.3 Shot 3

The beta decay data and the gamma data are averaged values of the decay of all the samples received at the site laboratory.

5.1.2.4 Shot 4

Beta decay was observed on a sample recovered aboard the YAG-39 (Project 6.4) at + 80 min. Gamma decay was started at + 4.8 hr. Both decays were initially observed on a GM counter. Due to the high background, high-counting samples were required. A gamma ionization decay

TABLE 5.1 - Gross Beta Decay

Shot 1		Shot 2		Shot 3		Shot 4	
t(days)	Relative Count						
7.46	1.87(b)	3.30	2.50(a)	3.62	0.962(a)	0.0575	30.6(b)
8.33	1.51	3.72	2.20	4.54	0.740	0.0596	27.7
9.10	1.26	4.28	1.82	5.10	0.648	0.0625	27.1
10.0	(1.00)			6.18	0.512	0.0646	26.0
10.2	0.987	5.21	1.42	7.33	0.397	0.0695	22.0
11.1	0.804	6.21	1.13	8.08	0.327	0.0708	21.4
12.0	0.676	7.21	0.898	9.12	0.258	0.0779	19.3
14.2	0.460	8.22	0.707	10.00	(0.215)	0.0800	17.5
15.1	0.393	9.21	0.574	10.2	0.210	0.0842	16.6
22.2	0.170(d)	10.0	(0.473)	12.1	0.146	0.0863	15.7
25.2	0.138	10.1	0.470	16.1	0.0860	0.0896	14.3
26.1	0.133(b)	11.1	0.372	22.2	0.0479(c)	0.0946	13.3
31.0	0.0970(d)	16.3	0.163	43.1	0.0186	0.0992	12.4
39.2	0.0673	21.1	0.102	48.2	0.0158	0.108	10.9
45.2	0.0540	25.1	0.0739	62.0	0.0108	0.115	10.3
53.2	0.0428	33.1	0.0459	99.1	0.00578	0.130	9.02
67.0	0.0304	54.1	0.0231	105.9	0.00524	0.149	7.48
75.8	0.0259	59.2	0.0201	110.9	0.00484	0.161	6.83
87.4	0.0212	72.9	0.0143	118.0	0.00460	0.164	6.70
		110.1	0.00782(c)	125.0	0.00427	0.169	6.40
		116.9	0.00713	131.9	0.00398	0.174	5.99
		121.9	0.00664	145.9	0.00345	0.185	5.87
		129.0	0.00624	161.1	0.00295	0.210	5.18
		136.0	0.00571	173.9	0.00269	0.219	4.53
		142.9	0.00532			0.234	4.44
		156.9	0.00461			0.274	4.24
		172.1	0.00402			0.325	3.59
		184.9	0.00365			0.370	3.22
						0.420	3.01
						0.464	2.78
						0.554	2.27
						0.628	2.04
						0.641	1.91
						0.747	1.72
						0.758	1.63
						0.943	1.33
						0.989	1.27
						1.02	1.20
						1.14	1.08

TABLE 5.1 Gross Beta Decay (Cont.)

Shot 1		Shot 2		Shot 3		Shot 4	
t(days)	Relative Count						
						1.29	0.932
						1.39	0.866(a)
						1.57	0.807
						1.69	0.742
						2.11	0.615
						2.60	0.511
						3.18	0.423
						4.14	0.323
						5.10	0.251
						8.95	0.121
						10.00	(0.100)
						11.00	0.0856
						24.1	0.0234(c)
						29.2	0.0173
						43.2	0.00910
						30.2	0.00431
						87.1	0.00392
						92.1	0.00367
						99.2	0.00330
						106.1	0.00304
						113.1	0.00288
						127.1	0.00248
						142.2	0.00211
						154.9	0.00190

- (a) Beta counter (gas flow)
- (b) Geiger counter
- (c) Beta counter #2, USNRDL
- (d) Beta counter, USNRDL (L. McIsaac)

The same superscript is implied for all undesignated quantities immediately following one that is designated.

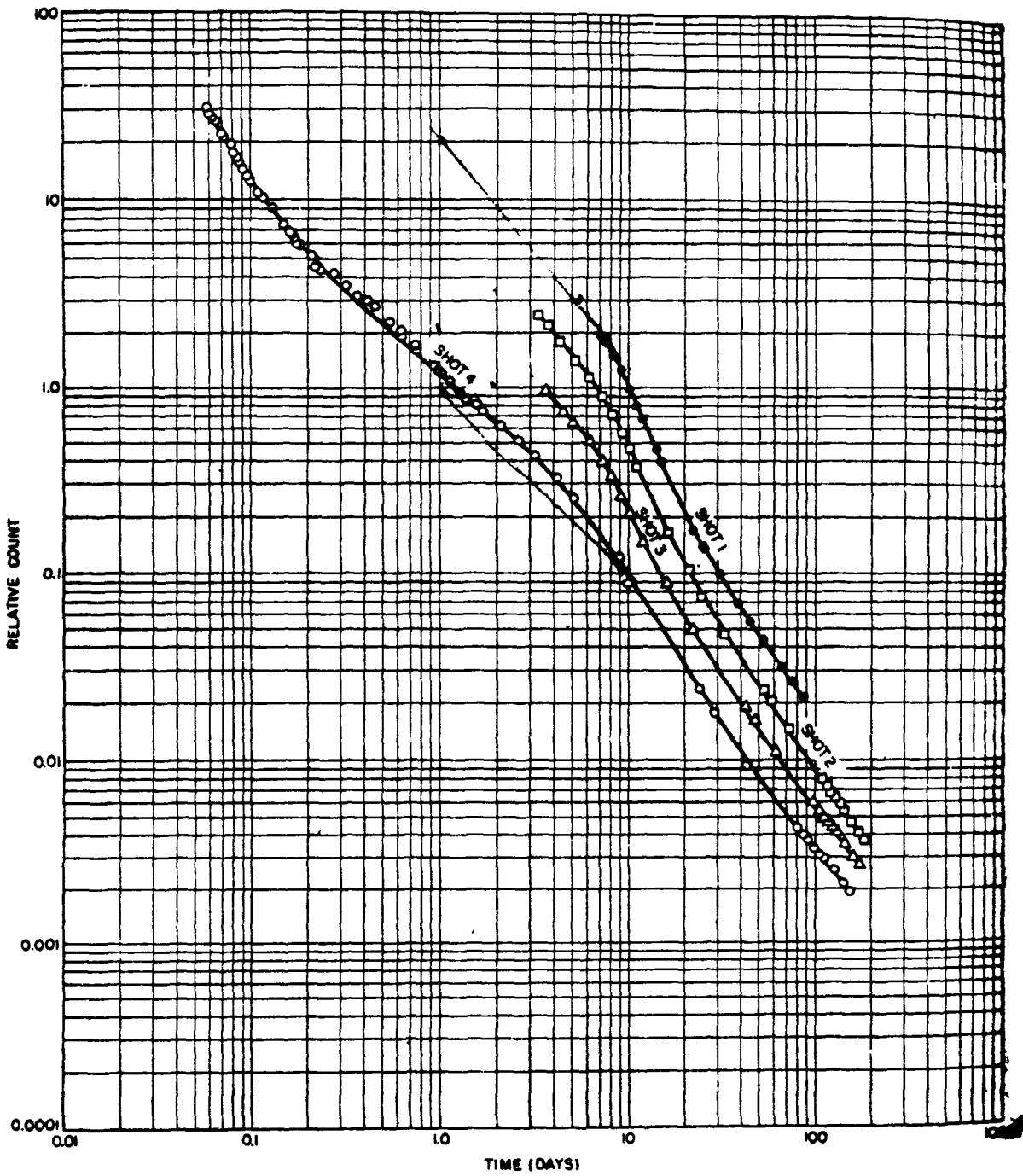


Fig. 5.1 Gross Beta Decay of Fallout Samples From Shots 1, 2, 3, and 4

TABLE 5.2 Gross Gamma Decay

Shot 1		Shot 2		Shot 3		Shot 4	
t(days)	Relative Counts						
5.41	3.05(a)	0.638	13.4(a)	3.38	1.06(b)	0.197	7.72(f)
5.62	2.97	0.664	13.3	3.51	1.00	0.207	7.13
6.10	2.64	0.690	13.0	3.60	1.00(c)	0.239	5.66
6.37	2.33	0.707	12.6	4.08	0.880	0.276	4.47
7.43	1.91	0.812	11.1	4.20	0.850(b)	0.328	3.46
8.08	1.52	0.896	10.3	4.32	0.811	0.374	2.77
8.29	1.46	0.979	9.50	4.48	0.785(c)	0.418	2.52
8.96	1.18(e)	1.06	8.94	5.10	0.674	0.468	2.26
9.10	1.23(a)	1.19	7.77	5.51	0.602(b)	0.548	1.86
9.15	1.20(b)	1.26	7.37	6.08	0.527(c)	0.635	1.57
9.52	1.11	1.44	6.39	6.55	0.471(b)	0.750	1.29
10.00	(1.00)	1.63	5.56	7.28	0.392(c)	0.932	1.08
10.03	0.995(abe)	2.04	4.38	7.50	0.374(b)	1.02	0.981
10.9	0.815(e)	2.48	3.56	8.20	0.325(c)	1.15	0.865
11.1	0.798(b)	3.07	2.88	9.08	0.260	1.29	0.743
12.1	0.656(abe)	3.38	2.45(b)	9.14	0.258(b)	1.42	0.726(c)
13.0	0.576(e)	3.51	2.28(a)	10.00	(0.215)	1.54	0.658(b)
14.0	0.474	3.53	2.31(c)	11.1	0.174	1.63	0.654(a)
14.2	0.461(b)	3.55	2.34(b)	12.1	0.143(bc)	1.70	0.635
15.0	0.416(e)	3.72	2.18(c)	14.1	0.0994(b)	1.81	0.594(b)
15.1	0.395(b)	4.03	2.00(a)	17.4	0.0635	2.12	0.522(ab)
16.0	0.356(e)	4.16	1.97(bc)	18.2	0.0550	2.22	0.508
17.2	0.304	4.55	1.79(b)	18.5	0.0528	2.39	0.490(b)
18.1	0.272	4.57	1.61(a)	21.6	0.0402	2.47	0.462(a)
18.2	0.255(b)	5.08	1.53(b)	22.2	0.0367(c)	2.66	0.448(ac)
19.0	0.245(e)	5.14	1.35(a)	29.1	0.0242(b)	3.13	0.386(ab)
20.0	0.218	5.20	1.47(c)	34.2	0.0184	3.35	0.357(c)
21.9	0.180	5.53	1.38(b)	37.1	0.0166	3.46	0.349(a)
22.4	0.164(a)	6.09	1.17(c)	38.1	0.0160	3.66	0.332
23.2	0.161(e)	6.14	1.11(a)	43.1	0.00992(c)	4.11	0.297(abc)
24.0	0.150	6.20	1.16(b)	52.1	0.00918(b)	5.10	0.243(c)
24.9	0.140	6.55	1.06	62.1	0.00476(c)	6.25	0.206(d)
25.8	0.130	7.11	0.921(c)	101.1	0.00190(d)	8.15	0.146
26.3	0.122(a)	7.17	0.818(a)	114.5	0.00163	8.92	0.126
27.0	0.119(e)	7.32	0.877(b)	125.0	0.00145	9.20	0.116
30.0	0.0992	8.10	0.719(c)	132.0	0.00133	10.00	(0.100)
30.2	0.0970(b)	8.49	0.610(a)	138.9	0.00124	10.1	0.0982
31.0	0.0928(e)	8.52	0.664(b)	145.9	0.00113	10.9	0.0837
32.0	0.0868	9.08	0.573(c)	161.1	0.00101	12.2	0.0710
33.0	0.0808	9.11	0.555(a)	173.9	0.000857	15.1	0.0449
36.1	0.0744	9.34	0.544(b)			16.1	0.0408
37.1	0.0698	10.00	(0.473)			16.9	0.0378

TABLE 5.2 - Gross Gamma Decay (Cont)

Shot 1		Shot 2		Shot 3		Shot 4	
t(days)	Relative Counts						
38.0	0.0640	10.1	0.461(c)			17.9	0.0339
39.0	0.0619	10.3	0.438(b)			21.9	0.0225
59.1	0.0354	11.1	0.375			23.1	0.0204
		11.2	0.371(c)			24.1	0.0184
		11.4	0.382(a)			25.0	0.0168
		12.2	0.295(b)			29.9	0.0127
		13.2	0.245			31.0	0.0118
		14.1	0.209			32.0	0.00983
		15.3	0.172			37.0	0.00748
		16.3	0.146(c)			43.1	0.00519
		16.5	0.142(b)			82.2	0.00154
		17.6	0.122			89.1	0.00141
		18.5	0.109			92.1	0.00131
		20.1	0.0895			93.1	0.00120
		21.1	0.0803(c)			106.2	0.00114
		23.1	0.0672			113.2	0.00104
		25.1	0.0564			127.0	0.000856
		25.2	0.0545			142.2	0.000741
		28.4	0.0447			154.9	0.000655
		32.6	0.0				
		33.3	0.0326(c)				
		40.1	0.0236(b)				
		45.2	0.0192				
		54.1	0.0138				
		59.2	0.0118				
		63.2	0.0105				
		73.0	0.00805				
		112.0	0.00358				
		122.0	0.00304				
		129.0	0.00288				
		135.9	0.00260				
		143.0	0.00243				
		150.0	0.00221				
		156.9	0.00199				
		172.1	0.00174				
		184.9	0.00153				

- (a) Gamma counter #1 (hut)
- (b) " " #2 (trailer)
- (c) " " #3 (cave)
- (d) " " #2 USNRDL
- (e) " " USNRDL (E. Schuert)
- (f) Geiger Counter

The same superscript is implied for all undesignated quantities immediately following one that is designated.

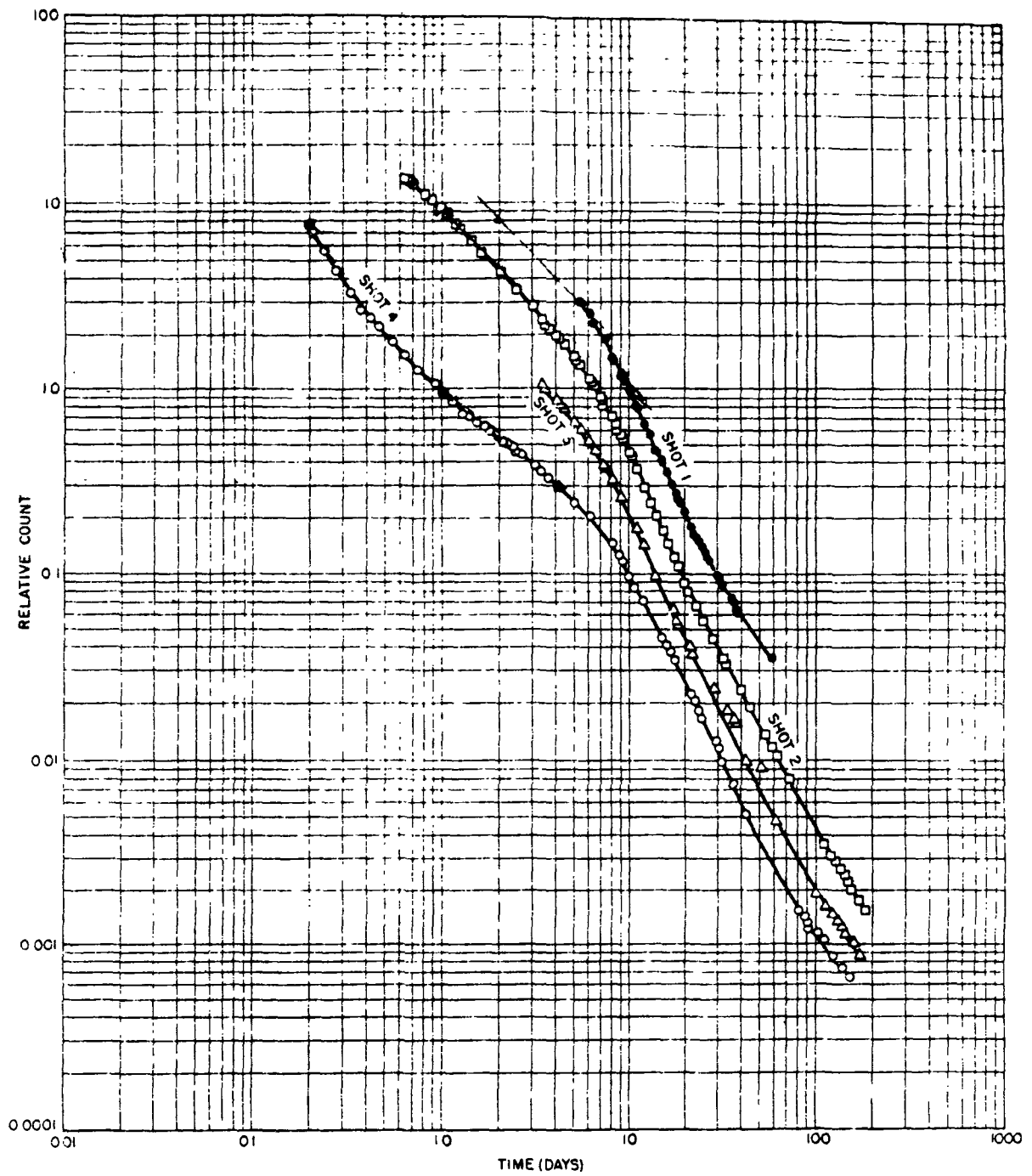


Fig. 5.2 Gross Gamma Decay of Fallout Samples From Shots 1, 2, 3, and 4

sample was prepared in which a Project 6.4 ion chamber was sealed and immersed in a 1-gal polyethylene bottle containing radioactive washdown water diluted sufficiently with dilute acid to give an activity within the operating range of the detector. The ionization decay data are given in Table 5.3 and are plotted in Fig. 5.3. Survey meter readings at the time indicated background within the shielding to be about 5 to 10 per cent of the room reading as measured at station 73A (Project 6.4 ion chamber). In general, the main background source was above the chambers; however, at + 7 hr the background increased rapidly due to higher concentrations of activity in the sea about the ship. With the background source being mainly from the hull, station 73A readings would be more affected than those of the sample since it was much nearer the hull. Accordingly, from + 7 to + 16 hr, 5 per cent of 73A was used as a background correction instead of 10 per cent as was used for all other readings. A new chamber was set up at USNRDL to continue the decay after return of the YAG's. The data for + 120 to + 150 days gave a decay of $t^{-1.4}$.

The high-counting samples as well as background on the YAG 39 proved to be in the severe coincidence loss region of the geiger tube. Before disembarking, two of the decay samples were utilized as split samples to determine the coincidence corrections at the operating counting rates. The readings are given in Table 5.4 along with the standard and background reading, R_b for the holder. The background readings show that attempts to keep the planchet holder clean were unsuccessful. However using the ratios for shelves 3, 4, and 5, and the background readings it was possible to calculate the true background. The observed reading was the sum of the plate contamination plus the background, or

$$R_b = B + a \frac{y}{x} R_x \quad (5.1)$$

in which $a \frac{y}{x}$ is the y to x shelf ratio, B the background, and R_x the contamination as read on shelf x. Values calculated by use of Eq. 5.1 are given in Table 5.5. The average value of B, 532 c/m, checks well with the value, 531 c/m, when a heavy Al absorber was interposed between the holder and the tube.

The coincidence loss for the GM counter was calculated from,

$$R^0 = R + R^2 T_1 + R^3 T_2 + R^4 T_3 + \dots \quad (5.2)$$

in which R is the observed count, the T's are constants and R^0 is the corrected count. The constants T_1 , T_2 and T_3 were determined from the split sample data.

Thus, for any set of split samples, the corrected total count was,

$$R_t^0 = R_1^0 + R_2^0 - B \quad (5.3)$$

After substitution for the corrected counts from Eq. 5.2, there resulted,

$$R_1 + R_2 - R_t - B = (R_t^2 - R_1^2 - R_2^2) T_1 + (R_t^3 - R_1^3 - R_2^3) T_2 + (R_t^4 - R_1^4 - R_2^4) T_3 \quad (5.4)$$

TABLE 5.3 - Gamma Ionization Decay of Sample 4-Y39

Time (days)	Sample Reading (mr/hr)	Station 73A Reading (mr/hr)	Sample Decay (corrected mr/hr)	Relative Count (b)
0.125	41.5	28	38.7	15.0
0.146	34.0	21	31.9	12.4
0.167	28.3	16	26.7	10.3
0.187	24.0	13	22.7	8.79
0.208	21.0	10	20.0	7.74
0.250	16.5	7.4	15.8	6.12
0.283	13.8	5.8	13.2	5.11
0.312	12.3	15	11.6(a)	4.49
0.350	11.2	17	10.3(a)	3.99
0.371	10.6	26	9.6(a)	3.7
0.383	10.3	21	9.2(a)	3.6
0.404	9.90	21	8.8(a)	3.4
0.446	9.10	17	8.2(a)	3.2
0.462	8.80	19	7.9(a)	3.1
0.558	7.40	16	6.6(a)	2.6
0.575	7.30	16	6.5(a)	2.5
0.600	7.03	13	6.4(a)	2.5
0.679	6.92	11	6.3(a)	2.4
0.688	6.41	11	5.8(a)	2.2
0.750	6.31	10	5.3	2.0
0.766	5.89	9.7	4.9	1.9
0.833	5.50	8.7	4.6	1.8
1.04	4.45	6.7	3.8	1.5
1.25	3.70	5.3	3.2	1.2
1.46	3.20	4.4	2.8	1.1
1.67	2.80	3.6	2.4	0.93
2.08	2.18	2.5	1.9	0.74
2.50	1.79	1.8	1.6	0.62
2.92	1.50	1.3	1.4	0.54
3.33	1.25	1.0	1.2	0.46
3.75	1.07	0.8	0.99	0.38
4.16	0.94	0.8	0.86	0.33
4.58	0.82	0.7	0.75	0.29
5.00	0.73	0.6	0.67	0.26
5.58	0.65	0.5	0.60	0.23
6.65	0.50	0.4	0.46	0.18
8.96	0.34	0.3	0.31	0.12

(a) Corrected by 5 per cent of station 73A reading.

(b) Normalized to 0.100 at 10 days.

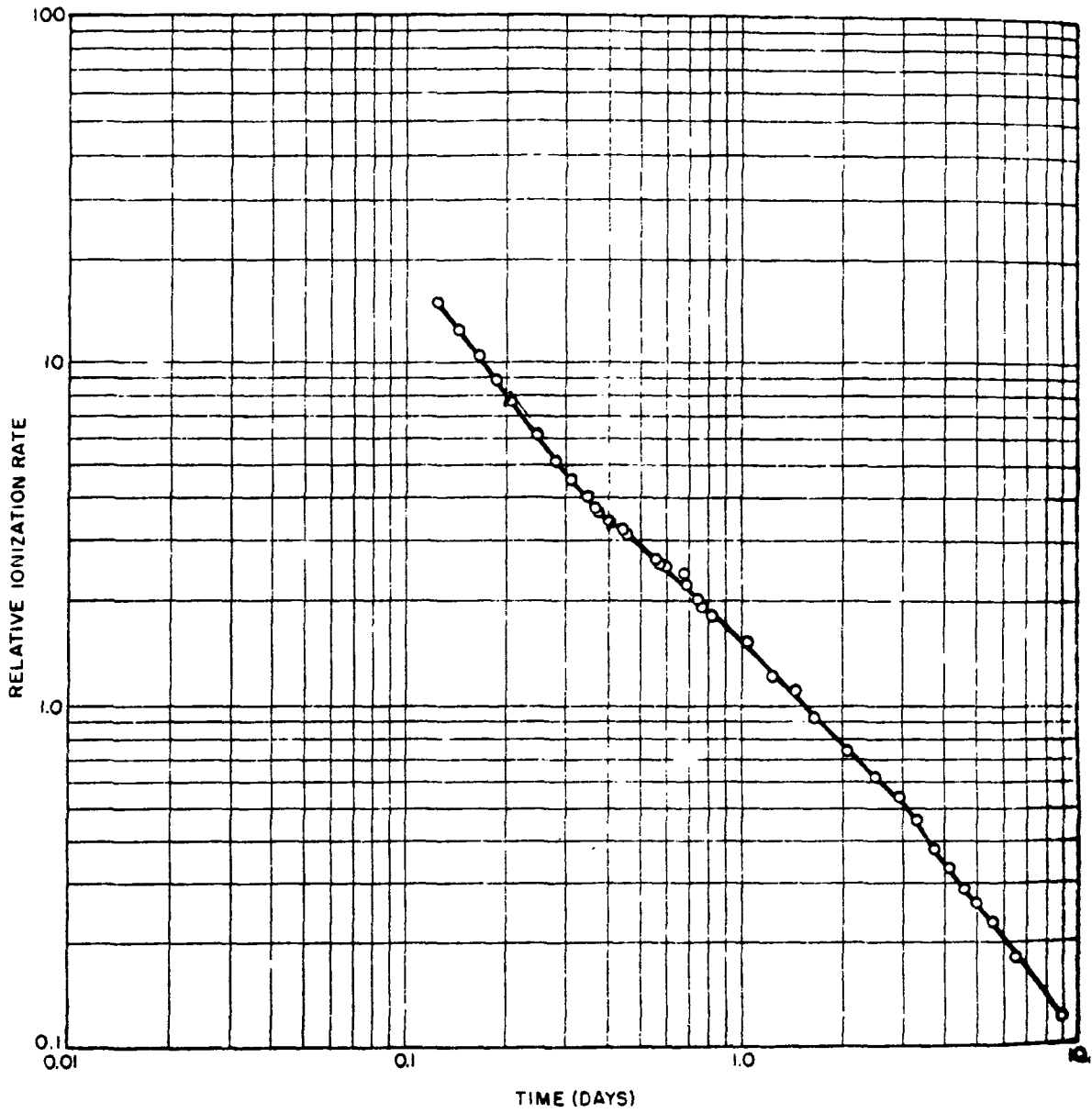


Fig. 5.3 Ionization Decay as a Function of Relative Ionization Rate

TABLE 5.4 - Data for Coincidence Loss from High Counting Samples from YAG 39

	Split Sample Readings (c/m)					
	Shelf 1	Shelf 2	Shelf 3	Shelf 4	Shelf 5	Shelf 5 - Absorber (a)
R ₁	43,148	14,978	7,318	5,675	4,170	1,263
R ₂	42,739	18,339	9,452	5,657	3,684	1,294
R _t	69,163	29,890	15,627	10,428	7,071	2,047
R _b	1,452	1,032	872	704	638	531
Std	10,128	3,650	1,588	847	500	-

(a) 1600 mg/sq cm of Al.

TABLE 5.5 - Calculation of Background from Shelf Ratios and Contaminated Plate Readings

Term	Shelf 3	Shelf 4	Shelf 5
$\frac{y}{a_3}$	1	0.533	0.315
$\frac{y}{a_4}$	1.875	1	0.590
$\frac{y}{a_5}$	3.176	1.693	1
R _x	351	176	102
B(a)	534	526	532

(a) Average 532 c/m.

Solving Eq. 5.4 with the data from Table 5.5 for shelves 1, 2, and 3 gave the values of the constants in Eq. 5.2. Hence,

$$R^0 = R + 2.820 \times 10^{-6}R^2 + 1.388 \times 10^{-10}R^3 - 6.738 \times 10^{-16}R^4 \quad (5.5)$$

Equation 5.5 may be expressed as,

$$R^0/R = 1 + y \quad (5.6)$$

$$\text{in which } y/R = 2.820 \times 10^{-6} + 1.388 \times 10^{-10}R - 6.738 \times 10^{-16}R^2 \quad (5.7)$$

These equations give an effective dead time of 200 μ sec at about 4000 c/m. The value of y for each observed sample and background count was read from a plot of y against R . From + 1.5 days, + 5 days, the sample was observed on a gas-flow counter at the site and from + 9 days it was counted at USNRDL on other gas-flow counters. The ionization and beta check well from about 0.4 to 10 days; at earlier times the ionization decay was somewhat faster.

Calculated beta decay curves for Shots 1 and 4 are plotted in Fig. 5.4. The decay of the induced activities for Shot 4 are included. The calculations were based on capture to fission ratios^{31/} and on the fission product d/m for 10,000 fissions at zero time.^{14/} The experimental beta decay for Shot 4 are superimposed on the plots by normalizing the 10-day values. Agreement between the observed and calculated curves is fair. The induced activities cease to effect the gross decay at + 60 days. The calculated decay curves exhibit some differences in the mode of decay between the radioactivities produced by Shots 1 and 2 for times less than + 60 days. The observed curves are all somewhat steeper at + 60 days and longer. The gamma decay of samples from Shots 2 and 4 at times shorter than + 10 days are different. Unfortunately only single samples were available for the early time decay for those two cases; and, further, the decays were observed on counters having different spectral responses. Hence there is no basis for determining the real significance, if any, of the differences. The ionization and gamma count decay could not be expected to agree with the calculated curves as closely as the beta decay; however, their divergence generally was not great for short intervals of time.

5.1.3 Gamma Spectrometer Measurements

Since the gamma analyser was converted from an alpha analyser after Shot 1, it was not available for early measurements on fallout samples from that shot. Gamma spectra were taken of gross decay samples from Shots 2 to 4 at various times after detonation. The results are summarized in Tables 5.6 through 5.9. In these tables the heights of the various peaks are shown relative to a value of one for the energy peaks nearest 0.1 Mev.

Since a small NaI crystal was used, the spectra were limited to the lower energy region and the peak at about 0.5 Mev was undoubtedly contributed to by annihilation radiation from gammas of higher energy than 1 Mev. However, the data were used mainly to compare the general

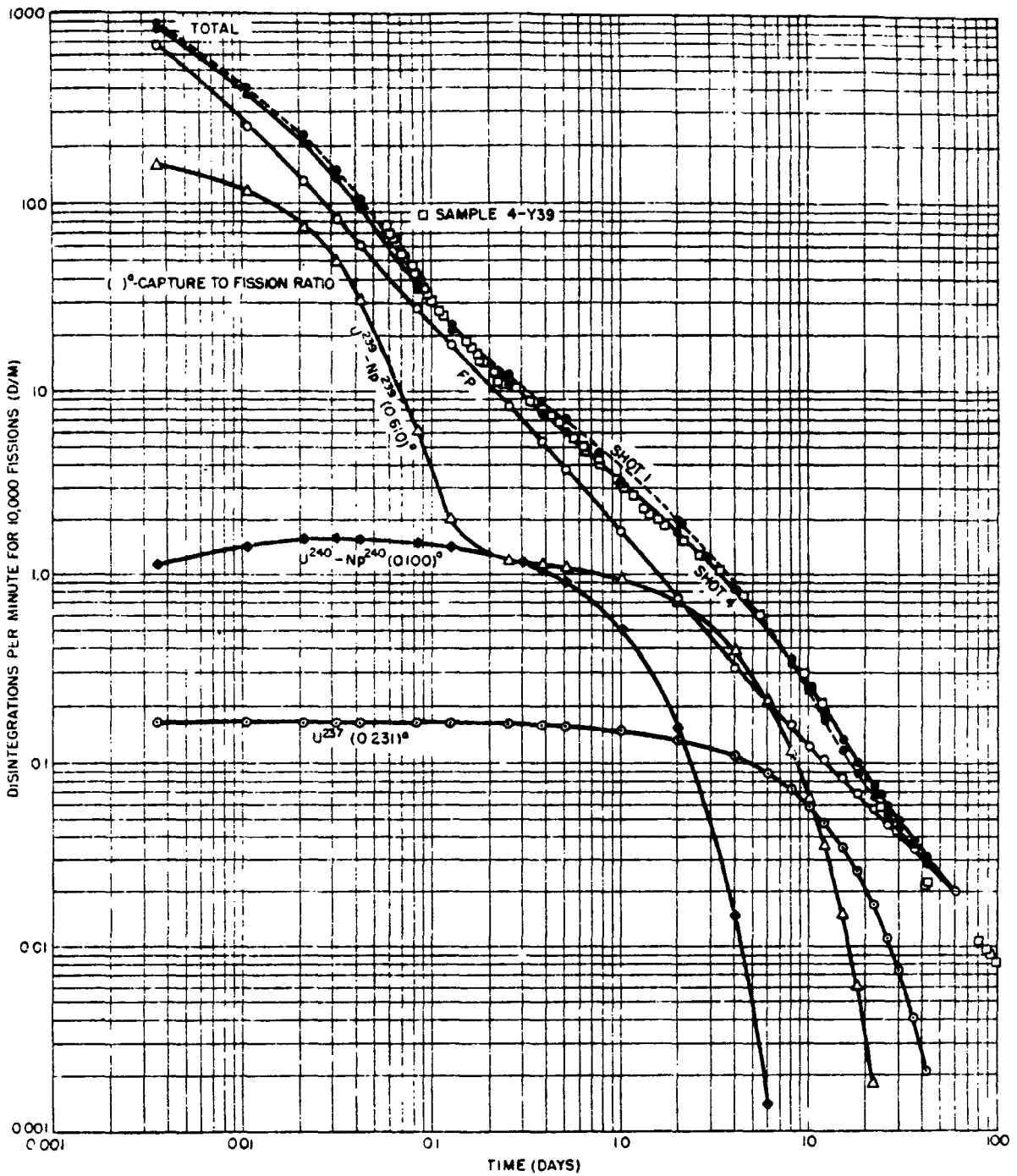


Fig. 5.4 Calculated Beta Curves

spectra from samples collected at different places and different shots with time. A comparative analysis for only one fallout sample from each shot is presented here.

5.1.3.1 Shot 1

A sample of fallout from Rongelap was analysed on + 29 and + 31 days after detonation. The results are shown in Table 5.6. Most of the same peaks show up for both curves with the exception of 0.03 and 0.27 Mev which do not appear at 31 days. Also the relative height of the 0.22 Mev curve is somewhat lower at 31 days. The 31 day curve shows a greater similarity to the other shots than the 29 day curve. In view of the fact that the calibration of the analyser was not completed at the time the first analysis was made the data collected on + 31 days are probably the more significant of the two analyses.

TABLE 5.6 - Gamma Energy Measurements from Rongelap Sample, Shot 1

Time after Shot (days)	Energy (Mev)								
	0.03	0.07	0.10	0.15	0.22	0.27	0.32	0.50	0.62
	Observed Peak Height Relative to 0.10 Mev Peak -								
29	0.67	0.80	1.0	0.86	0.59	0.35	0.17	0.18	0.05
31	-	0.57	1.0	0.57	0.12	-	0.12	0.15	0.05

5.1.3.2 Shot 2

On + 2 days there are significant peaks at 0.03, 0.08, 0.23, 0.30, 0.38, 0.62.

On + 3 days, the 0.30 has dropped way down, the 0.23 is about the same, the 0.08 is considerably higher and a very high peak has shown up at 0.12 Mev along with a smaller 0.15 peak. The higher energies, 0.38 and 0.62 have decreased considerably.

On + 4 days the high peak is still 0.12 Mev, the 0.08 and 0.15 are somewhat lower, and the 0.23 is about the same. There is a 0.28 peak slightly lower than the 0.23. The higher energies are still very low.

On + 6 days the 0.03 peak is the same as it was in all previous plots. There is very little change from R + 4 days.

On + 6.25 days. Very similar to R + 6 days. The 0.08 and 0.15 peaks are now symmetrical bulges on either side of the high 0.12 peak.

On + 9 days. Same as R + 6 except the 0.03 peak does not appear.

On + 11 days. Similar to R + 9 days except 0.03 peak again appears. There is a low but definite peak at around 0.50 which has been present since + 4 days.

TABLE 5.7 - Gamma Energy Measurements from Sample 2-A5, Shot 2

Time after Shot (days)	Energy (Mev)									
	0.03	0.08	0.09	0.12	0.15	0.22	0.28	0.36	0.50	0.70
	Observed Peak Height Relative to 0.12 Mev Peak									
2	0.55	0.63	0.45	-	-	1.0	3.8	1.26	0.37	0.45
3	0.25	0.75	-	1.0	0.47	0.22	-	-	-	-
4	0.20	0.42	-	1.0	0.36	0.18	0.11	-	-	-
5	0.20	0.40	-	1.0	0.40	0.17	0.11	-	0.03	-
5.3	0.21	-	0.45	1.0	-	0.16	0.10	-	0.34	0.45
9	-	0.50	-	1.0	0.46	0.25	-	-	-	-
11	0.39	0.42	-	1.0	-	0.21	0.05	-	0.04	-

5.1.3.3 Shot 3

It appears that for this sample which was observed from + 3 days to + 15 days, the amount of low energy (less than 0.1 Mev) radiation increased with time while the high energy (greater than 0.15 Mev) fraction decreased.

There is a very prominent peak at 0.10 Mev at all times up to + 16 days.

TABLE 5.8 - Gamma Energy Measurements from Sample 3 - Coca TC, Shot 3

Time after Shot (days)	Energy (Mev)									
	0.03	0.08	0.10	0.15	0.22	0.37	0.28	0.50	0.65	
	Observed Peak Height Relative to 0.10 Mev Peak									
3	0.27	0.39	1.0	-	0.16	-	0.10	0.014	-	
4	0.24	0.32	1.0	-	0.22	-	0.09	0.013	0.015	
5.6	0.36	0.54	1.0	-	0.19	-	0.09	0.022	0.015	
6	0.28	0.29	1.0	-	0.16	-	0.09	0.02	0.01	
7	0.31	0.31	1.0	-	0.18	-	0.09	0.03	0.02	
8.7	0.37	0.36	1.0	-	0.18	-	0.09	0.03	0.01	
9.3	0.41	0.47	1.0	-	0.22	-	0.12	0.04	0.02	
10	0.36	0.36	1.0	-	0.18	0.04	-	0.04	-	
11	0.42	0.45	1.0	0.21	0.12	0.05	-	0.02	-	
16	0.49	0.56	1.0	0.38	0.28	0.09	-	0.09	-	

5.1.3.4 Shot 4

These spectra have an unusually high component at 0.65 Mev. It was generally higher than the neighboring 0.50 Mev peak. There were few peaks below 0.06 Mev, at least up to the + 22-day curve where a 0.04 peak definitely occurs. These data do not change much with time.

TABLE 5.9 - Gamma Energy Measurements from Sample 4-Y39, Shot 4

Time after Shot (days)	Energy (Mev)											
	0.01	0.04	0.06	0.09	0.14	0.20	0.29	0.35	0.43	0.50	0.65	0.71
	Observed Peak Height Relative to 0.09 Mev Peak											
1.3	(1.57)	(1.87)	(4.0)	(1.0)	-	(0.15)	(0.13)	-	-	-	-	-
3.4	0.24	-	0.35	1.0	-	0.15	-	-	-	0.02	0.01	-
8.1	-	-	0.59	1.0	-	0.23	-	-	-	0.04	0.04	-
9.2	-	-	0.72	1.0	-	0.24	-	0.36	-	0.19	0.19	0.07
14.1	-	-	-	1.0	-	0.36	-	0.10	-	0.06	0.07	-
18.3	-	-	0.58	1.0	-	0.30	-	0.12	-	0.07	0.13	-
22.3	-	0.57	-	1.0	-	-	-	-	-	-	-	-
22.3	-	0.72	-	1.0	0.60	0.41	0.26	-	-	0.22	0.23	-

5.1.3.5 Comparisons of Spectra of Samples from Shots 1 through 4

In every curve studied the highest peak occurred at 0.09 ± 0.01 Mev. There was usually, but not always, one or more lower energy peaks near this energy. If the 0.09 Mev peak is given a relative height of 1.0, then the relative heights of the other peaks were about 0.5 for 0.01 Mev and 0.7 for 0.04 Mev. These relative heights decreased with time. There was another definite peak 0.20 Mev which ran about 0.30 of the highest peak. Higher energy peaks were observed at 0.50 and 0.65 Mev ranging from 0.1 to 0.2 of the highest peak. The 0.43 Mev peak however is doubtful since it appears in only one curve. The small NaI crystal which was used was not satisfactory for higher energies. In addition, the large amount of shielding required because of the high background at the site increased the scattering which resulted in very high counts in the low energy region and probably the peak at 0.50 Mev. The low efficiency of the crystal at the higher energies, however, was the chief reason for not taking spectra above the 1 Mev region.

The energies and relative heights of the peaks at 0.04, 0.06, 0.09, 0.20, and 0.29 Mev were very close to those observed in a pure Np^{239} spectrum which would indicate larger amounts of Np^{239} gammas. Some of these peaks gradually disappeared as the Np decayed out.

The following generalizations are evident from the analyses of the gamma spectra:

1. There did not appear to be any significant difference in the distribution of gamma-ray energies between the samples from the first four detonations.

2. The gamma analyzer curves showed no important differences between various samples from the same shot indicating that fractionation was not detectable by this method.

3. There was no great change in the relative heights of the various gamma peaks with time, although there was a detectable shift from the high 0.10 Mev peak toward both the low (0.03 Mev) and high (0.50 Mev) ends of the spectrum at later times.

4. There was a relatively large amount of 0.10 Mev gamma radiation present in the gross fallout mixture.

5. The relative peak height description permitted a general comparison of samples from different shots, from different locations for a given shot, and for the same sample at various times after burst. It should be emphasized that the descriptive technique used here, namely, analysis by relative peak height, is only a qualitative summary of the important photon energies present and has no relation whatever to the true photon-energy distribution of the radiation source.

5.1.4 Absorption Measurements

Aluminum absorption measurements were made with absorbers ranging in thickness from 0 to 3430 mg/sq cm. Before plotting, the aluminum absorber thickness was corrected for air and window thickness. Lead absorption measurements were taken with lead sandwiched between two aluminum absorbers. The aluminum absorber next to the counter window had a thickness of 1590 mg/sq cm and that just above the counting source 861 mg/sq cm. The lead absorbers ranged in thickness from 0 to 29.0 g/sq cm. The absorption measurements were taken at various times after detonation on one fallout sample from each of Shots 1 through 4.

5.1.4.1 Lead Absorption

A summary of gamma ray energies from the lead absorption curves is given in Table 5.10. These curves were analyzed into three components which give the "apparent" gamma energies although it is known that there are many different gammas contributing. The soft, medium, and hard components were then used to compare different samples with each other. The amount of each component was corrected by the counter efficiency for the apparent energy. The usual procedure of analyzing absorption curves was used; the "zero absorber" count rate was determined by extrapolating the three lines on a semilog plot to zero absorber thickness. The energy of each line was determined from Pb half-thickness curves; this energy was used to determine, from Fig. 2.1, the component crystal efficiency which was, in turn, used to weight the "zero absorber" count rate for each component to determine the relative amount of that component.

From these data the following conclusions may be drawn:

(1) Between 0.3 and 26 days there appeared to be no appreciable change in the energy of the soft gamma component. The average energy for all soft gammas observed was 0.16 Mev with a maximum deviation of 0.04 Mev.

(2) Between 0.3 and 26 days there appeared to be no significant change in the energy of the medium gamma component. The average energy for all medium gammas observed was 0.37 Mev with a maximum deviation of 0.11 Mev.

(3) There were larger variations in the energies of the hard gammas with respect to time especially for Shots 2 and 3. However, no definite trend is apparent as may be seen from Table 5.11 where the hard gamma component has been averaged for each shot. The over-all hard gamma energy average was 1.3 Mev with a maximum deviation of 0.5 Mev.

(4) There appears to be no trend common to all shots for the

TABLE 5.10 - Energies and Gross Distribution of Gamma Rays from Gross Fallout Samples

Shot Sample	Time After Burst (days)	Low Energy Gammas		Medium Energy Gammas		High Energy Gammas		
		Energy (Mev)	Amount (%)	Energy (Mev)	Amount (%)	Energy (Mev)	Amount (%)	
Shot 1								
1-251.03	3.77 ✓	5.4 30	0.16	42 1.29	0.32	29 2.55	1.1	29 2.57
" "	4.52 ✓	6.1 126	0.20	41 1.60	0.36	21 2.87	1.1	38 5.37
" "	3.35 ✓	7.4 178	0.17	46 1.38	0.30	27 2.59	1.0	27 7.78
" "	4.39 ✓	8.1 100	0.16	30 1.29	0.29	32 2.31	1.1	38 6.50
" "	4.73 ✓	8.3 101	0.18	47 1.44	0.38	23 3.03	1.5	30 11.20
" "	5.22 ✓	9.1 115	0.16	22 1.29	0.30	33 2.39	1.2	45 9.22
" "	3.83 ✓	10.1 142	0.14	48 1.13	0.32	21 2.55	1.15	31 8.87
" "	4.81 ✓	14.1 335	0.15	37 1.21	0.33	24 2.63	1.25	39 9.55
" "	6.20 ✓	22.4 157	0.20	32 1.60	0.48	17 3.81	1.3	51 9.84
" "	6.52 ✓	26.1 126	0.16	24 1.29	0.33	18 2.63	1.3	58 7.80
Shot 2								
Elmer	4.47 ✓	4.35 104	0.16	44 1.29	0.44	22 3.50	1.20	34 9.22
2-A5	3.78 ✓	3.7 88	0.17	66 1.38	0.40	16 3.19	1.80	18 13.10
"	3.19 ✓	6.1 146	0.13	68 1.65	0.48	15 3.81	1.5	17 11.20
"	4.07 ✓	8.16 110	0.165	62 1.33	0.40	16 3.19	1.70	22 12.43
Shot 3								
3-Coca T.C.	4.03 ✓	3.55 85	0.165	53 1.33	0.37	19 2.95	1.3	28 9.84
" "	3.02 ✓	4.2 101	0.16	71 1.29	0.38	12 3.43	1.35	17 10.20
" "	4.17 ✓	5.1 122	0.17	59 1.38	0.44	15 3.58	1.45	26 10.87
" "	4.27 ✓	6.1 146	0.16	47 1.29	0.36	21 2.87	1.25	32 9.86
" "	4.75 ✓	8.13 145	0.17	49 1.38	0.38	20 3.43	1.5	31 11.20
" "	(5.13) ✓	10.2 245	0.145	40 1.17	0.34	36 1.71	1.4	35 11.54
" "	6.45 ✓	13.1 317	0.17	37 1.33	0.42	18 3.36	1.6	45 11.80
Shot 4								
4-YAG-39	3.29 78.0		0.145	50 1.17	0.34	23 2.71	1.2	27 9.22
Plane Wipe	0.29 7.0		0.15	26 1.21	0.40	13 3.09	1.2	61 9.22
" "	1.63 19.2		0.16	38 1.29	0.34	19 2.71	1.0	43 7.78
" "	2.37 38.9		0.15	35 1.21	0.42	26 3.35	1.05	39 8.87
" "	2.67 64.0		0.135	35 1.69	0.31	27 2.47	1.2	38 9.22
" "	3.35 80.4		0.16	34 1.69	0.39	25 3.11	1.1	41 8.87
" "	5.13 123		0.135	36 1.69	0.29	29 2.31	1.0	35 7.78

variation of the proportion of different gamma components with respect to time after burst. The average percentages for the low, medium, and high energy gamma rays was 45, 22, and 35 per cent, respectively. However, the percentages varied considerably from one absorption curve to another. The lead absorption curves of 1-251.03 sample taken on + 22.4 and + 26.1 days show an exceptionally large proportion of high energy gammas.

TABLE 5.11 - Average Hard Gamma Energy for Each Shot

Shot	Average Gamma Energy (Mev)	Maximum Deviation (Mev)
1	1.2	± 0.2
2	1.55	± 0.35
3	1.41	± 0.19
4	1.11	± 0.11

Table 5.12 shows the percentage of each gamma component and their averaged energy for each shot at times less than 14 days.

TABLE 5.12 - Average Energy and Average Percentage of "Apparent" Gamma Components for each Shot at Times Less than 14 Days

Shot	Soft Gamma (%)	Max. Dev. (%)	Med. Gamma (%)	Max. Dev. (%)	Hard Gamma (%)	Max. Dev. (%)	Average Energy (Mev)
1	39	± 15	25	± 8	36	± 9	0.59
2	60	± 16	17	± 5	23	± 11	0.52
3	50	± 20	20	± 16	30	± 14	0.58
4	36	± 14	23	± 10	41	± 20	0.60

5.1.4.2 Aluminum Absorption

The only portion of the aluminum absorption curves analyzed was that for the highest beta energy. The upper portion of this high energy curve must be extrapolated over a large range of absorber thickness which would make any further analysis of the original curve doubtful. Analyses of aluminum absorption data for beta energies for all shots indicate that the energy of the hardest beta ray decreases with time in accordance with the theory.

The energies of the hard betas from Shots 1, 3, and 4 are listed in Table 5.13. The values for the maximum beta energy are nearly constant and approximate 2 Mev. The hard beta energy for sample 1-251.03 at later times appeared to be somewhat high compared to the samples from other shots. The beta-gamma ratio is 2 for most of the aluminum absorption curves although for Shot 3 at + 10.3 days the value was one and for one sample from Shot 4 at + 11.1 hr it was three.

TABLE 5.13 - Preliminary Summary of Beta Energies

Shot	Sample	Time after Burst	Max. Beta Energy (Mev)	Approximate Beta-Gamma Ratio(a)
1	251.03	10.2 days	2.1	2
1	251.03	14.05 days	1.3	2
1	251.03	22.15 days	1.9	2
1	251.03	26.1 days	2.2	1.5
3	Coca-TC	3.63 days	1.9	2
3	Coca-TC	4.63 days	1.85	2
3	Coca-TC	10.29 days	1.2	1
4	Y39	5.6 hr	2.6	2
4	Y39	11.1 hr	2.3	3
4	Y39	23.7 hr	2.3	2
4	Y39a	2.62 days	2.1	2
4	Y39a	3.53 days	2.0	2
4	Plane-wipe	8 hr	2.4	2
4	Plane-wipe	3.3 days	1.8	2

(a) Ratio of beta count rate to gamma count rate corrected for counter efficiency.

5.2 FISSION PRODUCT DETERMINATIONS

Radiochemical analyses of the fission produced radionuclides Sr^{89} , Y^{91} , Zr^{95} , Zr^{97} , Mo^{99} , Ag^{111} , Cd^{115} , Ce^{141} , Ce^{144} , Nd^{147} , Pa^{149} , Sm^{153} , Eu^{156} , Gd^{159} , and Tb^{161} were performed.

5.2.1 Radiochemical Procedures

Radiochemical determinations of the fission products were made according to standard published procedures⁷ which are outlined here.

Sr⁸⁹ was separated as the nitrate and purified by scavenging precipitations. It was determined as the carbonate.

Y⁹¹ was separated as the fluoride, purified by ion exchange, and determined as the oxalate.

Zr⁹⁵ and Zr⁹⁷ were exchanged with carrier Zr by use of HF, purified by scavenging precipitations and determined as the oxide.

Mo⁹⁹ was separated and purified as the alpha-benzoin oximate. It was determined as PbMoO₄.

Ag¹¹¹ was separated, purified, and determined as the chloride.

Cd¹¹⁵ was separated as the sulfide and purified by scavenging. It was determined as CdNH₄PO₄.

Ce¹⁴¹ and Ce¹⁴⁴ were separated as the iodate, purified by scavengings, and determined as the oxalate.

Yields of various fission product radionuclides were determined relative to the yield of Mo⁹⁹ and/or Zr⁹⁵. The determinations were made on different samples collected at various distances from ground zero. Comparison of relative yields among these reveals the extent of fractionation which occurred. In the absence of appreciable fractionation the relative amount of any fission product nuclide of interest is then obtainable from the measured fission yield curve.

5.2.2 Results

Analyses were made on all adequate samples obtained from the various events. The radiochemical results are presented in the form of R values where R is defined as follows:

$$R = \frac{C_r^i}{C_x^i} \bigg/ \frac{C_r}{C_x}$$

where C_r^i = counting rate at zero time of reference radionuclide in uranium thermal neutron fission.

C_x^i = counting rate at zero time of radionuclide of interest in uranium thermal neutron fission.

C_r = counting rate at zero time of reference radionuclide in event of interest.

C_x = counting rate at zero time of radionuclide of interest in event of interest.

Counting rates of a given radionuclide from the event of interest were measured under the same conditions of geometry and absorption as those used in measurements in thermal neutron fission. Counting rates were corrected for chemical yield. By inspection it is seen that an R value of 1 shows a relative fission yield the same as in thermal neutron fission of uranium, a value of greater than 1 shows a higher relative yield and one of less than 1 shows a lower relative yield. Results of the measurements are given in Table 5.14. The precision of measurement was 10 per

cent or better. Results of analyses on cloud samples are included to allow comparisons between fallout and cloud material. The cloud samples were portions of filter paper collections made for radiochemical determinations of weapon yield by LASL and UCRL.

5.2.3 Fractionation

5.2.4 Fission Yield Curves

5.3 INDUCED ACTIVITIES

Analyses for Na^{24} , K^{42} , Mg^{28} , Cl^{38} , Np^{239} , U^{237} , and U^{240} were performed on cloud and fallout samples. However, because of the difficulty of obtaining early samples only Na^{24} , Np^{239} , U^{237} , and U^{240} were detected. The fallout samples analyzed at the site were aliquoted as described in Section 3.1. The remainder of these samples and the cloud samples were analyzed at USNRDL.

5.3.1 Radiochemical Procedures

Radiochemical determinations were made according to either standard published procedures²¹ or those developed at USNRDL. They are outlined here and described more fully in Appendix A.

Na^{24} was separated from the gross activity by a two-step procedure. First, the alkali metal fraction was separated from the gross activity by ion exchange. Then, Na^{24} was isolated by a gravimetric procedure employing the specific precipitation of sodium zinc uranyl

acetate.*

K^{42} was separated from the alkali metal fraction as the $KClO_4$.
 Mg^{28} was isolated as the Mg hydroxyquinolate.

Cl^{38} was precipitated as $AgCl$ after removing the interfering activities by solvent extraction.

Uranium was separated and purified by ether extraction and deposited by electroplating to determine U^{237} and U^{240} .

Np^{239} was separated and purified by oxidized fluoride - reduced fluoride cycles and determined by electroplating.

5.3.2 Activities Induced in Environmental Substances

Neutron induced activities in environmental materials were considered a possible source of significant radiation contributors at early times from high yield devices. The nuclides considered as possible contributors were Na^{24} , K^{42} , Cl^{38} , and Mg^{28} . In general, the determination of most such induced activities requires an early delivery and processing of samples. In no case was an acceptable fallout sample recovered at a sufficiently early time to give reliable analysis for more than one induced activity (Na^{24}). Analyses were run on Shots 2 and 3.

An upper limit was established for K^{42} . Computations based upon this limit are made for purposes of comparing the relative contribution of Na^{24} and K^{42} .

5.3.2.1 Chemical Treatment of Samples

Only two representative samples were obtained for analyses. From them Na^{24} was isolated. This was accomplished by first removing the alkali metal fraction from the gross activity by ion exchange. Then Na^{24} was separated from this fraction by a gravimetric procedure. The alkali fraction contained approximately 10 per cent of the total activity of the gross sample. Decontamination of Na^{24} from Cs^{137} was done by a preliminary separation of cesium silicowolframate. Rubidium activity was not considered troublesome since all the significant rubidium activities formed in fission are short-lived (18 min or less). Interference of potassium was found to be negligible because of its relatively low yield.

In the procedure used for the isolation of Na^{24} , the sodium carrier was added before the ion exchange step. The effluent fraction from the column containing the sodium was treated with a solution of saturated sodium zinc uranyl acetate. The resulting precipitate was dissolved and precipitated twice more with the same reagent. The final precipitate contained 95-100 per cent as much sodium as the amount of carrier added originally. However, owing to the dilution of the Na^{24} in each precipitation step only about 3 per cent of the active nuclide

* The ion exchange step in this procedure was developed at the site when it became apparent that the isolation step did not give adequate purification. Several other radionuclides were fractionated in the ion exchange treatment. Details of these studies are reported in Appendix B

was recovered. A decontamination factor of at least 10^7 was obtained by this method.

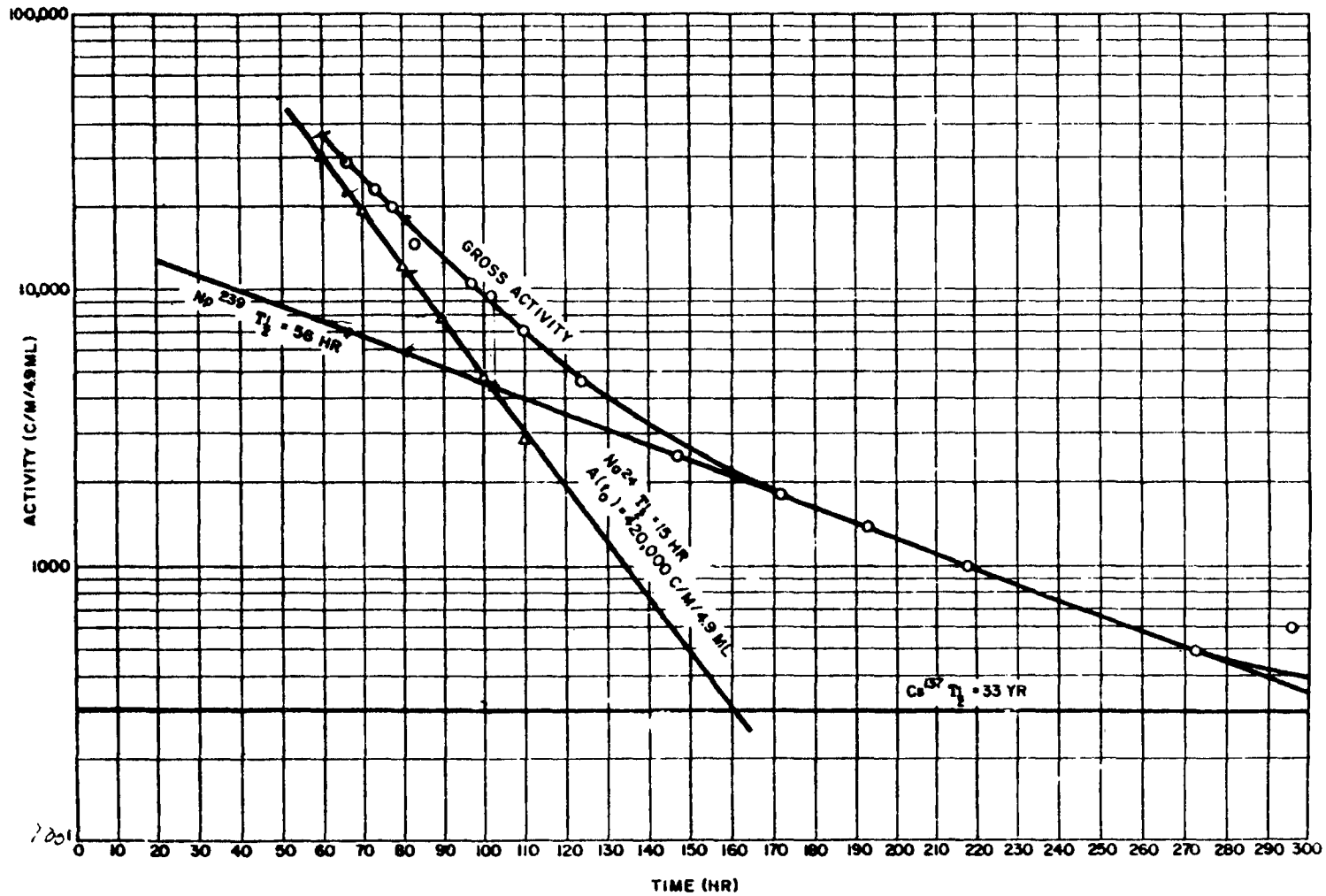


Fig. 5.5 Decay Curve of Na^{24} Sample from Shot 2.
 Sample was Collected 51 Nautical Miles
 from Ground Zero on Bearing 330°

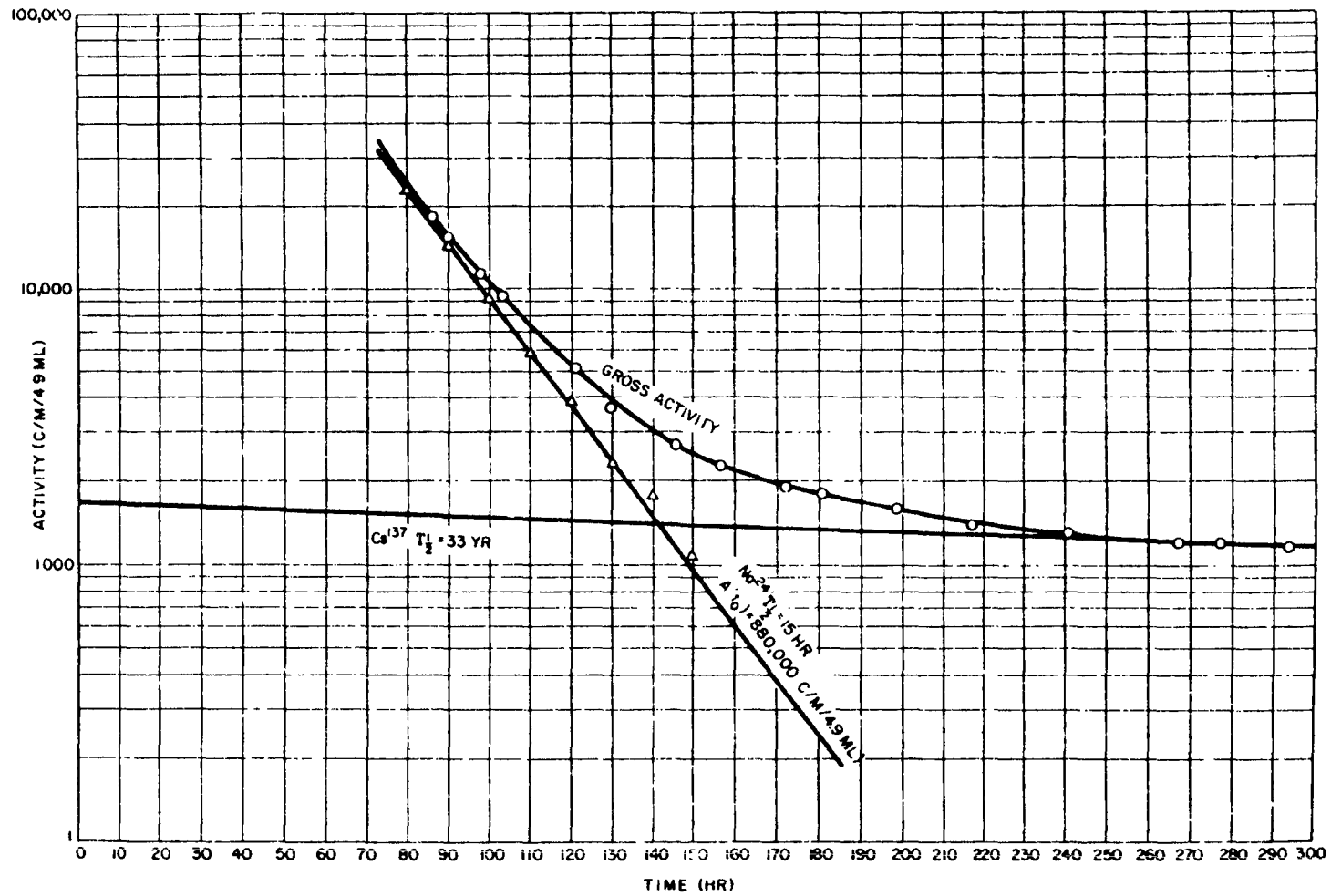


Fig. 5.6 Decay Curve of Na²⁴ Sample from Shot 3.
 Sample was Collected at Coca Head 6
 Nautical Miles from Ground Zero on
 Bearing 70°

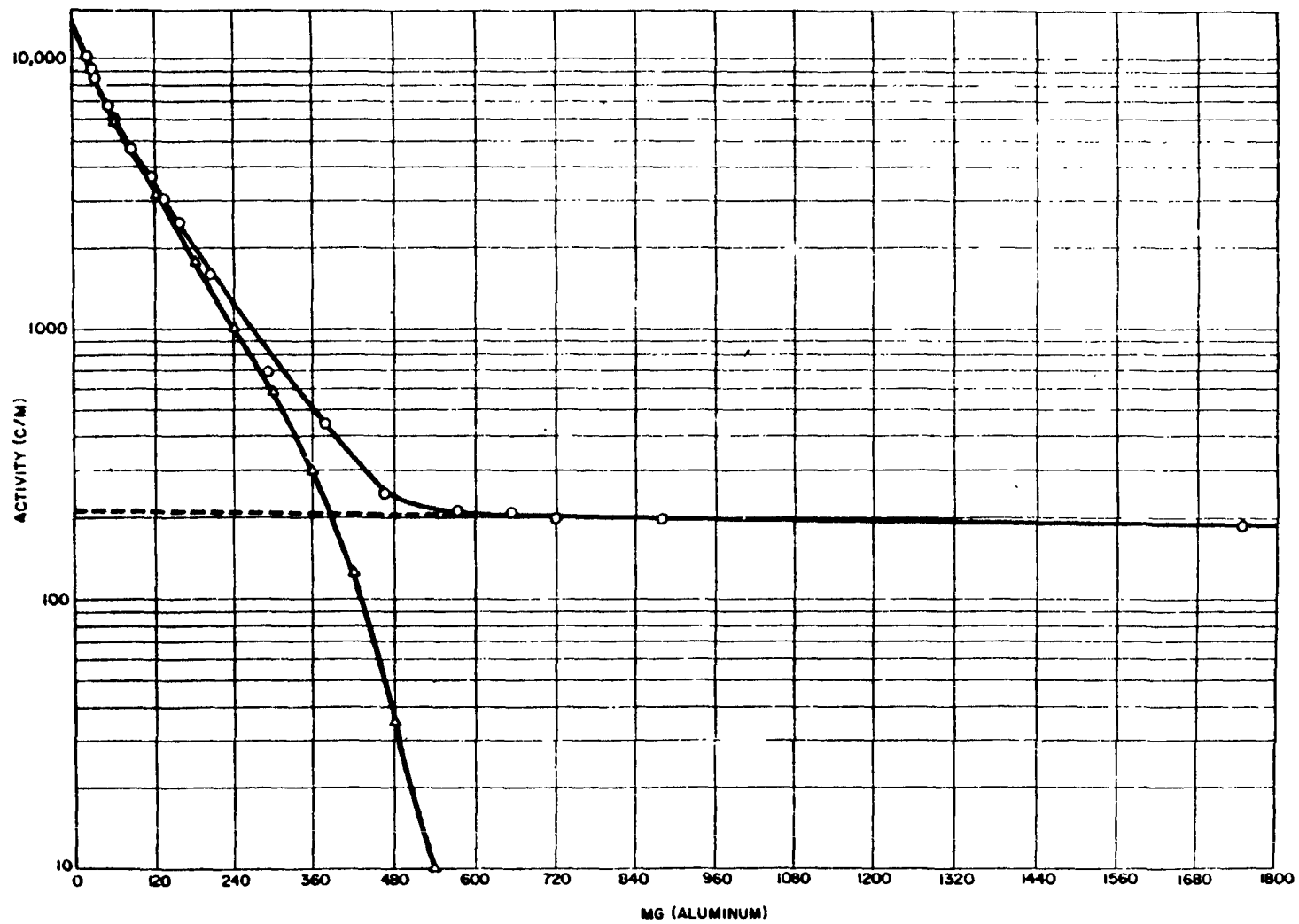


Fig. 5.7 Aluminum Absorption Curve for Na^{24} Sample from Shot 3

in cloud material: Na and K were found to undergo extensive fractionation in JANGLE. 20/

5.3.3 Activities Induced in Device Components

The most important radionuclides produced by neutron reactions in the device components are Np^{239} , U^{237} , and U^{240} . (U^{239} is also important but is too short-lived to have been seen in our measurements). They were produced in sufficiently high yields to affect the gross decay rates of the residual contamination and to contribute significantly to the radiations from the contaminant.

5.3.3.1 Results

To illustrate the extent to which these radionuclides contribute, their counting rates measured at the same shelf geometry and corrected for chemical yield and decay are presented in Table 5.16. In order to allow comparisons of their activity levels with those of fission products, corrected counting rates for Mo^{99} at the same shelf geometry are also presented.

Conversion of the above relative counting rates to relative numbers of atoms requires determination of counting efficiencies. These have been obtained for all of the above radionuclides except U^{240} . Consequently, there are presented in Table 5.17, for each sample, the number of atoms of Np^{239} and U^{237} produced relative to the number of fissions occurring as measured by Mo^{99} .

5.4 FRACTION OF BOMB IN FALLOUT SAMPLES

Radiochemical methods can provide an accurate determination of the fraction of the bomb included in fallout samples. The data required are the total number of fissions occurring in the detonation and the number of fissions giving the activity in the fallout sample. These determinations have been made by radiochemical means, the first at Los Alamos Scientific Laboratory, 28/ and the second here.

5.4.1 Results

CHAPTER 6

SUMMARY

6.1 GENERAL

Characterization of cloud and fallout samples from CASTLE has furnished information useful for (1) deducing the mechanism of the formation and subsequent reactions of the debris from nuclear detonations, (2) assessing the radiological situation in the areas of fallout, (3) synthesizing simulants for use in decontamination tests and (4) interpreting data obtained in proof testing atomic warfare countermeasures for ships.

6.2 MECHANISM OF FORMATION AND SUBSEQUENT REACTIONS OF NUCLEAR DETONATION DEBRIS

The composition of the debris varied with the weapon type and the location of the shot point. For surface land shots the fallout consisted of irregular solid particles derived from coral with associated bomb products which were usually concentrated at or near the particle surface. The outer layer of the particle was chiefly calcium carbonate; the inner part a mixture of calcium oxide and hydroxide. Apparently the coral grains were taken into the fireball as discrete particles and calcined to the oxide in the high temperature environment. The bomb products collected on the surface of these particles and as they fell through the humid atmosphere they were slaked to the hydroxide and the surface layers reconverted to carbonate.

Surface water shots produced fallout with relatively little solid matter. Small particles less than 10μ in diameter appear to have arrived at the earth's surface in the solid or semi-solid state. Liquid drops having a range of size up to several millimeters in diameter were also detected. The mode of formation and subsequent reactions of these fallout particles is not so well understood as that from the surface land shots. It is apparent that the bomb debris mixed to some extent with the large amount of sea water and the relatively small quantity of coral that were taken into the fireball. Evaporation of the water probably led to the formation of condensation nuclei derived from the sea water constituents. These small particles then collected the condensed bomb

products. Much of the water condensed in the cloud gathering additional bomb products. As the particles fell they probably changed their composition through reactions with atmospheric constituents. Their exact nature at the time of arrival at the earth's surface is not known. The measurements of the aerosols collected on the YAG's indicated small solid particles and larger liquid droplets. Results of the decontamination studies of the YAG's (Project 6.4) and special panels (Project 6.5) could be explained best by assuming a contaminant whose constituent radionuclides were largely in the ionic form. The gross fallout samples had little solid matter. In fact, the fallout was invisible both in the air and on the surfaces where it was deposited. A large fraction of the radionuclides was water soluble.

6.3 ASSESSMENT OF RADIOLOGICAL SITUATION IN FALLOUT AREAS

One of the factors needed to estimate the radiological situation in the fallout zone is the decay rate of the radiation field. This was determined by direct measurement on land areas wherever it was possible in moderate radiation fields. In other instances, it was estimated from measurements of the decay rates of samples collected in the areas of interest. The observed beta and gamma decay rate curves compared well with calculated curves based on the radiochemical composition of the samples. There was little difference in the decay rates of fallout samples collected at various distances after any single shot. This fact showed that fractionation was unimportant in determining the gross decay rate. Small variations were observed in the decay rates of samples from different shots. The decay rate changed considerably with time; at 60 days after the induced activities had decayed to a negligible level, it achieved a relatively constant value consistent with the $t^{-1.2}$ law.

Radiochemical measurements on debris from detonations in CASTLE gave information on the shape of the fission yield curve, on fission product fractionations, on contributions of neutron induced radionuclides, and on the fraction of bomb in fallout material.

The shape of the fission yield curve from these detonations was altered in respect to that from thermal neutron fission of U^{235} . The valley of the curve was raised by a factor of about 20 while the heavy wing was raised by a factor of about 6 at mass 156. Fractionation of several fission products was found to occur. That of Sr^{89} was the most extensive among the limited number of elements which could be studied. Neutron induced radionuclides were demonstrated to be very important contributors to the radioactive mixtures resulting from the detonations. Most important were U^{239} - Np^{239} , U^{240} , and U^{237} ; Na^{24} was only a minor contributor. Ratios of amounts of the important induced radionuclides to amounts of fission products showed that at certain times the uranium and neptunium isotopes contributed as much as 50 per cent of the total beta activity. Since the energy of the Np gammas is low as compared with the average of those from fission products, its contribution to the total radiation field is less than indicated by the beta ratio. Values of fraction of the bomb falling out at certain locations were determined radiochemically. These were useful in connection with the fallout studies of Project 2.5a.

6.4 SYNTHESIS OF SIMULANTS FOR DECONTAMINATION TESTS

Characterization of the contaminants from the surface land and water shots has furnished information needed for synthesizing simulants for laboratory decontamination studies. For the surface land shots the composition and physical characteristics of the fallout were documented adequately. A relationship between the radiation level and the quantity of fallout per unit area was established. The physical nature of the fallout from surface water shots is somewhat uncertain but its chemical composition and radiochemical properties were determined. The ratio of radiation field to the quantity of fallout per unit area is much lower than that for the surface land shots.

6.5 PROOF TESTING AND COUNTERMEASURES FOR SHIPS

The information regarding the nature and distribution of the fallout has been useful to Project 6.4 in interpreting the effectiveness of the countermeasures on the YAG's. A knowledge of the chemical and radiochemical properties of the contaminant aided in their decontamination studies. Information regarding the physical properties of the aerosols was used in determining the effectiveness of various protective systems for the ship's ventilation air. The rates of decay and energy measurements of the fallout from the various shots have been useful in evaluating the data from the radiation detection devices aboard the ships. This information is also useful in determining the shielding provided by the ship's structure.

APPENDIX A

CHEMICAL AND RADIOCHEMICAL PROCEDURES

A.1 DETERMINATION OF OXIDATION STATES OF NEPTUNIUM

The procedures employed in determining the oxidation states of Np are given below.

1. To the sample in a 100-ml beaker add concentrated HCl dropwise while warming gently; keep volume as small as possible.
2. If solid material remains undissolved, centrifuge, retain supernatant, and add additional HCl to precipitate, boil, centrifuge; add supernatant to that already obtained and discard precipitate.
3. Measure total volume of sample in graduate cylinder for activity assay. Take an aliquot for gamma spectrum and decay.
4. Evaporate solution to 6N-HCl.
5. Dilute solution to 2N-HCl and transfer to a separatory funnel.
6. Add approximately 20 cc of 0.4 M TTA in benzene to the solution and stir vigorously for 30 min.
7. Separate the phases. Wash the benzene phase containing Np IV with 5 cc 8N-HCl (saturated with TTA) for 10 min and then discard the benzene.
8. Treat the 8N-HCl which now contains the Np IV by the procedure given below starting with step 9. Also treat the aqueous phase containing Np V and Np VI starting with step 9.
9. Add several drops of 30 per cent H_2O_2 and 10 cc concentrated HCl keeping the volume as small as possible.
10. Boil the solution to destroy the H_2O_2 to bring the HCl concentration to 6N and to reduce volume.
11. Dilute the solution to 2N and transfer to a 125-cc separatory funnel.
12. Add 20 ml of 0.4 M TTA in benzene to the solution and stir vigorously for 30 min.
13. Separate the phases. The benzene phase contains Zr, Pa, and a small amount of Np. Wash this with 5 ml of 8N-HCl (saturated with TTA) for 10 min and discard the benzene phase. The 8N-HCl which now contains the Np is retained for later use.
14. The aqueous phase from the extraction contains all of the other substances including the greater fraction of the Np. Add 2 ml of formic

acid and 10 ml of concentrated HCl to this solution and boil for about 10 min to about 25 ml in 6N-HCl.

15. Dilute this solution to 2N-HCl and then extract with 10 ml of 0.4 M TTA in benzene for 10 min.

16. The aqueous phase containing the fission products, U, and other heavy metals is discarded.

17. Wash the benzene phase containing Np IV with 5 ml of 2N-HCl (saturated with TTA) for 2 min and discard the wash solution.

18. Back-extract the Np for 10 min from the benzene with the 5 ml of 8N-HCl retained in step 12. Discard the benzene.

19. Add 1 ml of concentrated formic acid and 10 cc HCl to the solution in 8N-HCl and boil for 10 min under a watch glass cover.

20. Transfer the solution to a separatory funnel, dilute to 2N-HCl, and extract with 10 ml of 0.4 M TTA in benzene for 10 min.

21. Discard the aqueous phase.

22. Wash the benzene phase with 2 ml of 2N-HCl (saturated with TTA) for 2 min.

23. Wash with 1 ml 0.1N-HCl (saturated with TTA) for 2 min.

24. Back-extract the Np from the benzene with 5 to 10 ml 8N-HCl (saturated with TTA) for 10 min.

25. Separate the phases. Measure the total volume. Take an aliquot for assay, gamma spectrum, and decay.

A.2 SEPARATION OF SODIUM ACTIVITY

The procedure used for the isolation of sodium activity from the gross activity was accomplished in two parts. Part I consisting of separating the alkali fraction from other radionuclides by ion exchange is discussed more fully in Appendix B. Part II consisted of a gravimetric procedure employing the specific precipitation of sodium zinc uranyl acetate. The complete procedure is given below.

Step 1. Transfer an aliquot of the original sample to a 100-ml beaker. Acidify solution with a minimum amount of HCl (usually to a pH of 5). This is usually sufficient to dissolve any of the solids present in the sample. Then the solution is evaporated down to approximately 2 ml.

Step 2. This volume is absorbed on the top of a cation exchange resin column along with added Na carrier (5 mg). After rinsing the column with de-ionized water, the column is eluted with 0.5N-HCl. In the water wash, I, Cl, Br, other anions, and some colloids are eluted. In the 0.5N-HCl elution, U and Np are first eluted. The second peak of activity contains the alkali metals. The Na breakthrough is determined by a Pt-wire flame test for the Na carrier. The alkali fraction is removed in approximately 50 ml of solution at a rate of 8 to 10 drops per minute.

Step 3. Evaporate the alkali fraction to 2 ml. Add 20 mg of Na carrier plus 10 to 20 mg of Cs⁺ and K⁺ carriers. Acidify with 10 ml of dil. HCl and then add 5 drops of 0.13 M silicowolframic acid (see Note 1). Allow to stand with occasional stirring for about 5 min. Centrifuge, and wash the precipitate twice with 5 ml of 6N-HCl. Combine supernatant and washes (see Note 2).

Step 4. Evaporate filtrate to 2 ml. Add 25 ml of zinc uranyl acetate reagent (see Note 3). Allow to digest with intermittent stirring for 4 to 5 min. Filter. Wash 5 times with small portion of zinc uranyl acetate. Wash twice with 2 to 3 ml of ethyl alcohol (see Note 3). Use 2 to 3 ml of hot dil. HCl to wash the precipitate into a 50-ml centrifuge tube. Cool in ice bath.

Step 5. Add 5 mg Cs^+ + 5 mg K^+ . Then add 15 ml of zinc uranyl acetate reagent for 15 min. Centrifuge, and discard supernatant. Wash precipitate 2 times with 5 ml of n-propyl alcohol. After washing, slurry precipitate in 10 ml of n-propyl alcohol and precipitate NaCl with HCl gas (see Note 4).

Step 6. Filter on a weighed filter paper disc in a small filter tower, and wash 3 times with 5 ml of n-propyl alcohol. Dry the precipitate at 110°C for 10 min, weigh as NaCl, and mount on a counting disc.

A.2.1 Notes

1. Unless otherwise noted, all solutions are to be kept in an ice bath during the entire procedure.
2. It may be necessary to repeat the centrifugation 2 to 3 times to assure complete precipitation of cesium and silica.
3. Zinc uranyl acetate reagent was saturated with sodium zinc uranyl acetate; n-propyl alcohol was saturated with NaCl; ethyl alcohol was saturated with sodium zinc uranyl acetate. These solutions were filtered into a fresh container before using.
4. Gas flow was continued for 10 min.

A.3 SEPARATION OF POTASSIUM ACTIVITY

Potassium is first separated with the alkali metal fraction obtained from 0.5N-HCl elution of the cation resin column (see sodium procedure). Purification is then accomplished by the following procedure.

Step 1. To 2 ml of the alkali metal fraction add 1 ml of Cs^+ (10 mg/ml), 2 ml of K^+ (10 mg/ml) and 10 ml of 6N-HCl in a 50-ml centrifuge tube. Add 0.5 ml of 0.13 M silicowolframic acid and allow to stand with occasional stirring for 5 min. Centrifuge and wash precipitate twice with 5 ml of 6N-HCl. In a 100-ml beaker combine washes with supernatant and discard precipitate. Add 2 drops of silicowolframic acid. If precipitate forms repeat centrifugation and washes. Repeat until the formation of a precipitate is no longer observed.

Step 2. On a hot plate evaporate solution to dryness. Cool and then add approximately 5 ml of 10 per cent HCl solution. Break up lumps of silica with a stirring rod. Transfer solution to a 50-ml centrifuge tube and centrifuge. Wash residue three times with 2 ml of 10 per cent HCl solution. Evaporate combined centrifugate and washings by swirling over a burner until the volume is approximately 3 ml. Cool for 2 min.

Step 3. Carefully add 5 ml of 70 per cent HClO_4 . Evaporate by swirling over a burner until dense fumes of HClO_4 are evolved. Cool for 5 min in air, then place in an ice bath. To the cold solution add 15 ml of absolute ethanol.

Step 4. Filter on a weighed filter paper disc in a small filter

tower. Wash 3 times with 5 ml of absolute ethanol. Dry precipitate at 110°C for 10 min. Cool in a dessicator. Weigh as $KClO_4$. Mount and count.

A.4 SEPARATION OF CHLORINE ACTIVITY

Apparatus for chlorine determinations permitted the analyses of three samples in duplicate in less than 60 min. The procedure for determining Cl^{38} is given below.

Step 1. Transfer 3 ml of the gross activity to a 50-ml centrifuge tube. Add 3 drops of Fe^{+3} (20 mg/ml); 3 drops of BrO_3^- (20 mg/ml) and 3 drops of IO_3^- (20 mg/ml). Add concentrated NH_4OH drop by drop until the precipitate of $Fe(OH)_3$ is formed. Add one drop in excess. Centrifuge and decant the supernatant into a separatory funnel.

Step 2. To the supernatant solution add $NaHSO_3$ dropwise until a colorless solution is observed. Adjust solution to pH 2 with concentrated HNO_3 .

Step 3. Add approximately 25 ml of 0.25 M TTA in CCl_4 to the solution of Step 2. Pour the mixture through the side arm of the separatory funnel and stir for 2 min.

Step 4. Separate the CCl_4 layer and wash aqueous fraction with pure CCl_4 . Separate again. To the aqueous phase add an equal volume of CCl_4 and while the mixture is being stirred add approximately 3 ml of concentrated HNO_3 . The characteristic violet color of iodine will then form in the CCl_4 phase. Remove this layer and wash the aqueous phase repeatedly with CCl_4 until the violet color is barely discernible. Then add 5 drops of a saturated solution of $NaNO_2$ and wash again with CCl_4 . Separate by removing the lower (organic) phase.

Step 5. Stirring the aqueous phase add dropwise 0.1 M $KMnO_4$ until a brown residual color is observed. At this point add $NaNO_2$ drop by drop until the aqueous phase becomes colorless. Extract with CCl_4 until no color is observed in the CCl_4 phase. Then do an additional extraction.

Step 6. Transfer the aqueous phase to a boiling flask which contains 5 g of crystalline $KMnO_4$ (see Note 1). Heat gently. The resultant Cl_2 -air mixture is bubbled through a solution of 0.1 M $NaHSO_3$.

Step 7. Acidify the $NaHSO_3$ solution with concentrated HNO_3 . Add $AgNO_3$ solution in excess and precipitate $AgCl$.

Step 8. Collect precipitate on a pre-weighed filter paper using a small filter tower. Wash 3 times with small portion of acetone. Mount precipitate on a planchet and count. After decay counting is completed, heat the precipitate for 10 min at 110°C. Cool precipitate in a dessicator and weigh to a constant reading.

A.4.1 Notes

1. The boiling flask is so constructed that when it is attached to a Vigreux column and receiver, air may be drawn through the system by aspiration.

APPENDIX B

PARTIAL FRACTIONATION OF FALLOUT COMPONENTS BY CATION EXCHANGE

B.1 EXCHANGE COLUMN PROCEDURE

An ion exchange procedure was utilized to separate the Na^{24} activity from the fallout samples. The procedure was developed at the site after Shot 1 when it became evident that the fallout samples were smaller than anticipated. It was designed for utilizing small samples of fallout combining the Na and I analyses. The ion exchange column consisted of 50 to 65 mesh Dowex 50 in a 80-mm i.d. glass tube 15 cm long. Washing and eluting solutions were fed into the column from a constant-head polyethylene bottle through polyethylene tubing; after passing through the column, the solution was carried below a GM tube by 1.5 mm i.d. thin-walled polyethylene tubing and into a collecting beaker. The tubing was threaded through two small holes drilled into a lead shield which held the GM tube. The radioactivity passing beneath the counting tube was recorded on an Esterline-Angus recorder through a General Radio Co. Model 1500-B rate meter.

After acidifying the samples with a minimum amount of HCl (usually to a pH of 5), the samples were adsorbed on the top of the column together with a measured amount of Na carrier. The column was then washed by eluting with de-ionized water. The water elution carried out anions and some colloidal materials. When the eluted wash water activity counted background, the column was eluted with 0.5N-HCl. The Na breakthrough was detected by means of a Pt wire flame test. Occasionally, after no Na was detected, other eluting reagents were used for further elutions. Sampling beakers were changed at the desired points, the volume of sample measured, and an aliquot was taken for counting. Gamma decay and spectral measurements were taken on the various fractions.

B.2 RESULTS

One elution is given by the chromatogram in Fig. B.1. The circled letters or numbers are the eluted fractions which were noted on

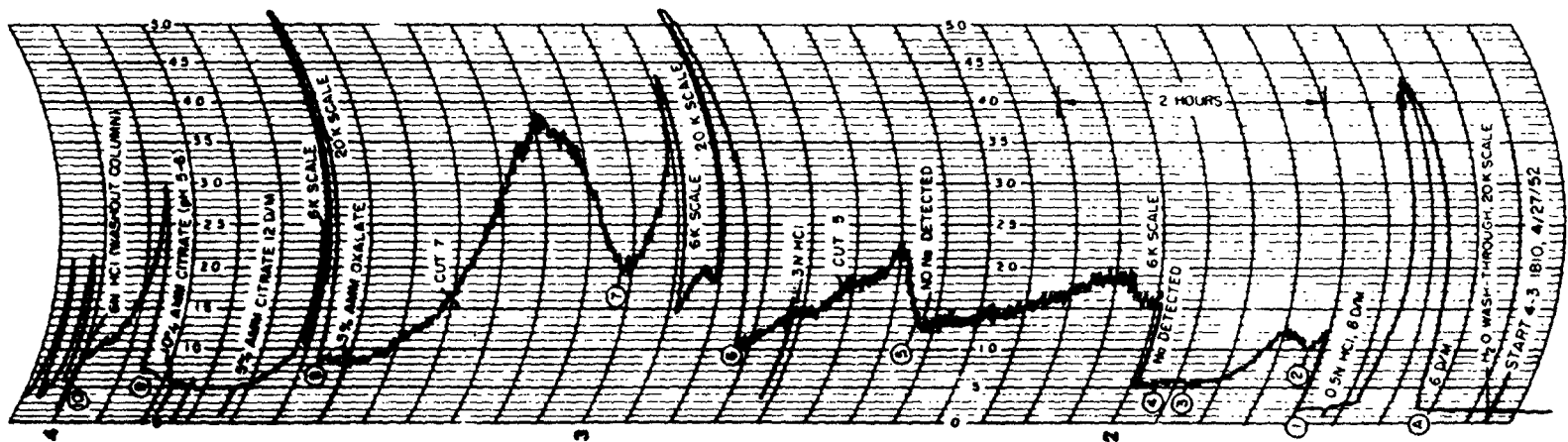


Fig. B.1 Facsimile of Chromatogram Taken from the Esterline-Angus Recorder

the chromatogram at the time the collection of the fraction was begun.

Analysis of the decay data for the first four fractions of Sample 4-3 (Shot 4, third elution run) of the chromatogram is shown in Figs. B.2 through B.5. Since Sample 4-3 did not contain sufficient Na activity to increase the count at the Na breakthrough (Fraction 4-34), the analysis of the decay of Fraction 4-24 from Sample 4-2 which did show Na activity is given in Table B.1 and is plotted in Fig. B.6. Sample 4-2 was run about 24 hr prior to Sample 4-3. When the elution of Fraction 4 did not give an activity peak, the fraction was not further analyzed for Na²⁴. The spectra of the five fractions at various times are summarized in Table B.1; only the major photon peaks are listed. The probable radioactive constituents of the first five fractions are given in Table B.2. The first, or anion fraction, contained the iodine activities and also activities from the insoluble (acidic) elements Ru, Rh, Te, Tc, and possibly some Mo. The relative amounts depended, of course, on time after burst when the elution was made and on the pretreatment of the sample. The elution of fallout samples from the island shot which were dissolved with strong HCl and diluted to pH 5 generally gave smaller peaks for the water wash which, in turn, contained relatively smaller amounts of the insoluble (acidic) elements. However, small amounts of these materials tailed along into the HCl elution until the alkali Fraction 4 where Mo⁹⁹ peaked along with the alkalis. The Te (Fraction 3) usually gave a higher peak than that shown by the chromatogram - especially at earlier times. The Np (Fraction 1 and 2) usually contained less Te impurity than that shown in Table B.1. At +3 to +5 days, when the Np activity reaches a maximum percentage of the total activity, it was often difficult to detect the Te (or other) impurity in those fractions. When the fallout sample was treated with a reducing agent prior to adsorbing it on the column, the Np peak did not appear. The alkali elements (Fraction 4) then came off first in the acid elution. Hence, the Np in Fractions 1 and 2 must be in the +5 (or +6) oxidation state. The general double peaking of Te, and perhaps of Ru and Mo, first in the water wash and again later at different places in the HCl elution, seems to indicate a distribution of oxidation states for these elements. First, they did not tail off in the usual manner, and secondly, radionuclides of each element appeared to have fractionated to some extent. Since the stability of the chloride complexes and the acidic properties of Ru, Rh, Te, and Mo depend upon the oxidation state of the element, the latter would therefore determine the ion exchange behavior. Further exploitation of ion exchange methods in the analysis of fallout materials in future field tests such as this would be extremely useful in the detailed characterization of the contaminant - especially for the important radioactive constituents.

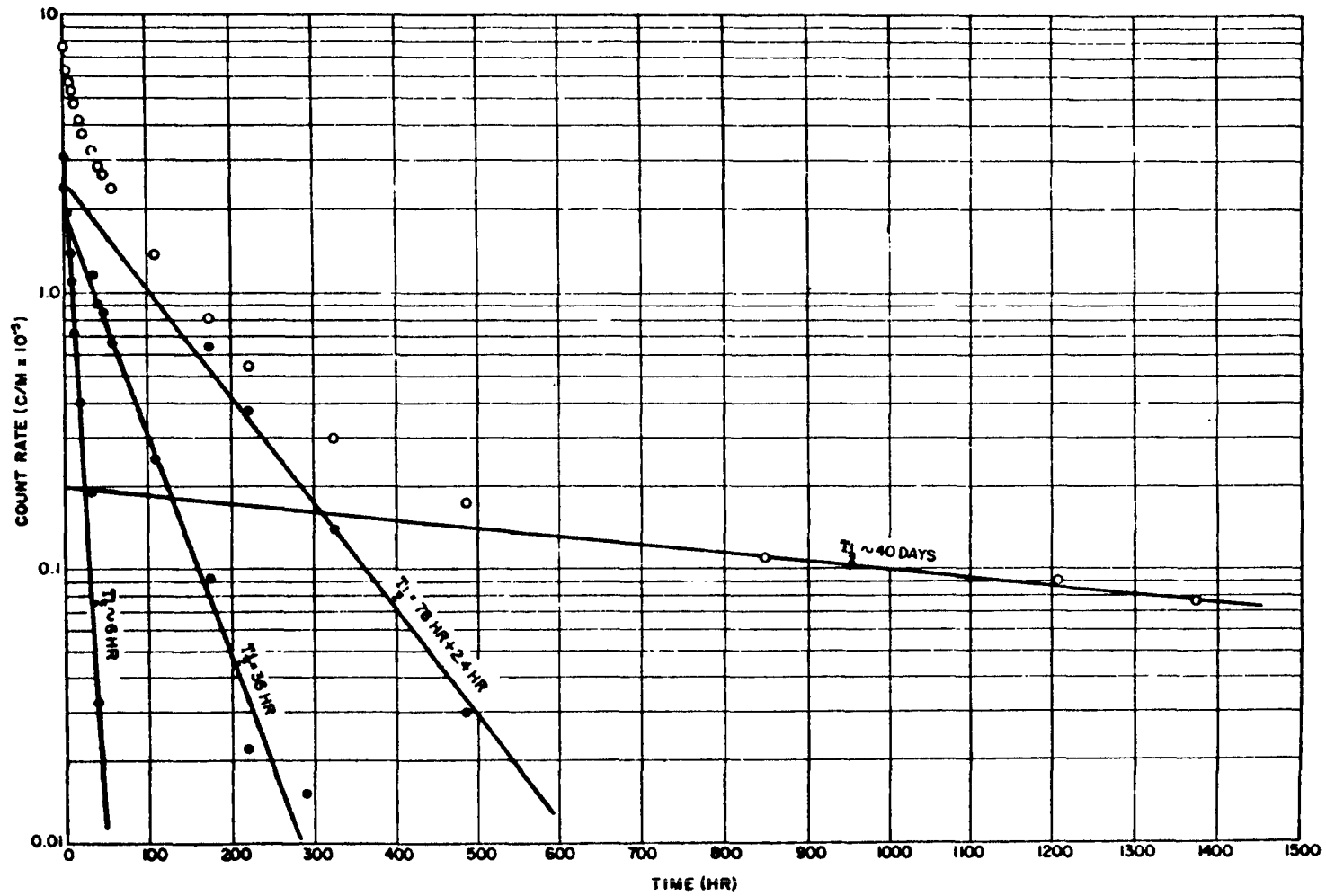


Fig. B.2 Decay of Fraction 4-34

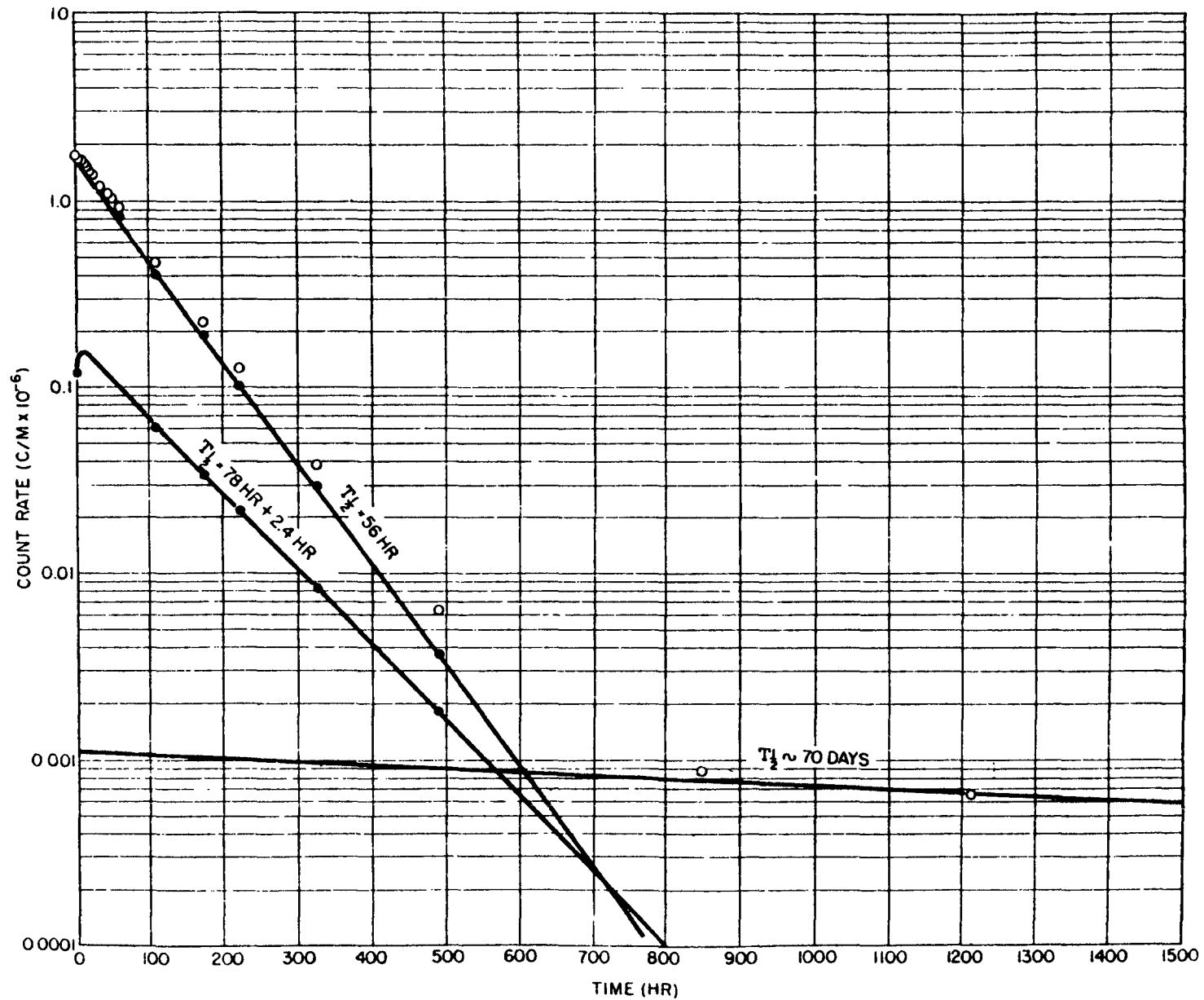


Fig. B.3 Decay of Fraction 4-31

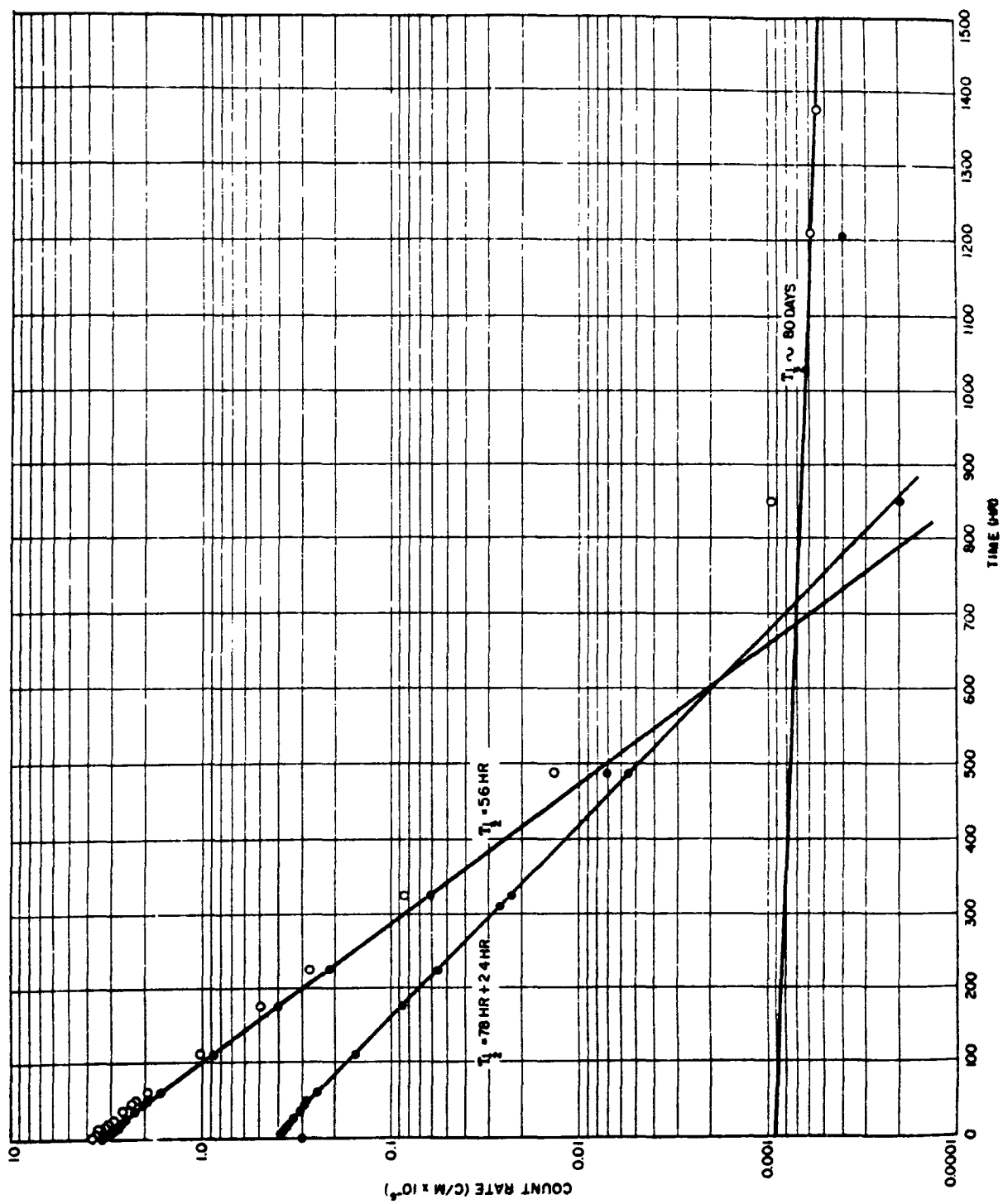


Fig. 3-A Decay of Fraction 4-32

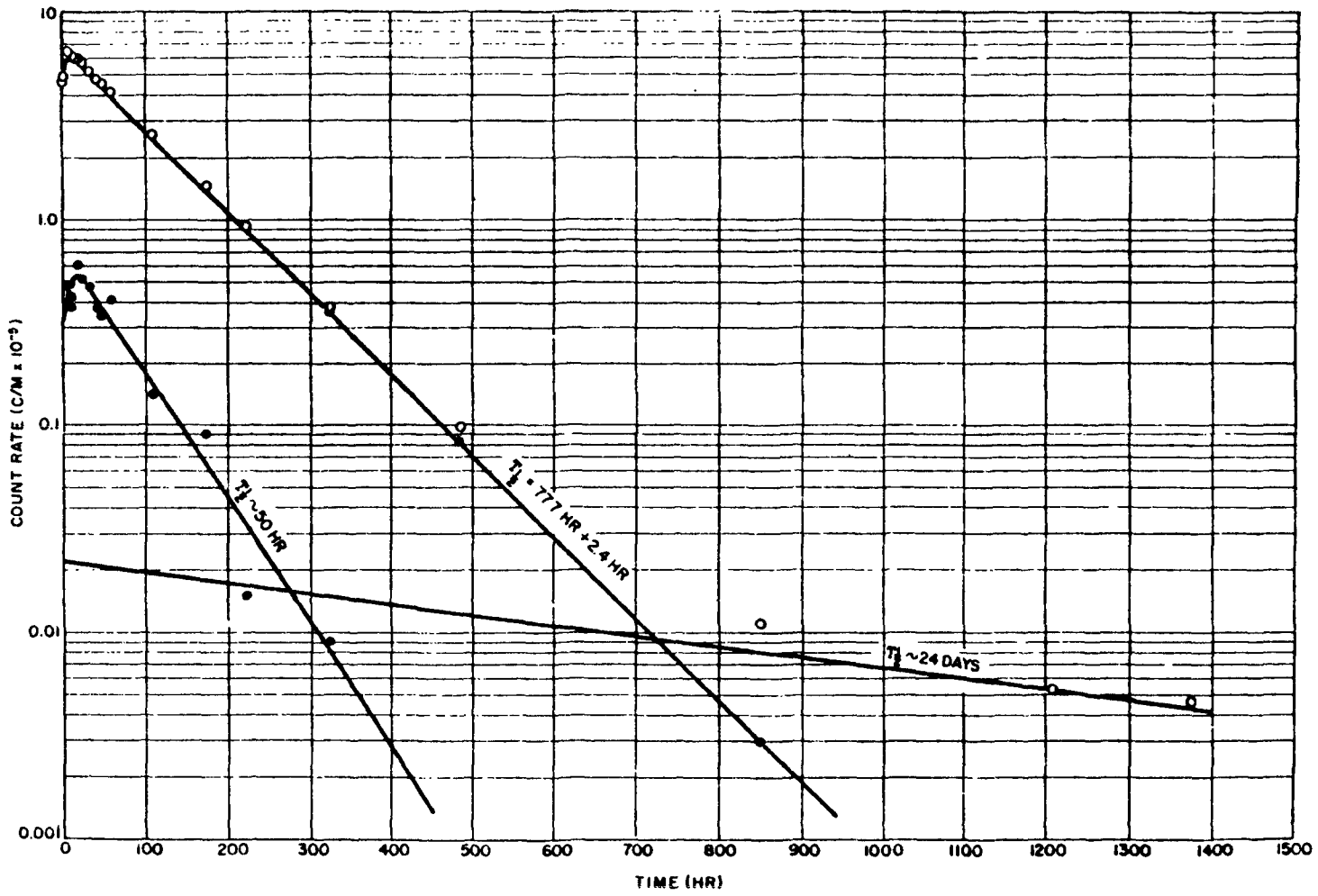


Fig. B.5 Decay of Fraction 4-33

TABLE B.1 - Summary of Major Photon Spectra Peaks of Ion Exchange Fractions

Time After Burst (days)	Peak Values (Mev)
	<u>Fraction 4-3A</u>
2.2	0.04, 0.05, 0.09 to 0.18, 0.24, 0.31 to 0.33, 0.45, 0.50 to 0.53, 0.65, 0.70, > 0.7
9.0	0.07, 0.105, 0.15, 0.21, 0.27, 0.48, 0.66, 0.76
23	0.07, 0.14, 0.23, 0.30, 0.38, 0.46, 0.48 to 0.57, > 0.6
40	0.04, 0.06, 0.24, 0.29 to 0.33, 0.37, 0.52, 0.61, 0.68
	<u>Fraction 4-31</u>
2.2	0.03, 0.06 to 0.14, 0.22, 0.24, 0.28, 0.46, 0.52, 0.65, 0.73
9.1	0.105, 0.21, 0.27, 0.49, 0.69, 0.74, 0.78
23	0.07, 0.105, 0.14, 0.18 to 0.20, 0.23, 0.27, 0.38 to 0.43, 0.46, 0.48, 0.58
	<u>Fraction 4-32</u>
2.2	0.07 to 0.15, 0.24, 0.28, 0.50, 0.67, 0.74
9.2	0.075, 0.12, 0.22, 0.27, 0.51, 0.69, 0.77
23	0.085, 0.105, 0.14, 0.18, 0.20, 0.22, 0.27, 0.46, 0.59, > 0.6
	<u>Fraction 4-33</u>
2.2	0.05, 0.08, 0.15, 0.21, 0.24, 0.33, 0.62, 0.64
9.2	0.13, 0.22, 0.36, 0.66, 0.77, 0.95, 1.1, > 1.3
23	0.02, 0.14, 0.22, 0.35, 0.46, > 0.6
40	0.02, 0.10, 0.23, 0.35, 0.41, 0.52, 0.68
	<u>Fraction 4-24</u>
2.1	0.02, 0.07, 0.15, 0.18, 0.28
2.2	0.02, 0.08, 0.14, 0.24, 0.29, 0.54, 0.65, 0.73, > 0.9
9.2	0.10, 0.14, 0.22, 0.34, 0.44, 0.49, 0.65, 0.73, 0.93, 1.1
40	0.08, 0.105, 0.16, 0.23, 0.34, 0.48, 0.52, 0.69

177

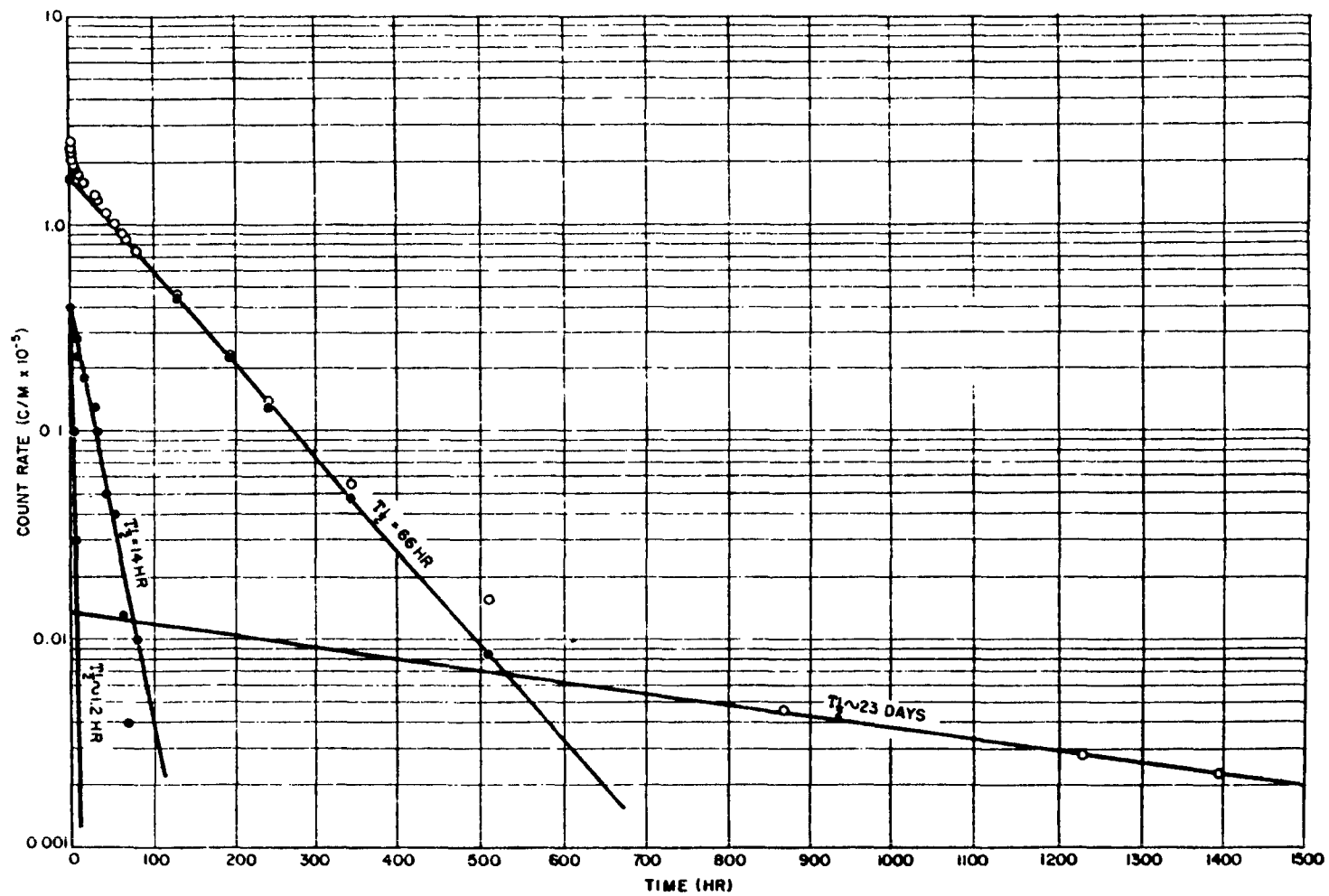


Fig. B.6 Decay of Fraction 4-24

TABLE B.2 - Major Gamma Emitters in Ion Exchange Fractions

Fraction	Half-Life	Initial Gamma Count (c/m) $\times 10^{-5}$	Fraction of Initial Gamma Count (%)	Probable Contributing Nuclides	Gamma Energies of Probable Nuclides (MeV)
4-3A	ca 40 days	0.20	2.6	Ru ¹⁰³ -Rh ^{103m}	0.04, 0.50
	78 hr	2.39	31.2	Te ¹³² -I ¹³²	0.23, 0.69, 1.4, 2.0
	36 hr	2.00	26.0	Rh ¹⁰⁵ (Te ^{129m})	0.32 (0.106, 0.3, 0.8)
	ca 6 hr	3.08	40.2	Te ^{99m} (I ¹³⁵)	0.14 (0.25, 0.52, 1.3, 1.8, 2.4)
4-31	ca 70 days	0.011	0.06	Te ^{127m} (Ru ¹⁰³)	0.09 (0.04, 0.50)
	78 hr	1.20	6.8	Te ¹³² -I ¹³²	0.23, 0.69, 1.4, 2.0
	56 hr	16.4	93.1	Np ²³⁹	0.070, 0.105, 0.23, 0.28
4-32	ca 80 days	0.0092	0.02	Te ^{127m} (Ru ¹⁰³)	0.09 (0.04, 0.50)
	78 hr	3.00	8.0	Te ¹³² -I ¹³²	0.23, 0.69, 1.4, 2.0
	56 hr	34.6	92.0	Np ²³⁹	0.070, 0.105, 0.23, 0.28
4-33	ca 24 days	0.022	0.5	Te ^{129m}	0.106, 0.3, 0.8
	78 hr	4.48	98.0	Te ¹³² -I ¹³²	0.23, 0.69, 1.4, 2.0
	ca 50 hr	0.07	1.5	Te ^{131m} -I ¹³¹	0.08, 0.16, 0.18, 0.28, 0.36, 0.64, 0.72
4-24	ca 23 days	0.013	0.5	Te ^{129m} (Cs ¹³⁶)	0.106, 0.3, 0.8 (0.9)
	66 hr	1.70	67.4	Mo ⁹⁹	0.04, (0.14), 0.18, 0.37, 0.74, 0.78
	14 hr	0.40	15.8	Na ²⁴	1.38, 2.76
	ca 1 hr	0.41	16.3	?	-

BIBLIOGRAPHY

1. Adams, C.E., Poppoff, I.C. and Wallace, N.R.
The Nature of Individual Radioactive Particles I. Surface and
Underground ABD Particles from Operation JANGLE
U.S. Naval Radiological Defense Laboratory Report
USNRDL-374, November 1952 (SECRET)
2. Adams, C.E.
The Nature of Individual Radioactive Particles II. Fallout
Particles from M-Shot Operation IVY
U.S. Naval Radiological Defense Laboratory Report
USNRDL-408, July 1953 (SECRET)
3. Adams, C.E.
The Nature of Individual Radioactive Particles IV. Fallout
Particles from the First Shot, Operation CASTLE
U.S. Naval Radiological Defense Laboratory Report
USNRDL-TR-26, January 1955 (SECRET)
4. Callou, N.E. and Bunney, L.R.
Nature and Distribution of Residual Contamination, II
JANGLE Project 2.6c-2 Report
WT-397 (in WT-373) June 1952 (SECRET)
5. Bigger, M.M., Rinnert, H.R., Sherwin, J.C., Kawahara, F.K. and
Lee, H.
Field Effectiveness Tests of a Washdown System on an Aircraft
Carrier
U.S. Naval Radiological Defense Laboratory Report
USNRDL-416, June 1953 (CONFIDENTIAL)
6. Conway, J.G. and Moore, M.F.
Spectrographic Analysis of Radioactive Materials
Analytical Chemistry, 24:463-464 (1952)
7. Coryell, C.D. and Sugarman, N. (Editors)
"Radiochemical Studies: The Fission Products, National Nuclear
Energy Series", Div. IV
Vol. 9, McGraw-Hill, New York, 1951

8. "Effects of Atomic Weapons, The"
U.S. Government Printing Office
Washington, D.C., 1950
9. Farlow, N.H.
A Physico-Chemical System for Water Aerosol Measurement
U.S. Naval Radiological Defense Laboratory Report
USNRDL-TR-49, May 1955
10. Gevantman, L.H., Pestaner, J.F., Singer, B. and Sam, D.
Decontaminability of Selected Materials: Decontamination by
Spraying with and Immersion in Liquid
U.S. Naval Radiological Defense Laboratory Report
USNRDL-TR-13, August 1954 (CONFIDENTIAL)
11. Greendale, A.E. and Ballou, N.E.
Physical State of Fission Product Elements Following Their
Vaporization in Distilled Water and Sea Water
U.S. Naval Radiological Defense Laboratory Report
USNRDL-436, February 1954
12. Heidt, W.B., Jr., LCDR, USN, Schuert, E.A., Perkins, W.W. and
Stetson, R.L.
Nature, Intensity and Distribution of Fallout from M-Shot, Opera-
tion IVY
IVY Project 5.4a Report, April 1953 (SECRET RESTRICTED DATA)
WT-615
13. Honma, M.
Flame Photometric Apparatus for Determination of Radioactive
Materials
Paper presented at Amer. Chem. Society Meeting September 11, 1955
Minneapolis, Minnesota
14. Hunter, H.F. and Ballou, N.E.
Fission-Product Decay Rates
Nucleonics, 9: No. 5, C1-7 (1951)
15. Johnstone, C.W.
A New Pulse Analyzer Design
Nucleonics, 11: No. 1, 36-41 (1953)
16. LaRiviere, P.D. and Ichiki, S.K.
Autoradiographic Method for Identifying Beta-Active Particles in a
Heterogeneous Mixture
Nucleonics, 10: No. 9, 22-24 (1952)
17. Laurino, R.K., Poppoff, I.G.
Contamination Patterns at Operation JANGLE
U.S. Naval Radiological Defense Laboratory Report
USNRDL-399, April 1953 (SECRET RESTRICTED DATA)

18. Macdonald, D. and Zigman, P.E.
Influence of Surface Roughness on Contamination and Decontamination Behavior of Materials
U.S. Naval Radiological Defense Laboratory Report
USNRDL-415, September 1953 (SECRET)
19. Maxwell, C.R., et al
Nature and Distribution of Residual Contamination, I
JANGLE Project 2.6c-1 Report
WT-386 (in WT-373), June 1952 (SECRET RESTRICTED DATA)
20. Maxwell, R.D.
Radiochemical Studies of Large Particles
JANGLE Project 2.5a-3 Report
WT-333 (in WT-371), April 1952 (SECRET RESTRICTED DATA)
21. Meinke, W.F.
Chemical Procedures Used in Bombardment Work at Berkeley
University of California Radiation Laboratory Report
UCRL-432, August 1949
22. Miller, C.F., Cole, R. and Heiman, W.J.
An Investigation of Synthetic Contaminants for an Atomic Burst in Deep Sea Water
U.S. Naval Radiological Defense Laboratory Report
USNRDL-411, August 1953 (SECRET RESTRICTED DATA)
23. Miller, C.F., Cole, R., Heiman, W.J. and Nuckolls, M.J.
Decontamination of Fission Products and Other Atomic Bomb Detonation Debris
U.S. Naval Radiological Defense Laboratory Report
USNRDL-439, November 1953 (CONFIDENTIAL)
24. Cole, R., Heiman, W.J., Miller, C.F.
Effect of Harbour Bottom Material on the Decontamination of Various Elements in a Synthetic Sea Water Contaminant
U.S. Naval Radiological Defense Laboratory Report
USNRDL-TR-43, February 1955 (CONFIDENTIAL)
25. Poppoff, I.G., et al
Fallout Particles Studies
JANGLE Project 2.5a-2 Report
WT-395 (in WT-371) April 1952 (SECRET RESTRICTED DATA)
26. Quan, J.T.
A Split-Image Film Comparator for X-ray Diffraction Powder
Review of Scientific Instruments, 25: No. 4 (1954)
27. Schmidt, A.C. and Wiltshire, L.L.
A Constant Flow Suction Unit for Aerosol Sampling Work
American Industrial Hygiene Association Quarterly, 16:2 June 1955

28. Spence, R.W.
Letter; LASL, J-11-96, WET 54-406D, August 6, 1954
29. Stetson, R.L., Schuert, E.A., Perkins, W.W., Shirawasa, T.H. and Chan, H.K.
Distribution and Intensity of Fallout at Operation CASTLE
CASTLE Project 2.5a Report (SECRET RESTRICTED DATA)
WT-915
30. Sverdrup, H.J., Johnson, M.W. and Fleming, R.K.
"The Oceans, Their Physics, Chemistry and General Biology"
Prentice-Hall, New York, 1942
31. Transmittal of CASTLE Device Data
Document T.U. 13-54-106S, 4 May 1954 (SECRET RESTRICTED DATA)
32. Werner, L.B.
Contamination-Decontamination Phenomenology
JANGLE Project 6.2 Report
WT-400 (Ch. 8) June 1952 (SECRET)
33. Wittman, J.P., and Goodale, T.C.
An Automatic Water Drop Collector for Field Use
Bulletin of the American Meteorological Society
Vol. 36, No. 2, February, 1955